Experimental investigation of microbial growth in subsurface environment

Mohammad Hussein Essa

Civil Engineering

July 1993

Abstract

An experimental investigation was conducted to quantify the permeability reduction caused by enhanced biological growth in a porous media. Studies were conducted using columns packed with sand of three different sizes (0.2, 0.3, and 0.4 mm). Phenol was used as a growth substrate. The study involved three distinct Phases with three different concentrations of phenol (15, 50 and 100gm/l). Variations in piezometric head, substrate concentration, and biomass measured as volatile solids, were monitored in space and time.

The reductions in permeability were found to be 78% for the coarse, 93% for medium size, and 93.7% for fine sand in Phase-I; Similarly in Phase-II, the reductions were 88.4% for coarse sand, and 94.6% for medium size sand. Finally, in Phase-III, the reductions were 95.5% for medium size, and 96.8% for fine sand. For aerobic sand media, volatile solids can be described as a function of influent substrate concentration respectively. The modified Kozeni-Carman equation was used to estimate the thickness of biological film, knowing the biofilm affected permeability. The estimated values of the film thickness varied from 0.06 mm to 0.09 mm. A good correlation was observed between porosity and biofilm thickness in low range values of thickness.

Experimental Investigation of Microbial Growth in Subsurface Environment

by

Mohammad Hussein Essa

A Thesis Presented to the

FACULTY OF THE COLLEGE OF GRADUATE STUDIES

KING FAHD UNIVERSITY OF PETROLEUM & MINERALS

DHAHRAN, SAUDI ARABIA

In Partial Fulfillment of the
Requirements for the Degree of

MASTER OF SCIENCE

In

CIVIL ENGINEERING

July, 1993

EXPERIMENTAL INVESTIGATION OF MICROBIAL GROWTH IN SUBSURFACE ENVIRONMENT

BY

MOHAMMAD HUSSEIN ESSA

A Thesis Presented to the

FACULTY OF THE COLLEGE OF GRADUATE STUDIES

KING FAHD UNIVERSITY OF PETROLEUM & MINERALS

DHAHRAN, SAUDI ARABIA

In Partial Fulfillment of the
Requirements for the Degree of

MASTER OF SCIENCE
In

CIVIL ENGINEERING

JULY, 1993

KING FAHD UNIVERSITY OF PETROLEUM & MINERALS
DHAHRAN 31261,SAUDI ARABIA.

COLLEGE OF GRADUATE STUDIES

This Thesis, written by **MOHAMMED HUSSEIN ESSA** under the direction of his Thesis Advisors and approved by his Thesis Committee, has been presented to and accepted by the Dean of the College of Graduate Studies, in partial fulfillment of the requirements for the degree of

MASTER OF SCIENCE IN CIVIL ENGINEERING

Thesis Committee

Dr. Shaukat Farooq
Chairman

Dr. Girgis F. Nakhla
Co-Chairman

Dr. Abu Nasser Khondaker
Member

Dr. Al-Farabi Sharif
Chairman
Department of Civil Engineering

Dr. Ala H. Al-Rabeh
Dean
College of Graduate Studies

Date : 11-12-93

123

ACKNOWLEDGEMENTS

Praise and gratitude be to **ALLAH**, Almighty, with whose gracious help it was possible to accomplish this work. Acknowledgement is due to King Fahd University of Petroleum and Minerals for extending the facilities to carry out this research.

I would like to express my gratitude and appreciation to my advisor Prof. Shaukat Farooq for his constant and valuable guidance and helpful suggestions throughout this study. Thanks are due to Dr. Girgis Nakhla and Dr. A. Nasser Khondaker for the valuable suggestions and contributions provided throughout this study.

Acknowledgement is also due to Mr. Essam Al-Deeb and Mr. M.K. Abdulappa of Environmental Engineering Laboratory for their help during the experimentation. Thanks are also extended to my friends especially Mr. Abdusalam Mohammed Ahmed, Mr. Ahmed Aidid Ibrahim, Mr. Mohammed Ali Moallim, and Mr. Ali Abdulaziz Shehata who all helped me in different aspects of this research.

I owe my family an expression of gratitude for their patience and understanding during my studies in KFUPM.

TABLE OF CONTENTS

List of Tables

List of Figures

ملخص بحث

الاسم: محمد حسين عيسى

مسمى البحث : بحث عملي عن نمو البكتريا في البيئات التحتية .

التخصص العام : هندسة مدنية (مصادر المياه والبيئة)

تاريخ الدرجة : يوليو ١٩٩٣

تم إجراد تجربة لتقدير حجم خفض التسرب بسبب النمو البكتيري في الوسط النفاذ ، وتم تطبيق دراسات باستعمال اسطوانات معبأة برمال بثلاثة احجام مختلفة (٢ر. - ٣ر. - ٤ر. مم) . وقد تم استعمال الفينول كوسط نمو . وقد تمت الدراسة في ثلاث مراحل مع ثلاث تركيزات للفينول (١٥ - ٥٠ - ١٠٠ ملجم / ١) .

وقد تبين أن خفض التسرب في المرحلة الأولى (النفاذية) هو ٧٨٪ في اكبر حجم للرمال (٤٠ر مم) و ٩٦٪ للحجم المتوسط و ٩٣ر٧ ٪ لأصغر حجم من الرمال . وفي المرحلة الثانية ٨٨ر٤ ٪ ٩٥ر٥ ٪ و ٩٦ر٨ ٪ بالترتيب .

وقد استعملت معادلة كوزيني كارماني لتقدير سمك الفيلم البيولوجي ، وقد تفاوتت قيم سمك الفيلم بين ٠٠٠٦ مم و ٠٠٠٩ مم . وقد لوحظ وجود علاقة تبادلية جيدة بين النفاذية وسمك البيوفيلم في قيم منخفضة المعدل .

درجة الماجستير في العلوم

جامعة الملك فهد للبترول والمعادن

الظهران - المملكة العربية السعودية

ABSTRACT

Name: **Mohammed Hussein Essa**

Title of Study: **Experimental Investigation of Microbial Growth in Subsurface Environment**

Major Field: **Civil Engineering (Water Resources & Environmental)**

Date of Degree: **July 1993**

An experimental investigation was conducted to quantify the permeability reduction caused by enhanced biological growth in a porous media. Studies were conducted using columns packed with sand of three different sizes (0.2, 0.3, and 0.4 mm). Phenol was used as a growth substrate. The study involved three distinct Phases with three different concentrations of phenol (15, 50, and 100 mg/l). Variations in piezometric head, substrate concentration, and biomass measured as volatile solids, were monitored in space and time.

The reductions in permeability were found to be 78% for the coarse, 93% for medium size, and 93.7% for fine sand in Phase-I; Similarly in Phase-II, the reductions were 88.4% for coarse sand, and 94.6% for medium size sand. Finally, in Phase-III, the reductions were 95.5% for medium size, and 96.8% for fine sand. For aerobic sand media, volatile solids can be described as a function of influent substrate concentration respectively. The modified Kozeni-Carman equation was used to estimate the thickness of biological film, knowing the biofilm affected permeability. The estimated values of the film thickness varied from 0.06 mm to 0.09 mm. A good correlation was observed between porosity and biofilm thickness in low range values of thickness.

MASTER OF SCIENCE DEGREE

King Fahd University of Petroleum and Minerals
Dhahran, Saudi Arabia

Chapter I

INTRODUCTION

Recently considerable attention has been paid to the microbial ecology of the subsurface environment and to the possibility of using indigeneous organisms in pollution remediation. Microbial growth in the subsurface environment plays an important role, particularly in the studies of microbial contamination of groundwater due to infiltration of wastewater, and in situ bioremediation of organic contaminants in groundwater. The injection of water into oil bearing formations is commonly used to increase recovery, but bacterial clogging of the formation near the injection well often occurs. This problem has been studied by Kalish et al. (1964), Raleigh and Flock (1965), and Show et al. (1985). All these investigations show that the permeability reduction can be related to bacterial characteristics, intrinsic properties of the formation, injection rates, and depth of bacterial penetration. It has long been known that various bacteria flourish in the subsurface waters. The growth of these bacteria has led to the suspicion that they might reduce the hydraulic conductivity of the porous media significantly. The microbial growth in the subsurface environment is a function of numerous natural and/or environmental factors, including temperature, characteristics of porous medium, moisture or water content, oxygen availability and the presence of

organic and inorganic nutrients in the system.

In a saturated porous media, bacteria can be suspended in the liquid phase or attached to the solid phase of the medium. Bacteria in the water phase are subject to convective and dispersive transport due to fluid motion, and may also move when a gradient in the growth substrate concentration exists. Bacteria grow and reproduce at the interface of the water and solid phases, increasing the biomass and extracellular material. The entire deposit is termed biofilm. As the biomass increases in volume due to bacterial growth, the microscopic geometry of the pore space is changed. Porous medium properties which are functions of the pore geometry, i.e.,porosity, permeability, and dispersivity, therefore change as a consequence of biofilm growth. The grain size distribution is the dominating factor of the charac- teristics of the porous medium.

The objective of the proposed study is to determine the effects of grain size distribution on the microbial growth and the removal of the hazardous pollutants in subsurface environment. Three different sets of experiments were designed to study the effect on the removal of phenol, microbial growth, and permeability of soil columns. Each set was conducted at a given concentration of phenol, i.e. 15, 50, and 100 mg/l. Furthermore, each set was comprized of several soil columns consisting of fine, medium, and coarse sizes of sand. These columns were dismantled at various stages to determine the increase in volatile mass as a result of biological growth.

Chapter II

LITERATURE REVIEW

Bacterial growth in a porous medium and the consequent reduction in hydraulic conductivity are cited in the literature only in a descriptive manner. This bacterial growth most of the times is associated with groundwater recharge, water treatment or disposal processes, enhanced oil recovery schemes, and, more recently, in situ bioremediation of organic contaminants in grounwater. Microbial contamination of groundwater due to wastewater injection or bioremediation projects may result in the contamination of well water supplies, since both processes inject water containing relatively high levels of growth substrate and inorganic nutrients, thus changing the properties of the media (Taylor , 1990).

2.1 Bioremediation of Contaminated Soil

Bioremediation of organic contaminated soil is a treatment technology that, depending on the site-specific conditions, can reduce the organic contaminants to an acceptable level which meets the remediation criteria estabilished by the regulatory agency. Biodegradation occurs naturally in all soils. Microorganisms use organic compounds which contain only carbon, hydrogen and oxygen. A wide variety of bacteria such as molds and yeasts and certain cyanobacteria have been shown to aerobically oxidize organic contaminants (Newton,

1990). The microorganisms feed on the organic chemicals found in the soil matrix, use the oxygen, and require water in order to survive.

In situ biodegradation involves the stimulation of this microbial activity. In situ biodegradation is generally appropriate in areas where the water table is relatively close to the surface. In arid areas, it is not economically viable because of the excessive pumping costs. Biodegradation is influenced by a variety of factors including dissolved oxygen level, soil moisture content, soil permeability, temperature, soil pH, nutrient availability, and natural microbial community (Robinson, 1990).

In more complex physical environment, biological activity is stimulated and maintained by implementing estabilished engineering practices, coupled with the management of otherwise constraining physical barriers such as geological and hydrogeological. A thorough understanding of the properties of the media such as hydraulic conductivity is needed before attempting to mention about the various aspects on it.

2.2 Hydraulic Conductivity

Conductivity may be defined as the rate at which a fluid passes through a porous medium of unit area under unit gradient. The simplest expression is the Darcy equation defined by the following:

$$Q = k\frac{AH}{L} \qquad (2.1)$$

$$q = k\frac{dh}{dl} \qquad (2.2)$$

where:

Q = is the flow rate (volume per unit time)

K = is the hydraulic conductivity

A = is the cross-sectional area of the soil column

H = is the difference in piezometric head at the two ends of the soil column.

L = is the length of the column

q = is the flow per unit area which is velocity

dh/dl = is the hydraulic gradient

The value of the coefficient of hydraulic conductivity of various soils varies greatly. In the laboratory, it can be determined by means of constant pressure head or falling pressure head tests. The constant pressure head test is more suitable for granular soils.

The following table provides the general range for the values of K for various soils (Table 2.1)

Coefficient of permeability k (cm/sec)	Type of soil
Greater than 10^{-1}	Medium to coarse gravel
10^{-3}	
10^{-1}	Coarse to fine sand
10^{-5}	
10^{-3}	Fine sand, silty sand
10^{-6}	
10^{-4}	Silt, clayey silt
10^{-7} *or less*	Clays

There is a relation between hydraulic conductivity and permeability. Hydraulic conductivity is related to the fluid and the properties of the medium through the following equation:

$$K = \frac{k\rho g}{\mu} \qquad (2.3)$$

Where

K = hydraulic conductivity

k = the intrinsic permeability of the medium

μ = the dynamic viscosity of the fluid

ρ = the viscosity of the fluid

g = acceleration due to gravity

From the above equation, the hydraulic conductivity is a function of the properties of the medium and the fluid properties. The intrinsic permeability is a function of the porosity, specific surface, and tortuosity. The change of porosity or specific surface will affect the intrinsic permeability and consequently the hydraulic conductivity (Taylor, 1990).

2.3 Change of Porosity with Biofilm Thickness

One of the goals of this investigation is to determine the biofilm thickness indirectly since the direct measurement is very difficult to accomplish. Growth of a biofilm in a porous media reduces the average size of the pores. The change in the pore space is easily quantified when certain geometric assumptions are made. We assume that the porous medium is rigid and saturated with a single fluid, the flow is Darcian, and the biofilm has negligible permeability. It is assumed also that the microbes are utilizing growth substrate under aerobic conditions. It follows that the problem is primarily one of relating changes in pore geometry, caused by biofilm growth, to changes in porosity. Many different modeling approaches for the treatment of single-phase porosity have been described in the literature.

Kozeni-Carman model has been extensively used to describe the change in porosity affected by biofilm thickness (Marshall, 1958; Taylor et al., 1990). In this study, the modified Kozeni-Carman

model developed by Taylor et al. (1990) is used. This model assumes the porous medium to be equivalent to a conduit, the cross section of which has a complicated shape but a constant area. From hydraulic theory it is known that the conduit diameter is taken to be 4 times the hydraulic radius. Combining the Hagen-Poisewille equation for laminar flow in a conduit with Darcy's law yields the Kozeni-Carmen equation.

$$K = c_0 n^3 / M^2 \qquad (2.4)$$

where n is the porosity, M is the specific surface, and c a constant for which Carman (1937) suggests a value of 1/5.

Assumptions regarding the packing of the solid phase are made. It is assumed that the solid phase is comprised of uniform spheres packed in a stable manner. In any arrangement, each sphere tangentially contacts a certain number of neighbouring spheres, and the number of contact points m can be used to characterize the packing arrangement. The value of m for the sphere arrangement is 6. The packing arrangement factor alpham for the sphere is 1.

Assuming that a biofilm develops in a porous medium comprised of spheres of equal diameter. Biofilm growth increases the volume and decreases the surface area of the solid phase. Expressions for the biofilm - affected porosity n and specific surface M can be derived from the geometry of the sphere coated with a constant biofilm thickness Lf.

$$n_b = 1-\pi/\alpha((2-m)/12(2lf/d)^3+(4-m)/8(2lf/d)^2+1/2(2lf/d)+1/602.5)$$

$$M_b = (\pi/\alpha*d)*((2-m)/2*(2lf/d)sup2+(4-m)/2*(2lf/d)+1 \qquad (2.6)$$

The biofilm-affected permeability for the sphere model is found by substituting the biofilm-affected porosity and specific surface into the equation 4.1, assuming that c does not vary with biofilm growth. hence the equation is as follows:

$$K_b = c_0(n_b^3/M_b^2) \qquad (2.7)$$

2.4 Reduction of Permeability by Bacteria

A literature survey has shown that limited information on the reduction of permeability in subsurface environment is available. Allison (1947) reported a laboratory investigation initiated to determin the reason for the decreasing rate of infiltration in agricultural soils under continuous submergence. He performed permeability tests on 43 undisturbed soil cores. The soil cores were obtained in steel cylinders 5 inches by 36 inches and they were taken at various depths in the upper San Joaquin Valley. Significant reduction in the hydraulic conductivity was observed in his study. Allison found marked reductions in the hydraulic conductivity of saturated porous media during prolonged flow and established that these reductions are caused by microorganisms The reduction in permeability was attributed to

clogging of the soil pores by bacterial cells and polysaccharides.

Gupta and Swarzendruber (1962) found that drastic reductions in hydraulic conductivity occured for bacterial numbers exceeding 400000 per gram of sand.

Raleich (1965) investigated the nature of pore clogging with bacteria and attempted to relate its characteristics to physical rock properties. He took fifteen core samples of four specific oil-bearing formation types. Two of the formation types were fairly uniform-grained sandstones and two were heterogeneous carbonates. The injection rate of the water was held constant during the experiment. The bacteria used for clogging purpose was a uniform-sized, dead bacteria, *Bacillus subtilis*, a microorganism commonly found in water, air and soils. He found that th majority of the clogging in the uniform grained sandstones was located near the input end of the cores. The heterogeneous carbonate cores behaved irregularly, and clogging was observed well within the core. He came to a conclusion that depth of clogging within porous rock is a function of the pore geometry. He also concluded that the two physical rock properties which are permeability and residual saturation did not appear to reflect directly the parameters for rate of clogging.

Kalish and Bennett (1964) in their investigation on the effect of bacteria on sandstone permeability, concluded that bacteria can not reduce permeability to zero and that their effect on permeability is subject to definite limitations. They have used three different oil

bearing formations . The injection fluid used in all tests was a 25000 mg/l calcium chloride brine. A calcium rather than sodium brine was used because it minimized the sensitivity of the sandstone without having any marked physical effects on the bacteria tested. The bacteria used throughout the study were species which had been found in several oil field water injection systems. They were *Pseudomonas aeruginosa*, *Pseudomonas fluorescens*, *Bacillus cereus*, *Micrococcus roseus*, *Micrococcus citrius*, *and Proteus vulgaris*.

Show et al. (1985) used a sintered glass bead core to simulate a porous medium. The passage of the bacteria through this medium initially promoted adherent bacterial microcolonies on available surfaces. Bacteria within these microcolonies produced large amounts of polysaccharides and formed a plugging biofilm that caused significant decreases in core permeability.

Jenneman et al. (1984) and Raiders et al.(1986) studied the feasibility of using microorganisms to selectively plug high permeability zones of a formation and improve the oil recovery efficiency during water injection. They have shown that in situ microbial growth can selectively plug high permeability zones and tends to drive an initially heterogeneous permeability field toward homogeneity.

Brian D.Wood et al.(1993) studied the in situ measurement of microbial activity and controls on microbial carbon dioxide production in the subsurface environment. They have measured carbon dioxide concentrations at various depths and times of two hydraulically and

geochemically contrasting fields. They have determined the microbial activity quantified as carbon dioxide production (respiration). In their study they examined the possibility of relating carbon dioxide production rates determined from gas phase measurements to the number of subsurface microorganisms and the subsurface temperature. They also found that cases in which microbial numbers and subsurface temperature do not correlate with production would suggest that other factors may have greater relative importance in controlling subsurface microbial carbon dioxide production rates.

Taylor and Jaffe'(1990) reported in a series of publications the biofilm growth and the related changes in the physical properties of a porous medium. In the first paper, Taylor and Jaffe'(1990-a) have conducted an experimental investigation to quantify the permeability reduction due to biological growth in a porous medium. They have used two column reactors (5.08 cm diameter and 52 cm long) packed with ASTM C-190 test sand. The sand was of nearly uniform size and consisted of grains ranging from 0.59 to 0.84 mm in diameter. The bacteria used in the study were derived primary sewage and activated from primary sewage and activated sludge (Princeton Sewage Treatment plant, Princeton, New Jersey). Methanol was used as a growth substrate. They concluded in this experiment that there is a limit on permeability reduction, which was found to be $K/k' \ 5*10^{-4}$ where k' is the initial permeability.

In the second paper Taylor and Jaffe'(1990-b) presented the analytical estimation of the magnitude of the permeability change caused by biofilm growth in a rigid porous medium . In this paper they set the theoretical framework for a rigorous interpretation of the experimental results of the first paper.

In the third paper, Taylor and Jaffe'(1990-c) investigated the change in dispersivity resulting from the growth of a biofilm in a porous medium. They estimated the dispersivity from experimental data. They conducted experiments in biofilm column reactors and estimated dispersion coefficients by solving the inverse solute transport problem by nonlinear least sqares regression.

In the fourth paper, Taylor and Jaffe'(1990-d) presented a model for the transport of substrate and biomass in a porous medium. The model was calibrated and verified against experimental data.

M.W.O'Neil et al.(1993), studied the extraction of organic contaminants from a loamy soil. The organic contaminants used in their study were phenol and aniline. They found in this study that the nature of the material onto which the organic contaminant sorbs is important, the properties of the organic contaminant compound and the solvent medium also influence the sorption process. They also found that aniline was much more difficult to desorb than phenol.

Christiansen (1944), explained the effect of entrapped air upon the permeability of soils. He conducted an experiment to determine

the amount of air entrapped and the effect of variations in density upon the permeability and the air entrapment. He filled eighteen tubes with sandy loam with appropriate compaction. The tubes were weighed and then set in beakers of water and allowed to stand in water overnight. The tubes were again weighed and at the end of the experiment they were weighed a third time. He concluded that the difference in weight at the beginning and the end of the experiment is an approximate measure of the pore space initially occupied by air and subsequently by water. He found a good correlation between the amount of entrapped air and the relative increase in permeability when air is eliminated.

Thomas and Brown (1992) reported depth variations in hydraulic conductivity within a compacted clay. Compacted clays were formerly used as the sole liner for landfills and impoundments, but current regulations require double liners and currently compacted clay liners are commonly used as components of the lower portion of composite double liner systems for hazardous waste containment. They performed laboratory test using two subsoils: a fine, montmorillonitic soil and a fine-loamy soil. They characterized representative samples of each soil through a series of laboratory tests including: texture, Atterberg limits, optimum moisture content, swelling, and water retention. Compaction of the two soils was achieved with a mechanical compactor. After the compaction sufficient volumes of these two soils were air dried and passed through a 2.5, 5, 7.5 cm mesh screens to produce batches of soils. Each batch of soil was brought to its

optimum moisture content by adding water to the soil, gently mixing, and allowing the moistened soil to equilibrate for one week in a closed 200 L drum. After that, 10 Kg of moist soil were put on top of a 4 mm thick geotextile. A pressure of 1.38 MPa was applied on top of the soil. The soils were then immediately covered with plastic to prevent evaporation and moved to a place where they were equipped with a head tank. The head tank was filled with water to provide approximately 1 m of head. Water levels were measured daily using a hook gauge. Effluent was collected and measured daily. Effluent measurements were continued until the effluent volume was within 95% of the inflow. When equilibrium was reached, the liquid head was drained and the head tank was removed. A total 7.5 cm of soil was carefully removed in three increments of 2.5 cm each. The head tank and liquid were replaced and the conductivity measurements were repeated for the remaining soil (approximately 15 cm) until equilibrium was reached. Again, 7.5 cm of soil were removed in 2.5 cm increments and the hydraulic conductivity of the remaining 7.5 cm of soil was measured. From the experiment they concluded that soil bulk density was poorly correlated with hydraulic conductivity and indicated that measuring the bulk density of a compacted soil is an inadequate method for assuring low hydraulic conductivity. Measurements of the time to the first appearance of leachate indicated that 8 to 17 days are required for water to penetrate a 23 cm thick compacted liner with an average conductivity of $1*10^{-7}$ cm/sec.

In the present work, an experimental study is initiated to investigate the effect of grain-size distribution on the bacterial growth in soil columns using groundwater and phenol. The effect of three different phenol concentration (15, 50, and 100 mg/l) on the microbial growth pattern is investigated for the different type of soil samples of various grain size distributions. The overall effect of biomass growth on the medium hydraulic conductivity has been also investigated in the laboratory.

2.5 Microbial Life in the Soil

As we know, the variability of microbial life in the soil reflects both their physiological characteristics and a wide range of environmental factors. Growth of microbes depends upon a supply of free energy through chemical and photochemical reactions and the ability to duplicate cellular constituents through biosynthetic reactions. Specific growth rates are deeply influenced by environmental factors such as temperature, pH, and others.

2.5.1 Principles of Microbial Growth:

All living systems require sources of energy to develop and sustain their population. In biological treatment, the contaminant is usually one of the sources of food and energy for single species thriving in the contaminated environment. The activity of organisms responsible for contaminant destruction is controlled by several environmental factors, notably nutrients, water and oxygen availability, temperature

and pH. In addition, activities can be inhibited by the presence of toxic organic compounds, metals, or high salt content (Chiang, 1989). Nutrient requirements play an active role in the metabolism of any organism on the organism growth rate. When the concentration is 0, no growth occurs. As the concentration is increased the growth increases, then becomes constant, and eventually declines back to 0. When the growth rate increases with concentration the substance is considered stimulatory; when the growth rate declines with concentration the substance is considered toxic.

During the microbial growth process, organisms incorporate certain amounts of nutrients, such as nitrogen and phosphorous, particularly during growth of their population to produce biomass. Available nitrogen and phosphorous must be maintained as sufficient as possible in the contaminated environment to assure that only the contaminant is the only limiting nutrient (Ellis, 1991). Generally, the range of carbon: nitrogen: phosphorous is between 100: 10: 1 to 100: 10: 0.5 depending on the type of treatment used, and the phase (liquid or solid) in which the contaminant is found. Orgamisms can survive in otherwise inhibitory and toxic environments because of change in their metabolic or physical characteristics developed during a process of acclimation.

There are four phases of growth which are: the lag phase in which little if any growth occurs; the exponential phase (or logarithmic phase) in which the logarithm of the number of cells increases

linearly with time; the stationary phase in which growth does not occur; and the death phase in which the viable population declines (Hattori, 1973).

2.6 Aerobic Attached Growth

The process description of the aerobic attached growth is as follows: The organic material which is present in the wastewater is degraded by by microorganisms attached to the soil media. Adsorption of organic material on the biological film takes place; therefore the organic material is degraded by aerobic microorganisms. As the micro- organisms grow , the thickness of biofilm increases.

As the biofilm increases in thickness, the fluid shear stress at the water-biofilm interface increases. Also, as the thickness of the biofilm increases, the potential for substrate, electron acceptor, or nutrient limitation in the deeper portions of the biofilm is increased. These limitations may weaken the biofilm matrix and enhance the shear or detachment of biomass from the solid phase of the porous media. Taylor et al. present data that shows that detachment rate increases with increasing fluid shear stress and with increasing biofilm mass (1990).

2.7 Biosorption Phenomena

In the aerobic attached-growth tratment processes, biosorption of substrate could contribute significantly to the removal of substrate.

Interaction between substrates and microbial cells can occur through the sorption of substrate to cell surfaces. The kinetics of substrate sorption on the cell surfaces is very complicated. The kinetics thought to be physical adsorption at the cell surface is very rapid and occurs a short time after the microorganism comes into contact with the substrate. Dead cells accumulate substrate also on their surfaces. This kind of sorption is called biosorption (Asku, 1990).

2.8 Monod's Equation of Microbial Growth

The growth of microbial cells includes a great variety of reactions linked together as a complex network, and growth of a microbial population involves complex mechanisms. Nevertheless we can find basic quantitative characteristics of microbial growth in Monod's three equations

When microbial cells of biomass M (expressed as mg/ml) are growing exponentially with a supply of all nutrients required by the microbes or all cell constituents are increased proportionately over the same period of time, the growth rate is determined by the following three equation:

$$\frac{dM}{dt} = \mu M \tag{2.8}$$

here t is the time and μ is a specific growth rate for the organism.

The second Monod equation is concerned with the relation between

the specific growth rate (mu) and concentration of the substrate (s) affecting the growth rate:

$$\mu = \mu_{max}(S/K_s + S) \qquad (2.9)$$

where μ_{max} is the maximum growth rate and Ks a constant called a Saturation Coefficient.

The third equation expresses the relationship between newly synthesized biomass and amount of the substrate consumed by microbes:

$$-d(S)/dt = (1/Y)*dM/dt \qquad (2.10)$$

where y is the growth yield relative to a given substrate. In these equations, Monod considered that the growth yield is a constant.

2.9 Nature of the Contaminant (Phenol)

The complexity of the organic material often determines the likelihood of the molecule to be degraded. For example, longchained aliphatic hydrocarbons, aldehydes, and ketones are rapidly degraded to end products of carbon dioxide and water. In contrast polynuclear aromatic (PNA) compounds with four or more rings are degraded slowly. Heterocyclic compounds containing nitrogen, sulphur and oxygen are also often difficult to degrade. The extent to which degradation of the important halogenated compounds occurs varies depending on the structure of the molecule and the degree to which it is halogenated (Lapinkas, 1989). The contaminant that is used in this study (phenol), is reported to have been successfully treated bilogically in many occassions. In most of the studies conducted on

phenol biodegradation, pure cultures of microorganisms were used (Radhakhishan, 1974, and Davis, 1991). Radhakhistan et al. in their study have shown that Bacillus Cereus biodegrades phenol and that it can sustain up to 1000 mg/l of phenol concentration. Yang and Humphery (1975) have reported that *Pseudomonas Putida* species can biodegrade phenol up to an inhibition level which they found to be above 100 mg/l of phenol. Pawlowsky and Howell (1973) studied experimentally phenol biodegradation using a mixture of heterogeneous species isolated from soil and activated sludge.

2.10 Dissolved Oxygen Requirement

Dissolved oxygen is needed for the respiration of aerobic microorganisms as well as all other aerobic life forms. Since the rate of biochemical reactions that utilizes oxygen increases with increasing temperature, dissolved oxygen levels becomes critical during summer months. In fixed film biological treatment, the film development is influenced by the molecular diffusion of both substrate and dissolved oxygen (Ju-Chang Huang, 1985). Generally, the maximum biofilm thickness under an atmospheric condition was found to vary from a few hundred microns to several millimeters, depending on the substrate concentration and hydraulic shearing stress (huang, 1985). However, for a thicker biofilm, an aerobic condition cannot be maintained throughout its depth under atmospheric environment. It was further observed by Huang and his co-workers that aerobic biofilm were more effective in oxidizing organic matters than the anaerobic counterpart. In their study, "Biofilm growths with sucrose as substrate" Huang and his co-workers found that whenever the test DO was higher than 16 mg/l, the biofilm texture was loose and porous; therefore air and water were present in the biofilm. On the other hand, when the test DO was at a lower range, the biofilm appeared to be dense in structure without much porosity. They also found in their study that at the high DO environment (16 mg/l), the prevailing microorganisms were short rods, some of which were grouped in a chain. On the other hand, when the DO was reduced to a low level, the prevailing microorganisms were mainly large individual rods, none

of which appeared to be in chain groupings. Huang and his co-workers concluded that the difference in the microbial predominance and its associated metabolic patterns and products are probably responsible for the variations in biofilm density and structural density.

2.11 Effect of Temperature and pH

Temperature affects the rate of all processes occuring in microbes, and it may determine the type of reproduction, morphology, and the nutrients required. The optimum temperature is that at which the growth rate is the greatest. It has been observed that the rate of reaction for microorganisms increases with increasing temperature, doubling with about 10C of rise in temperature until some limiting temperature is reached. According to the temperature range in which they function best, bacteria may be classified as psychrophilic, mesophilic, and thermophilic. Bacteria with optima of approximately 15C and a range from 5 to 30C are called psychrophiles (psychro = cold). Those with optima of 30 to 37C and a range of moderate temperature are mesophiles and those with optima of 55 to 60C and a range from 40 to 80C are called thermophiles (Hattori, 1973).

pH also plays a vital role in the life and death of bacteria,as well as in other microscopic animals. It is a key factor in the growth of organisms. Most organisms can not tolerate pH levels above 9.5 or below 4.0. Generally, the optimum pH lies between 6.5 and 7.5 .

2.12 Need of the Study

The literature review presented shows that there is limited information on the studies relating biological growth in a porous medium and the cosequent reduction in permeability. Essentially no quantitative information is available about the growth of microorganisms in subsurface environment, although data exist about the reduction of permeability of porous media due to growth of microorganisms. This study will emphasize on the quantification of biological growth, during the various stages of the experiment, in the subsurface environment through plate counts and increase in volatile solids due to growth of microorganisms for a given phenol substrate. This study will contribute in the understanding of the dynamics of biofilm growth and substrate utilization on the reductions in permeability.

Chapter III

RESEARCH OBJECTIVES

This proposed research primarily consists of experimental work dealing with removal of phenol through the growth of microbial mass in soil columns. The detailed objectives of the study are given below:

1. Experimental study of the effects of the grain size distribution (0.2, 0.3, 0.4 mm) on microbial growth under contaminated conditions using groundwater and phenol.

2. To determine the effects of three different phenol (15, 50, 100 mg/l) concentrations on the growth of microorganisms in the subsurface environment.

3. To determine the effects of microbial growth on the saturated hydraulic conductivity of the porous medium.

4. To determine the effect of grain size diameter on the biofilm thickness.

It is believed that above work will significantly contribute in the understanding of the dynamics of biological growth, substrate utilization, and permeability reduction of the porous medium.

Chapter IV

MATERIALS AND METHODS

4.1 Description of Columns And Overhead Tank

Fifteen plexiglass columns used in this study were built in the KFUPM central workshop. Each of the columns has an internal diameter of 10 cm, and a length of 50 cm. The top as well as sides are made of 10-mm thick plexiglass sheet. The column reactors were equipped with three ports along its length. Each column is fixed with a perforated plate at the to in order to have a uniform distribution of flow throughout the entire width of the column. Each of the sampling port is also connected to its own piezometer so that spatial distribution of pressure head could be monitored at any time. All these columns were mounted on a wooden bench. A typical column reactor is shown in Figure 4.1.

The size of the head tank is 1.0 m * 1.0 m * 0.5 m. The head tank was also constructed from a plexiglass sheet. Three diffusers were installed inside the head tank to diffuse the pure oxygen in the feed solution stored in the overhead tank. The head tank was kept covered during the experiment. The height of the headtank can be changed from 2.5m to 5.0m. A heavy duty pump (Dynafilo, Davey Products, Australia) of 0.63 KW and 4.6 ampere, was used to pump

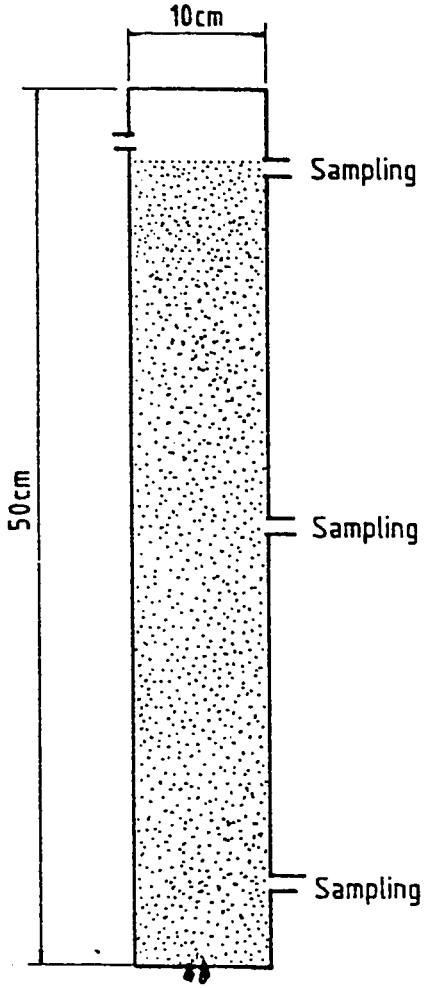

FIG. 14.1

the feed solution from a ground level reservoir to the overhead tank to a fixed water level. Any excess solution was allowed to flow back to the ground reservoir under gravity.

The columns were operated in a down flow mode. Water was pumped from an influent reservoir to an overhead tank, and from where it flowed under gravity to a set of 15 columns. Phenol feed was prepared in a storage tank, from where it was pumped to the overhead tank to a fixed water level. The phenol concentration in the first phase was 15 mg/l, and it was increased up to 50 mg/l in the second phase, and up to 100 mg/l in the third phase.

4.2 Core Sampling

For the determination of the distribution of biomass inside the columns five core samplers were made in the KFUPM central workshop. The core samplers were made from a stainless steel tube. The length of the sample was 50 cm and had an internal diameter of 2.5 cm. On the top of the sampler a 1 mm hole was made to expell the air from the column during the penetration of the sampler into the soil at the time of dismantling. The core comprized of two symmetrically equal sheets of stainless steel bonded together by bolts. After the core sample is taken, it is easy to unfold the two pieces of the sampler without disturbing the sample. Each time, once the core samplers were used, a thin layer of oil was applied inside and outside of the sampler to prevent corrosion problem.

The experimental procedure followed in this study is described below:

4.3 Soil Sample:

The raw sand was collected from SAFWA area (on the way from Dhahran to Ras Tanura) in the Eastern province of Saudi Arabia. Three homogeneous sand samples were sieved according to ASTM method 1980 Sand #1 was obtained by taking those sand particles which passed through sieve #20 and retained on sieve #40 (0.4mm). Sand #2 was obtained by taking sand particles which passed through sieve #60 and retained on sieve #80 (0.2 mm). Sand #3 was obtained by taking a mixture of 50% of Sand #1 and 50% of Sand #2 (0.3 mm).

4.4 Packing And Saturation of the Soil:

In order to simulate field density and to get uniform packing of the soil in the columns, hand compaction was used. To facilitate the workability of the soils, the soil was mixed with a suitable tap water content. This type of packing reduces finer particles present as dusts during the packing of the columns. The compaction was needed to avoid any kind of short circuiting of flow. The compaction was accomplished using round rubber hammer.

4.5 Source of Wastewater

In the present study, the raw sewage used for seeding was taken from North Aramco Watewater Treatment Plant, Dhahran. The raw sewage used as the seed was brought to the laboratory once a week, and was stored in the refrigerated room at 4 oC to retard biological activity. The desired amount of sewage was taken daily from that refrigerated sewage for seeding the columns. Detailed analysis was conducted immediately to determine its characteristics as listed in Table 4.1.

Table 4.1: Wastewater Characterization

Parameter	Average Concen.	Range
BOD (mg/l)	110	80-140
TSS (mg/l)	90	80-120
VSS (mg/l)	70	64-96
COD(mg/l)	200	180-250
Alkalinity (mg/l)	150	120-180
TKN (mg/l)	15	12-25
Total-P (mg/l)	5	4-7
pH		6.9

4.6 Experimental Setup

All experiments were carried out in three phases. The phase I, with feed phenol concentration of 15 mg/l, utilized all 15 columns. The first five columns were packed with 0.2 mm sand, another five with 0.3 mm, and the remaining with 0.4 mm sand. The detailed of all phase are given in Figure 4.2 along with column designations. A1-A5 refers to coarse size sand, B1-B5 refers to the medium size sand, whereas C1-C5 refers to the fine sand. All the columns were packed exactly in the same manner so that the columns can be dismantled at various time periods during the experiment to get the overall profile about the growth of the microorganism within the column.

All these 15 columns were connected to the same overhead tank, from where the feed solution was allowed to flow equally under gravity. During the first week of the operation only raw sewage was fed to all columns in order to develop bacterial culture inside the columns. The raw sewage was continuously oxygenated with pure oxygen at dissolved oxygen concentration of 26 mg/l. After one week the phenol solution was gradually mixed with raw sewage in the ratio of 3 to 1 before applying to the columns. Once the desired level of phenol was achieved in the feed, the application of raw sewage was completely stopped. This was achieved over a period of 5 days. During this total initial period of 12 days, the flow rate, and piezometric pressure were monitored daily. After 12 days the feed was completely switched to phenol solution of 15 mg/l, and regular monitoring of

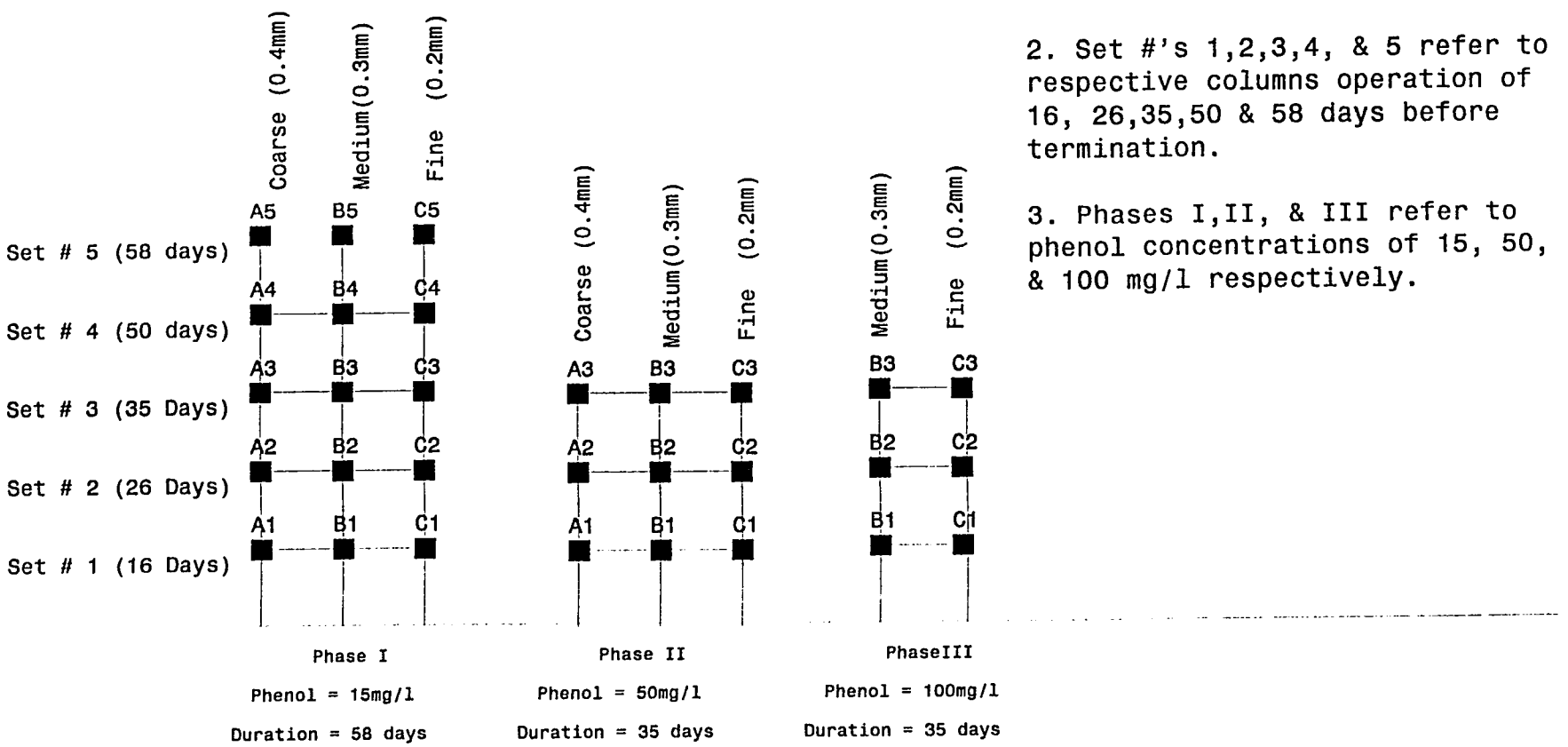

NOTES:

1. Column As, Bs, & Cs refer to the sand types of ccarse, medium, & fine, respectively.

2. Set #'s 1,2,3,4, & 5 refer to respective columns operation of 16, 26,35,50 & 58 days before termination.

3. Phases I,II, & III refer to phenol concentrations of 15, 50, & 100 mg/l respectively.

Fig. 4.2 Conceptual Design of the Experimental Setup.

detailed parameters was initiated. This monitoring included measurement of flow rates through columns, phenol concentration dissolved oxygen concentration, and checking of pH on daily basis.

After 16 days of regular operation, columns A1, B1, C1 were dismantled to determine the profile of volatile solids within the depth of the column. After another 10 days, i.e., 26 days from the start of regular monitoring, another 3 columns (A2, B2, and C2) were dismantled and analyzed. Similarly columns A3, B3, and C3 were dismantled after 35 days, followed by columns A4, B4, and C4 after 40 days respectively. During this period of 40 days the flow rate through colums A reduced from 60 ml/hr to 7.9 ml/hr. In this same period the flow rate through columns B reduced from 60 ml/hr to 6.o ml/hr, whereas for column 5C the flow reduced from 60 ml/hr to 6.8 ml/hr. The last three columns A5, B5, and C5 were dismantled after 53 days when changes in piezometric head and substrate concentration were small with respect to time (steady condition). Phase I was carried out during the period of february-april 1993. All columns of phase II were emptied, washed, and repacked.

Phases II and III with phenol concentration of 50 and 100 mg/l respectively were conducted simultaneously from April to June 1993. Phase II utilized 9 columns out of 15, whereas the remaining 6 columns were used in phase III. C1 to C3 refers to fine sand B1 to B3 to medium sand, and A1 to A3 to coarse sand. In this case only three columns for each sand was used as compared to 5 in phaseI.

This was possible due to the availability of data from phase I. Exactly the same procedure was used in this phase as in the previous one. After one week of feeding of raw sewage, the phenol concentration was increased to 50 mg/l over the period of next 3 days. The regular start of the experiment and monitoring started after 5 days. The first three columns (A1, B1, C1) were dismantled after 16 days , followed by A2, B2, and C2 after 26 days, and final 3 columns A3, B3, and C3 after 35 days respectively. This reduction in time was possible due to the heavy growth of microorganisms within the columns as a result of high concentration of phenol. The final flow rates after 35 days in columns B3, and C3 were 8.7 ml/hr and 4.4 ml/hr respectively. Incidentally the concentration of initial DO was 30 mg/l throughout the duration of phase II.

In phase III with feed phenol concentration of 100 mg/l, only six columns were used. B1 to B3 refers to the medium sand, while C1 to C3 refers to the fine sand. The time of raw sewage feeding is the same as in phase II. The regular start and monitoring started after 3 days . The first two columns (B1 and C1) were dismantled after 16 days, followed by B2 and C2 after 26 days, and final two columns (B3 and C3) after 35 days. The final flow rates after 30 days in columns B3 and C3 were 3.8 ml/hr and 4.6 ml/hr respectively. The concentration of initial DO was 34 mg/l throughout the duration of phase III.

4.7 Analytical techniques:

4.7.1 Substrate Determination

The phenolic solution used in the experiment was buffered by adding 1.3 g/l of KH2PO4 and adjusted to a pH of 7.0. Phenol concentrations were determined daily using Spectrophotometer -21. After the samples are taken from the respective ports of the columns, the samples are filtered using filter paper No 42. After that the pH of the samples are measured and adjusted. The wavelegth used is 269 nm. The minimum detectable quantity is 10 micrograms of phenol when a 5-cm cell and 100 mL are used. The standard calibration curves for the three phases of the experiment are given in Figures 4.3 and 4.4 respectively.

4.7.2 Total Count of Bacteria

Total bacterial count for the sand columns was determined by the method described by Wollum II. Soil samples were collected by using core samplers. Stainless steel core samplers, longitudinally divided into two pieces and held together with fastners and having an internal diameter of 2.5 cm and length of 50 cm, were pushed vertically down into the columns and capped to obtain samples. Two such samples were collected from each column at the end of the every set: one for the determination of volatile solids and the other for total bacterial count.

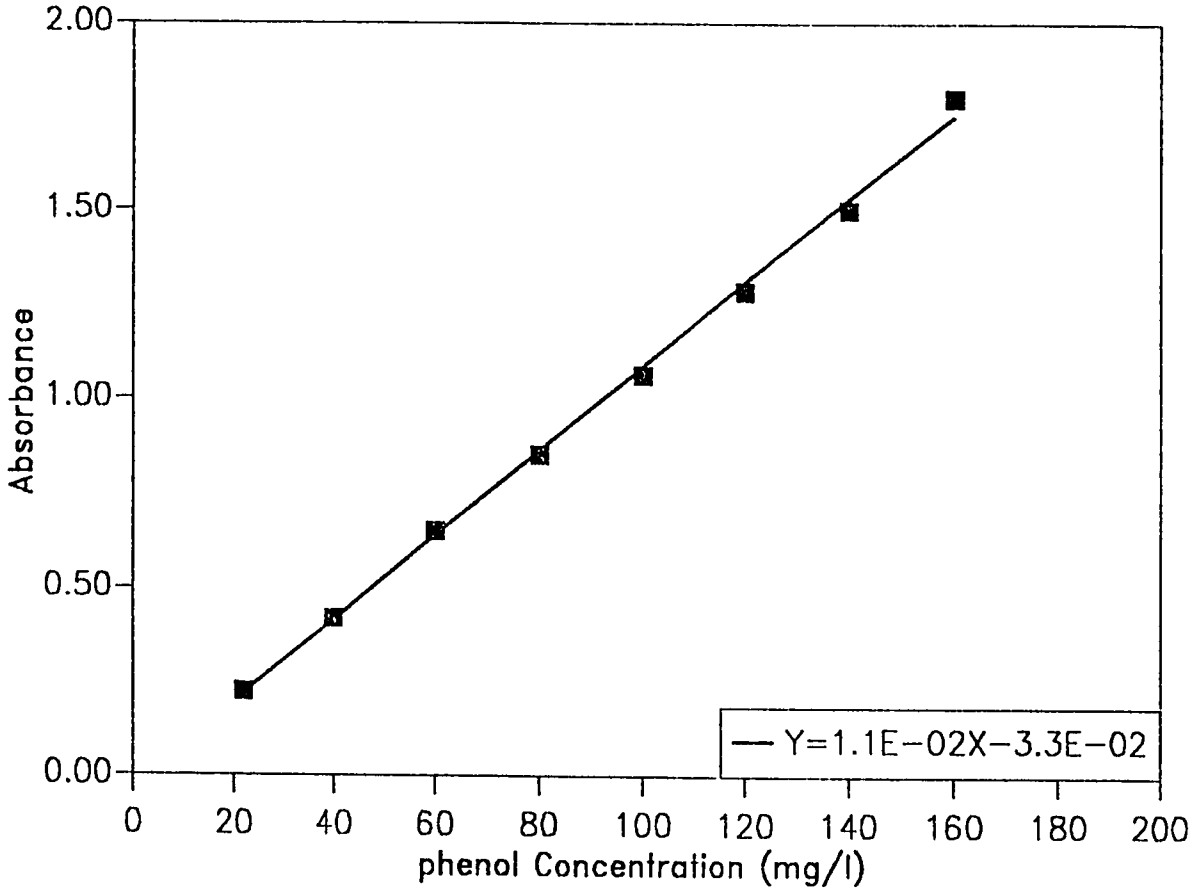

Figure 4.3: Phenol Calibration Curve

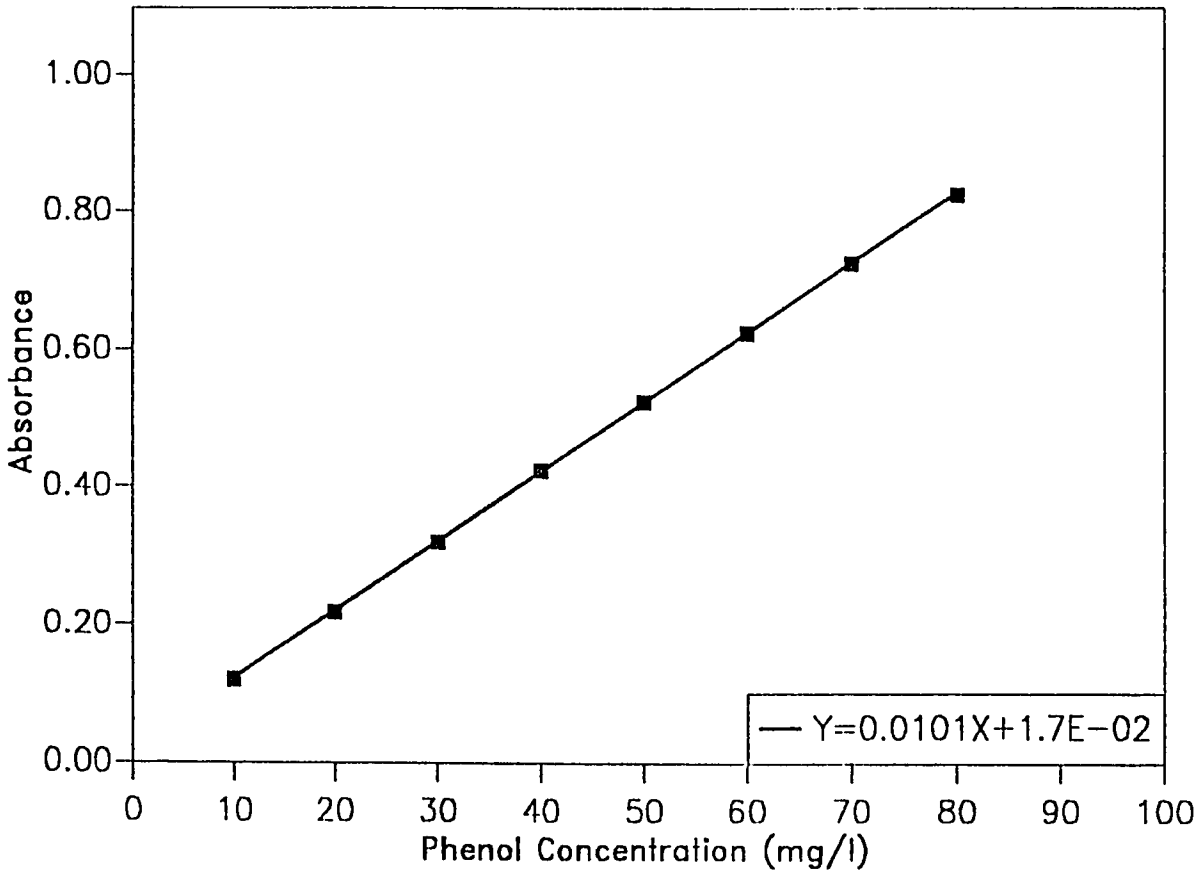

Figure 4.4: Phenol Calibration Curve (Phases II & III)

123

The samples were removed from the core samplers by separating the halves without disturbing the vertical profile of the sample. Since the soil depth in the columns was 35 cm, vertically the sand samples were segmented into seven portions of 2.5 cm depth for the analysis of total bacterial count and volatile solids. The samples were processed immediately after the collection to avoid any significant alterations in their biological properties (Clerk, 1965). Vertically segmented samples were numbered from surface to bottom. Each sample is homogenized to obtain a composite aliquot. The samples were suspended in diluent which in the present context is 10% peptone water. Sterilized 90 ml dilution blanks were made in glass bottles and 10 grams of homogenized sample was suspended in it. The soil suspension was stirred in a shaker for 1 hour. The dilution blank was sterilized at 1.05 kg/cms and 121 oC for 20 minutes in an autoclave.

After removing the sample from the shaker and just before using, the bottles were shaken vigorously. Immediately thereafter, 10 ml of the soil suspension were taken from the center of the suspension to a fresh 90 ml blank. This estabilished the 10^{2} dilution. After a vigorous shaking of the bottles, 10 ml of the suspension was removed as previously described. This sequence was continued until a dilution of 10^{10} is reached.

After that 15 ml of Standard Method Agar autoclaved at 1.05 kg/cms and 121 oC for 20 minutes was distributed in petridishes along with the diluted sample after thorough mixing. Samples were

distributed in three dilutions and in duplicates. The petridishes were then incubated at 35 oC for 24 hours. After the incubation period the dishes were examined under a Colony Counter and the colonies were enumerated. Volumetric values were then converted to colonies per gram of soil. Wherever the growth was found to be less, additional 24 hours more was given for the colonies to emerge. The dilution that yielded 30-300 colonies per plate only were selected.

The composition of Standard Methods Agar is given in Table 4.2

Parameter	Range
Peptone (gram)	5
Beef Extract (gram)	3
Yeast Extract (gram)	1
Agar (gram)	15
Distilled Water (ml)	1000

4.7.3 Volatile Solids

In this study the determination of biomass was accomplished by determining the volatile solids which refer to the portion of solids that evaporate during ignition of the soil sample at 550 C. The fixed solids after the evaporation of the volatile fraction constitute the biomass density. The sampe sampling technique used for total counts is used.

4.7.4 Dissolved Oxygen Measurement

Column influent and effluent dissolved oxygen were measured to check possible oxygen limitations. The influent DO was measured every three days using the Winkler method, whereas the effluent DO Measurements were done daily using Dissolved Oxygen Probe. The DO concentrations at the effluent were always sufficient to prevent oxygen limitations.

4.7.5 Measurement of Hydraulic conductivity:

Hydraulic conductivity were measured using Darcy's law, although in the measurement of any parameter in porous media is affected by a certain degree of uncertainty. The flow rates through the columns were measured daily by collecting the effluent from the outlet tubes into graduated cylinders for a predetermined short period of time. Similarly, several sets of piezometric head were measured daily. To facilitate the cumbersome calculation of hydraulic conductivities using Darcy's law, it was developed a small program which took care of all the steps involved in the calculation of hydraulic conductivity. A sample of this program is given in the appendices.

4.8 Analysis of The Soil

4.8.1 Physical Analysis of the Soil

In this particular analysis a gradation test of the soil is performed. Samples of dry soils, from the three types of soil used in this study, were shaken mechanically through a series of square-mesh sieves with successively smaller openings. Since the total mass of each sample was known, the percentage retained or passed each size sieve was determined by weighing the amount of soil retained on each sieve after shaking. The procedure followed was the one specified by ASTM (1980).

4.8.2 Chemical Analysis of the Soil

The parameters determined in the chemical analysis were the organic carbon present in the soil, the conductivity of the soil, the soil reduction (pH). The methodologies followed in this analysis were taken from Chopra's Book "Analytical Agricultural Chemistry, 1980).

4.8.2.1 Determination of Organic Carbon

For the determination of organic matter or organic carbon in the soil Walklay rapid titration method was used. In this method the soil was digested with chromic and sulphuric acids making use of the heat of dilution of sulphuric acid. The excess of chromic acid, not reduced by the organic matter of the soil, is determined by titration

with standard ferrous ammonium sulphate solution. The reagents involved in this method are Potassium dichromate, Sulphuric acid, Phosphoric acid, Diphenylamine indicator solution, and Ferrous ammonium sulphate.

4.8.2.2 Determination of the Conductivity of the Soil

It is known that all soils contain varying amounts of salts in the soluble form as carbonate, bicarbonate, sulphate, nitrate, etc. The soil may be saline or alkaline depending on the nature and quantity of the salts present. For the determination of the conductivity of the soil it was used conductivity cell. This apparatus was calibrated to read directly the electrical conductance with a given cell.

4.8.2.3 Measurement of the pH of the Soil

For the pH measurement the Glass pH meter was used. 10 grams of soil were added to 25 ml of distilled water and shaken for about 30 minutes. After that the calomel electrode was dipped in the soil suspension. The electrodes were connected to the pH meter which has already been checked with a standard buffer of known pH. The resistance in the external circuit was increased and decreased till the potential of the electric power equalized the potential of the cell containing soil suspension and the galvanometer needle stood at zero. In this moment the pH of the soil was read from the scale.

The results of this chemical analysis of the soil is summarized in the following Table 4.3

Table 4.3 Chemical Analysis of the Soil

Soil Type (Diameter)	pH	Conductivity	% Organic Matter
0.4 mm	7.18	120 uhmos	0.683
0.3 mm	7.20	180 uhmos	1.252
0.2 mm	7.10	740 uhmos	1.407

Chapter V

RESULTS AND DISCUSSIONS

a) Phase I

5.1 Hydraulic Conductivity Reductions

Piezometric head measurements obtained in this study were used to estimate the reduction in hydraulic conductivity due to the growth of biomass in the porous media of the reactors. Flow rates were measured at 24-h intervals. From these data, together with reactor geometry, conductivity values were computed using Darcy's law.

5.1.1 Hydraulic conductivity measurement:

$$Q = k\frac{AH}{L} \tag{5.1}$$

where:

Q = is the flow rate (volume per unit time)

K = is the hydraulic conductivity

A = is the cross-sectional area of the soil column

H = is the difference in piezometric head at the two ends of the soil column.

L = is the length of the column

The flow rates through the columns were measured daily by collecting the effluent from the outlet tubes into graduated cylinders for

a predetermined period of time (24 hours). Similarly, several sets of piezometric head were measured daily. To facilitate the cumbersome calculation of hydraulic conductivities using Darcy's law, a small computer program was developed which took care of all the steps involved in the calculation of hydraulic conductivity.

There is a relation between hydraulic conductivity and permeability. Hydraulic conductivity is related to the fluid and medium properties through the following equation:

$$K = \frac{k\rho g}{\mu} \qquad (5.2)$$

Where

K = hydraulic conductivity

k = the intrinsic permeability of the medium

μ = the dynamic viscosity of the fluid

ρ = the viscosity of the fluid

g = acceleration due to gravity

While the hydraulic conductivity is a function of the properties of the medium and the fluid properties, the intrinsic permeability is a function of the porosity, specific surface area, and tortuosity. The change of porosity or specific surface area will affect the intrinsic permeability and consequently the hydraulic conductivity (Taylor, 1990).

The temporal profiles of the observed conductivity reductions for

all three sand sizes are plotted in Figures 5.1 to 5.3. To facilitate comparison, the data from the last set of dismantled columns is depicted in Figure 5.4. In all the plots there are usually three distinct stages: an initial stage in which the conductivity decreases; a second stage during which the conductivity increases and a third stage where the conductivity decreases again till steady state is reached.

The initial decrease in the hydraulic conductivity is due to the air entrapped in the soil upon wetting which lowers appreciably the conductivity regardless of how the soil is wetted. On highly permeable soils the initial decrease is small, while for relatively impermeable soils it may be appreciable and continue for some time before the second stage of increase is apparent. Another possible reason for the initial decrease in hydraulic conductivity could be due to structural changes resulting from swelling and dispersion of the dry soil upon wetting. This is followed by an increase in hydraulic conductivity due to physical mechanisms which include the release of entrapped air bubbles, the filtration of solid particles suspended in the percolating liquid, and the progressive disintegration of the soil structure (Cunningham, 1991). As the air is dissolved and removed in the percolating fluid, the hydraulic conductivity gradually increases, attaining a maximum value when all of the entrapped air is removed. Finally, the conductivity decreases with time and this is mainly due to the clogging of the pores by microbial cells and their synthesized products and polysaccharides (Vandevivere, 1992). In the early stage of

the experiment, data presented in Figures 5.1 to 5.3 show no significant reduction in conductivity due to insignificant biofilm growth. With time, the clogging propagates into the columns, although conductivities less than 10^{-4} of the original conductivity were not observed in any column.

Conductivity profiles presented in Figure 5.1 after 58 days show that the biomass has penetrated the entire lengths of columns, thus reducing the hydraulic conductivity from the initial value of 10.2 cm/min to a value of 0.0058 cm/min near the end of the experiment. Figure 5.2 depicts the time profile for conductivities of the fine sand. After 58 days of continuous operation the conductivity decreased from an initial value of 2.2 cm/min to 0.0033 cm/min. In case of column B (medium sand), the conductivity profile with time is shown in Figure 5.3. As it is evident from the figure, after 58 days of operation, the conductivity decreased from a clean bed value of 5.6 cm/min to a final value of 0.0034 cm/min.

Similar experimental work was conducted by Taylor *et al.* (1990). They have used sand of nearly uniform size which consisted of grains ranging from 0.59 to 0.84 mm in diameter at a temperature of 15 C. In their study methanol (7.2 mg/l) was used as a growth substrate. Their columns were inoculated by pumping a solution of bacterial culture , 7.2 mg/l solution of methanol, and mineral salts medium through each column for a minimum of 4 hydraulic retention times. They stopped the operation for 1 hour to let the inoculum settle

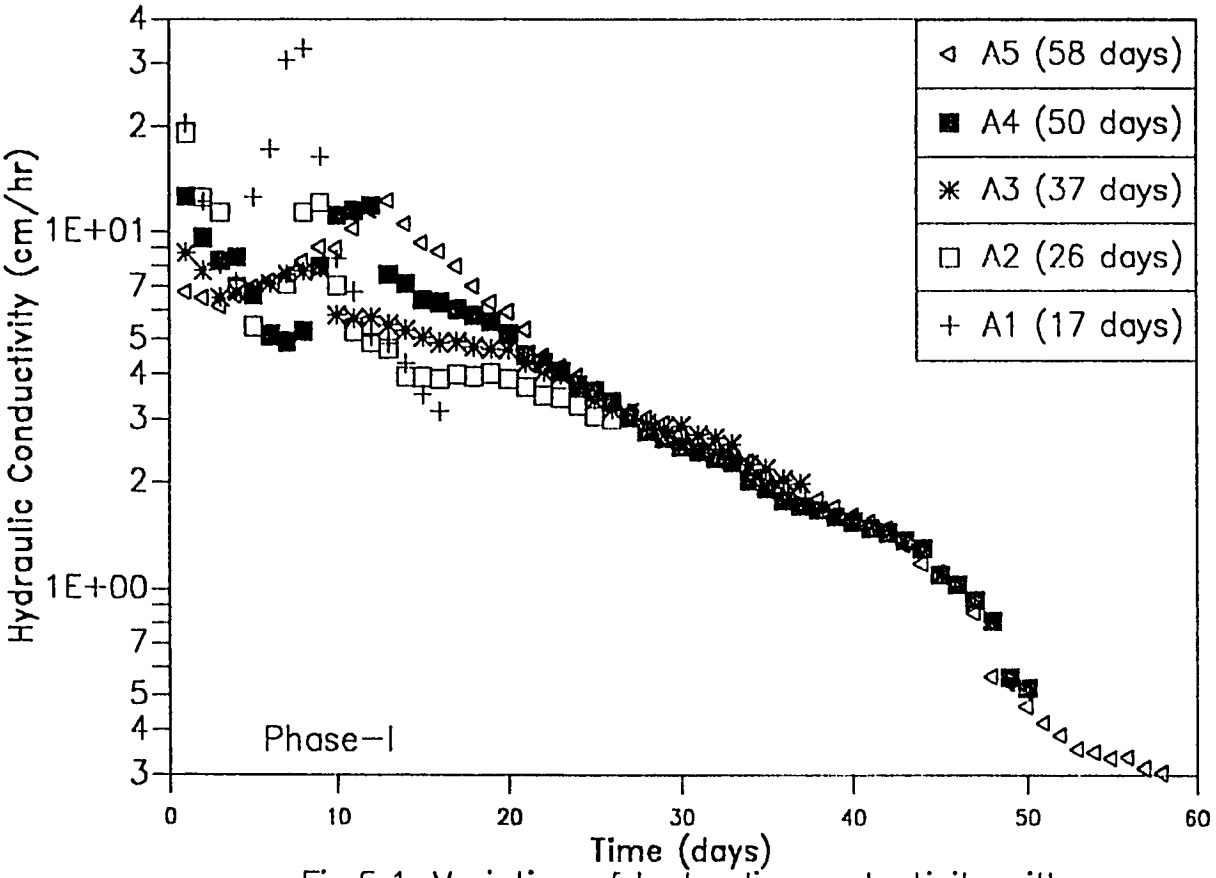

Fig.5.1: Variation of hydraulic conductivity with time through columns A1–A5 in the coarse sand

123

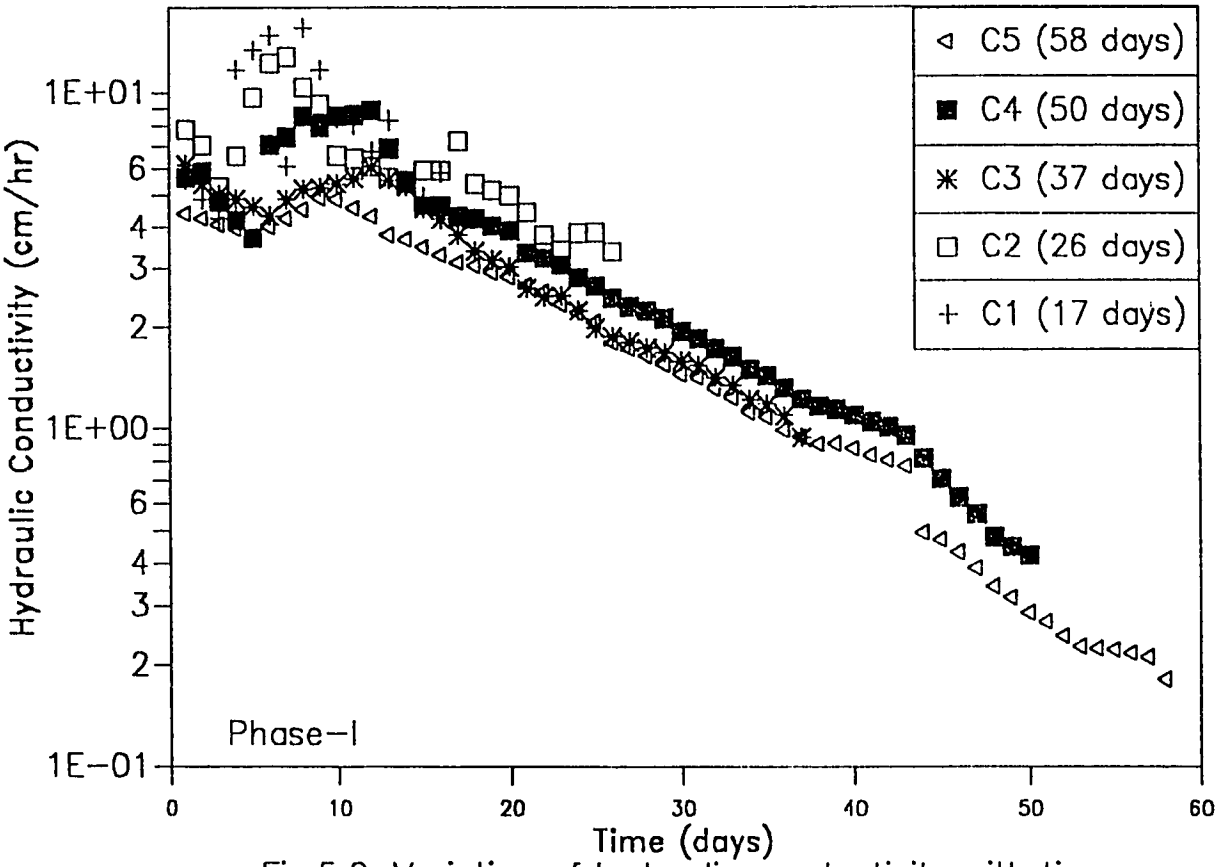

Fig.5.2: Variation of hydraulic conductivity with time through columns C1–C5 in the fine sand

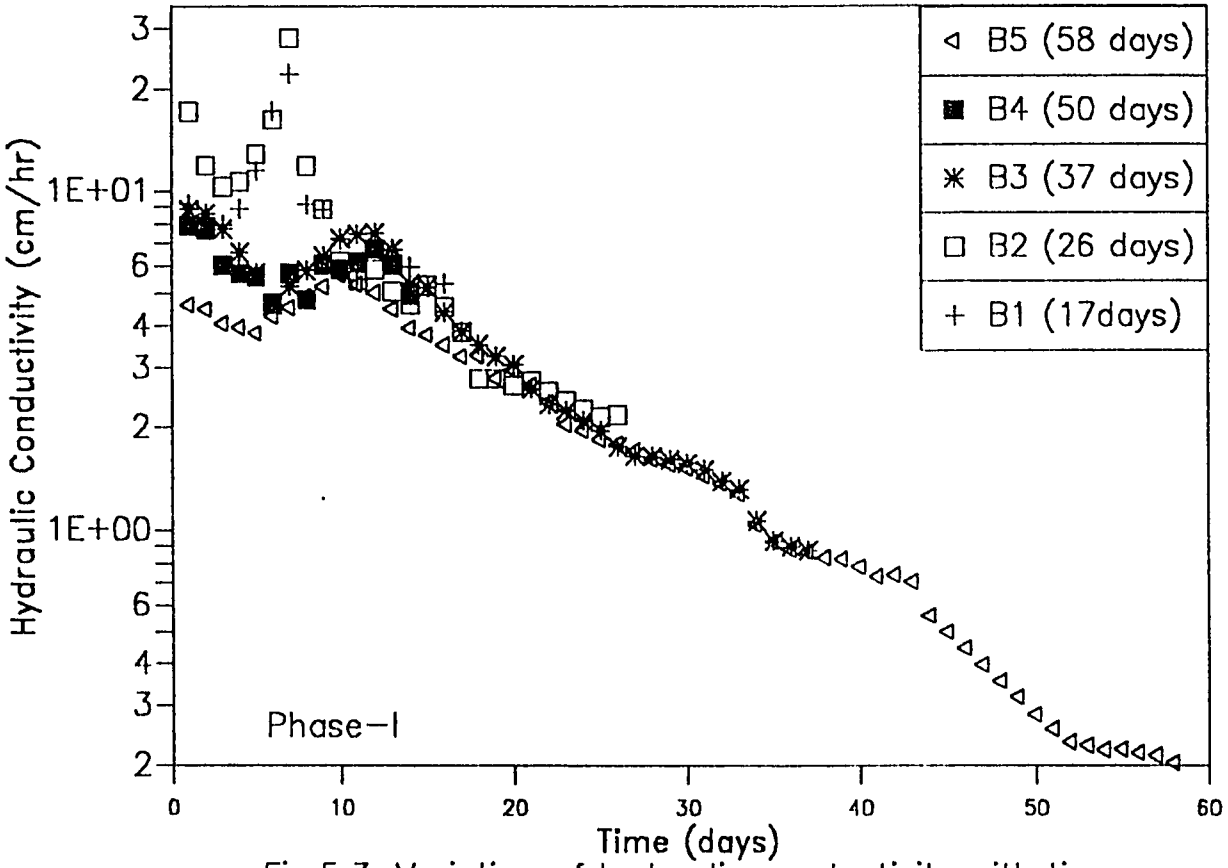

Fig.5.3: Variation of hydraulic conductivity with time through columns B1–B5 in the medium sand

123

onto the soil. Results from their study show that in the first 15 days the hydraulic conductivity decreased from the original value of 15.2 cm/min to 2.5 cm/min, compared to the results of this study where a decrease from an original value of 10.2 cm/min to 0.53 cm/min was achieved. The relatively rapid clogging reported in this study is mostly attributed to the relatively high substrate concentration, although bacterial yields are comparable, and the much higher specific surface area of the medium that consequently retains higher biomass densities. Another possible reason could be that the time for acclimation in this study was much greater (7 days) than in their case (2 days).

Figure 5.4 shows decrease in hydraulic conductivity for three different sizes of sand at the final termination of the columns after 58 days of operation. In the first 10 days, the decrease in hydraulic conductivity was same in the fine and medium size sands. During this time, the hydraulic conductivities in the fine and medium size sand were 0.097 cm/min, and 0.091 cm/min respectively, compared to the coarse sand conductivity of 0.21 cm/min. However, after 58 days of operation, this conductivity in the fine & medium size sands reached a value of 0.0033 cm/min, whereas in the coarser sand it reached 0.0058 cm/min.

These data also show that there appears to be a limit beyond which further reductions are insignificant as reflected by the uniformity of conductivity between days 50 & 58. This could be due to

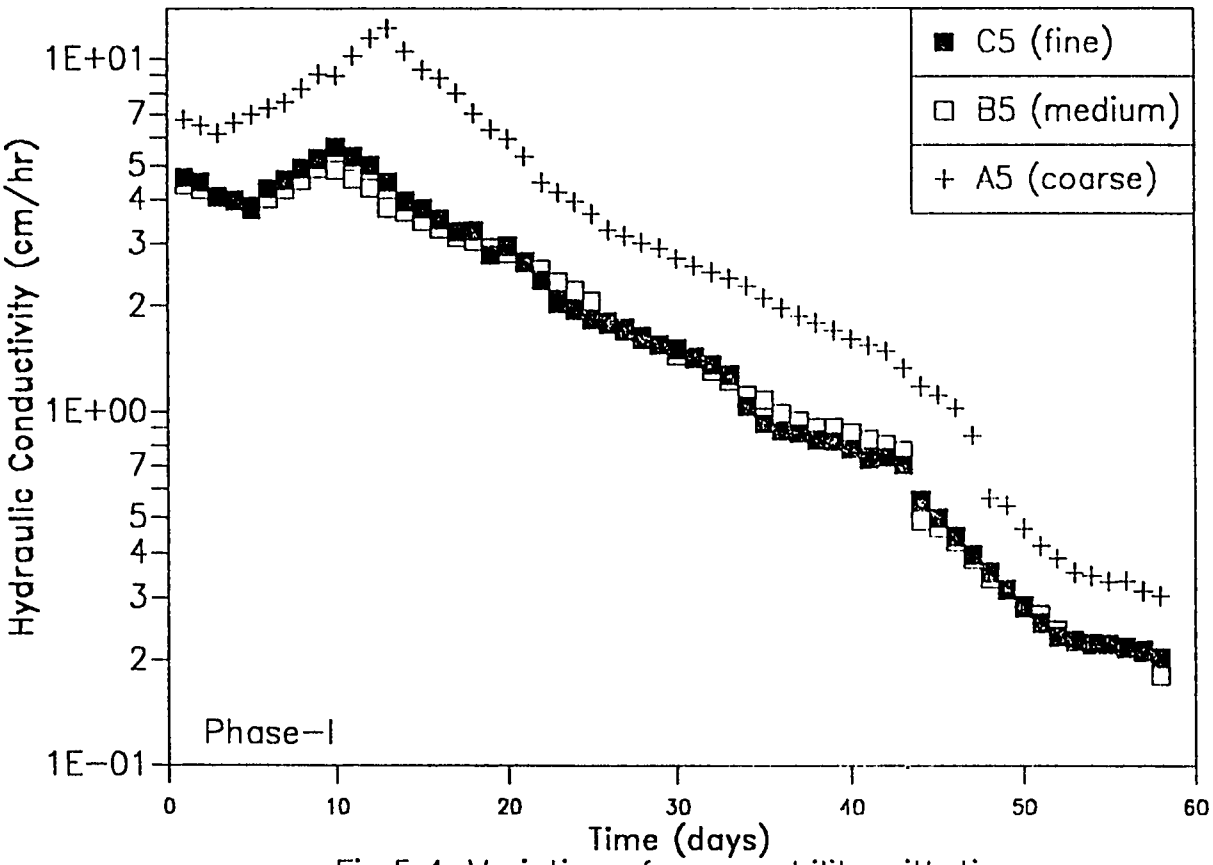

Fig.5.4: Variation of permeability with time through different sizes of sand

123

the fact that the net rate of biomass removal due to shearing and filtration balances the net biofilm growth rate. In the present study, the ratio of the final to initial values of hydraulic conductivity, K/k_0, for the coarse, medium, and fine sand were $5.8*10^{-4}$, $5.9*10^{-4}$, and $1.5*10^{-3}$ respectively.

The findings of this study concur with those of Taylor *et al.* (1990a) who reported a permeability reduction of $K/k_0 = 9.9*10^{-4}$, after 55 days of operation using a uniform size sand of 0.7mm at a temperature of 15 C. The k_0 value in Taylor's study was 15.2 cm/min compared to the values of 10.2, 5.6, and 2.2 cm/min for the coarse, medium, and fine sands respectively. From these results it can be deduced that conductivity reduction is most severe for the fine sand since it has large surface area compared to the other two sizes, and therefore it could accomodate larger number of bacteria.

5.2 Substrate utilization

Substrate concentrations were monitored daily over the course of the column experiments. The profiles for the three types of sand are plotted in Figures 5.5 to 5.8. Figure 5.5 depicts an effluent phenol concentration of 1 mg/l corresponding to a removal efficiency of 93.3% in the coarse sand. Profiles for the other two sizes of sand are shown in Figures 5.6, and 5.7. The phenol removal efficiencies for the fine and medium sizes sand reached 99.3% and 98.6%, respec-

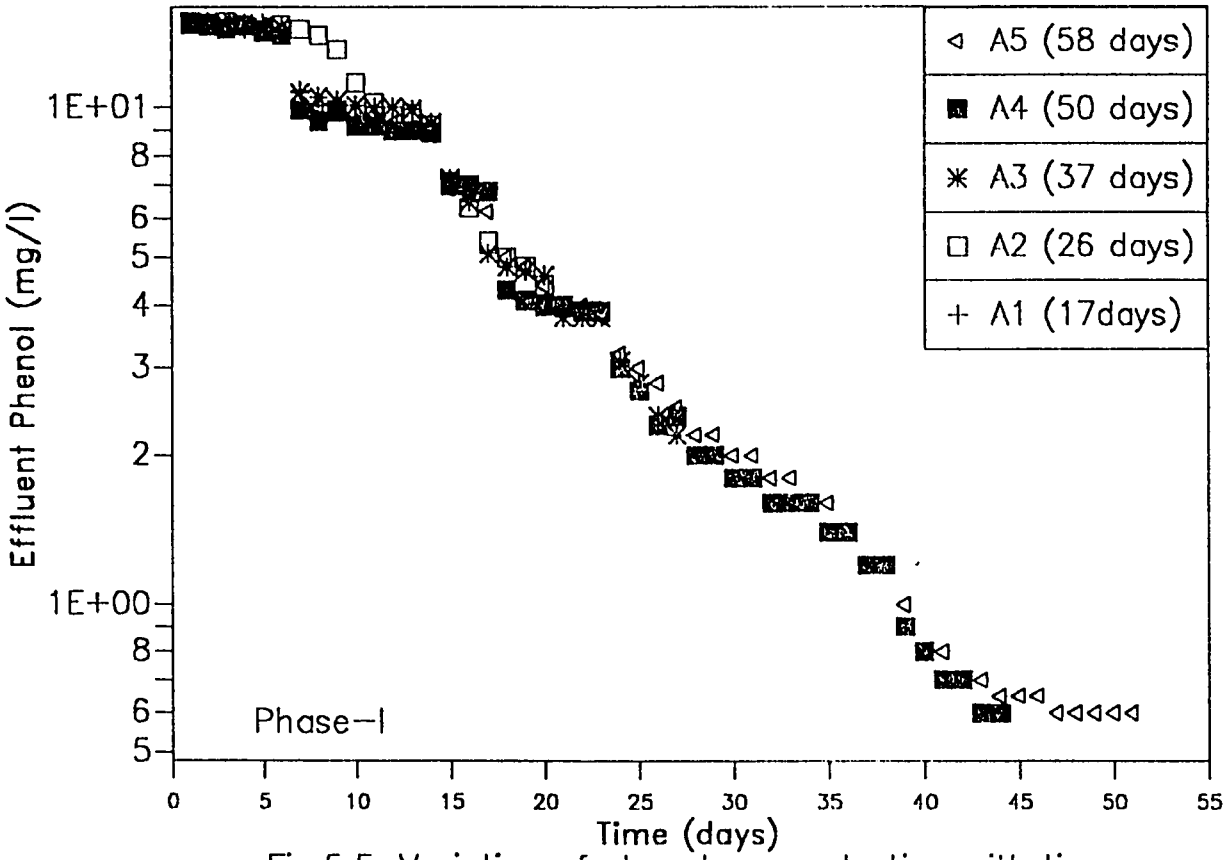

Fig.5.5: Variation of phenol concentration with time through columns A1–A5 in the coarse sand

123

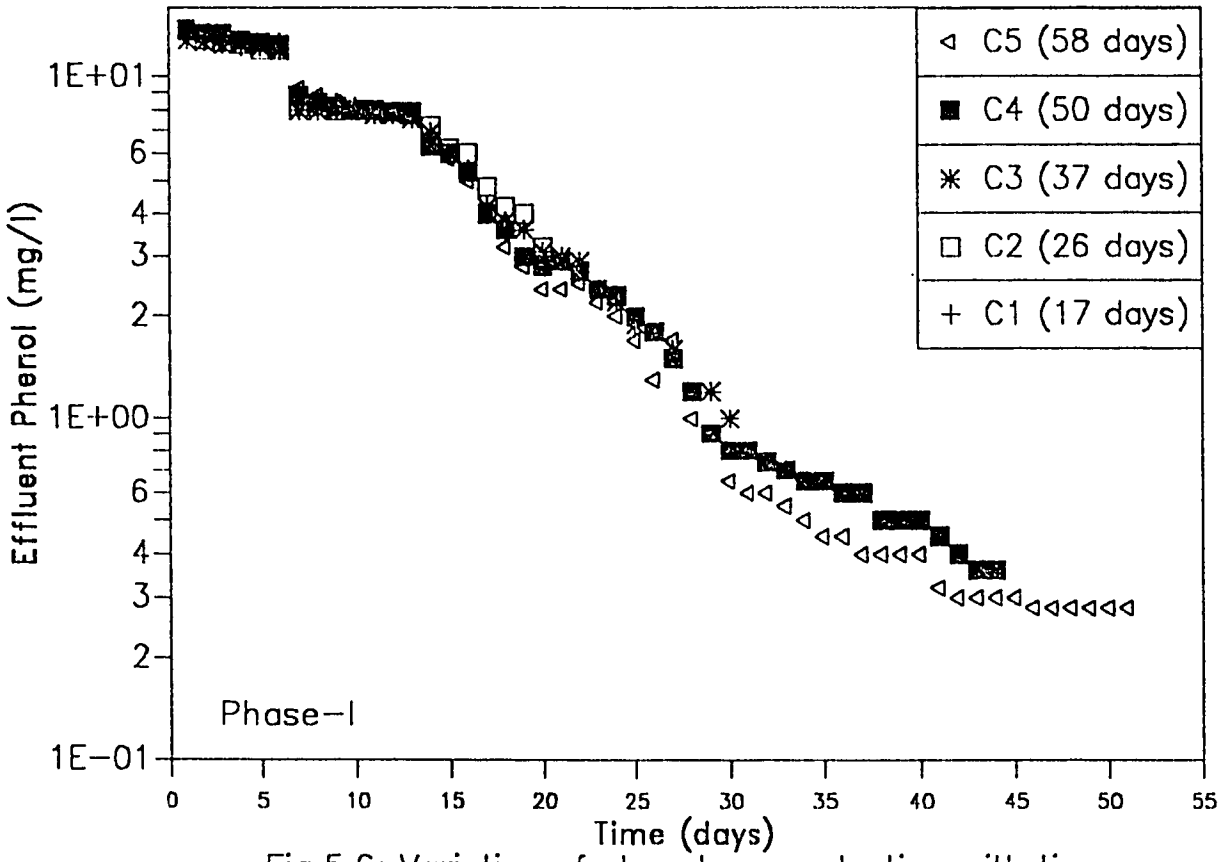

Fig.5.6: Variation of phenol concentration with time through columns C1–C5 in the fine sand

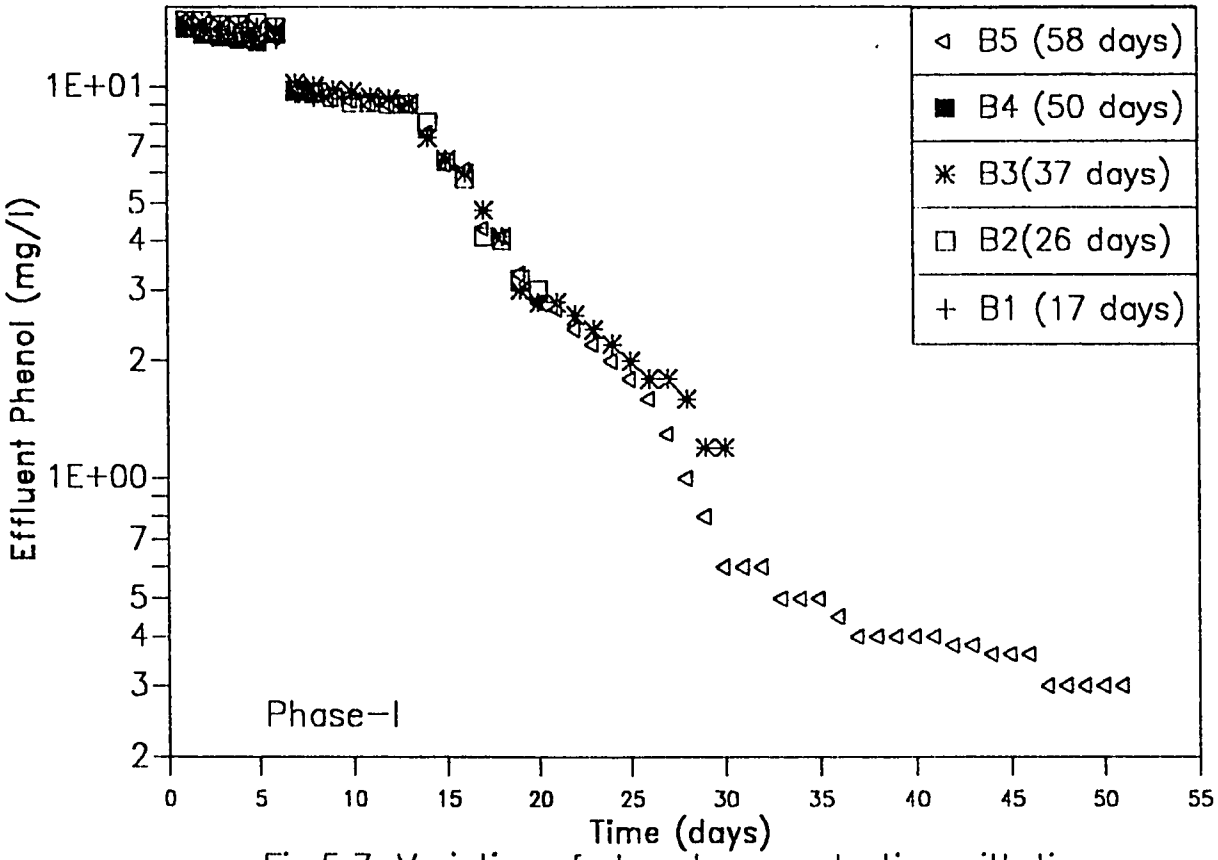

Fig.5.7: Variation of phenol concentration with time through columns B1–B5 in the medium sand

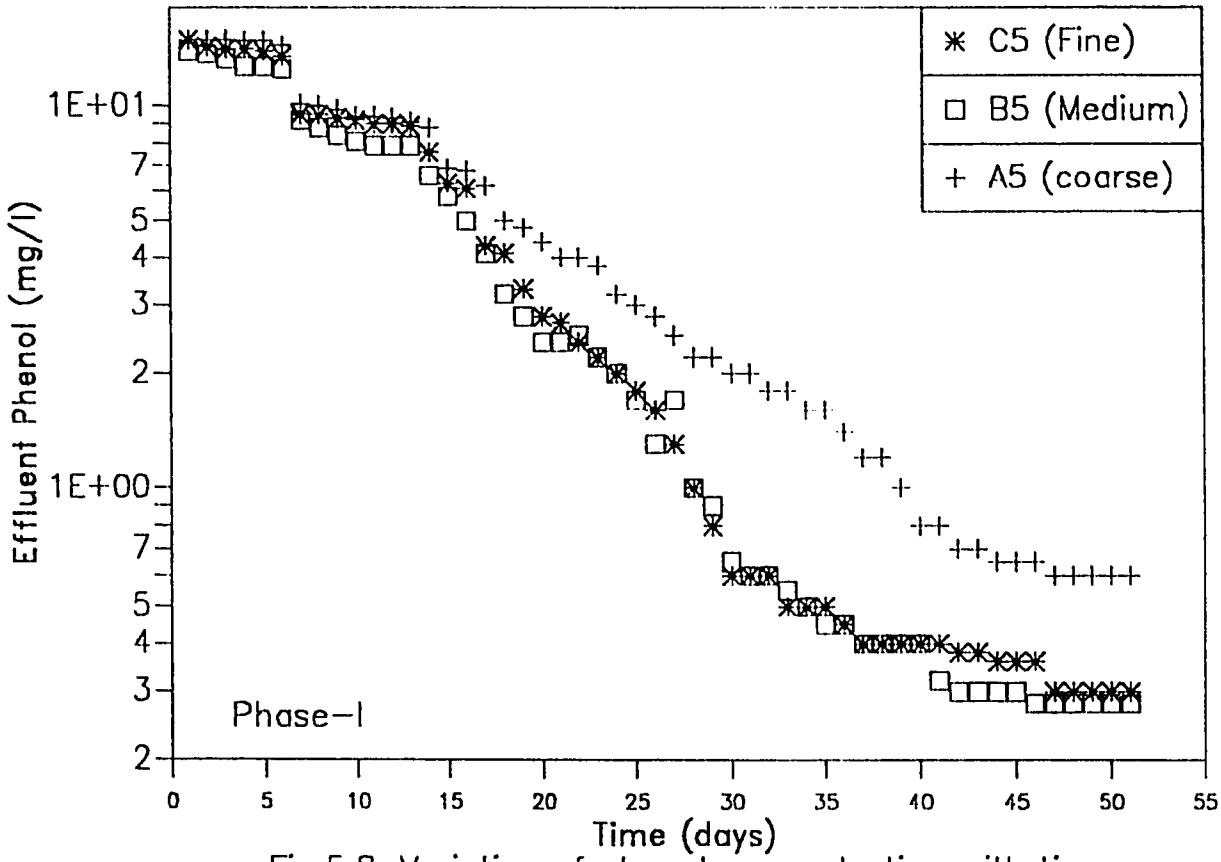

Fig.5.8: Variation of phenol concentration with time through different sizes of sand

tively.

Taylor *et al.* (1990a), have plotted substrate (methanol) profiles with depth at selected times. Their data show that after 196 days from the start, the substrate removal was 94%, whereas in this study, after 58 days, the removal was 99.3% for the fine sand. Again, this difference could be primarily due to the same reasons given earlier.

Figure 5.8 displays the variation of effluent phenol concentration with time through columns of three different sizes of sand. It is apparent from the figure, after 58 days of operation, the removal efficiencies were 99.3% in the fine sand, 98.6% in the medium size sand, and 93.3% in the coarse sand, and also the fine and medium size sand reached the steady state before the coarse sand. This is due to the difference in surface area which exists among the three sands. The estabilishment of steady-state effluent phenol concurs with the uniformity of hydraulic conductivity after day 50, depicted in Figure 5.4.

5.3 Volatile Solids

Volatile solids were determined to measure the biological growth. During the various stages of this study, a set of columns was dismantled. A total of 14 samples were thus taken from each column and their contents were assayed for volatile solids determination. The spatial distributions of the volatile solids of each column are

given in Figures 5.9 to 5.12. The data show the volatile solids to be a decreasing function of column depth, and depict the higher density of biomass at the inlet due to easy availability of the substrate.

Figure 5.9 shows the variation of volatile solids with depth through coarse sand (A1 to A5). Initially, for the first two weeks, very low biomass is observed in the lowest 5 cm of the columns, giving rise to a high volatile solids concentration gradient between top and bottom of the soil reactor. At the same time substrate removal efficiency is very low with effluent phenol concentration approaching the influent. Thus a more uniform distribution of biomass is expected. However, nonuniform seeding and relatively poor acclimatization at this short time may lead to the uneven distribution of biomass. After 58 days of operation, the biomass density at the top and bottom sides of the fifth column (A5) reached a value of 9.2 mgVSS/g, and 4.04 mgVSS/gr.of soil, respectively. At the same time biomass density variations between the top and bottom ranged from 11.2 to 6.2 mgVSS/g in the medium sand and from 11.8 to 6.2 mgVSS/g in the fine sand. It is interesting to note that following the establishment of high biomass concentrations at the inlet initially, biomass detachment due to high shear stresses combined with increased biomass transport downwards as a consequence of higher pore velocities tend to more evenly distribute the biomass inside the reactor with time.

Taylor *et al.* (1990a) also plotted the spatial distribution of the

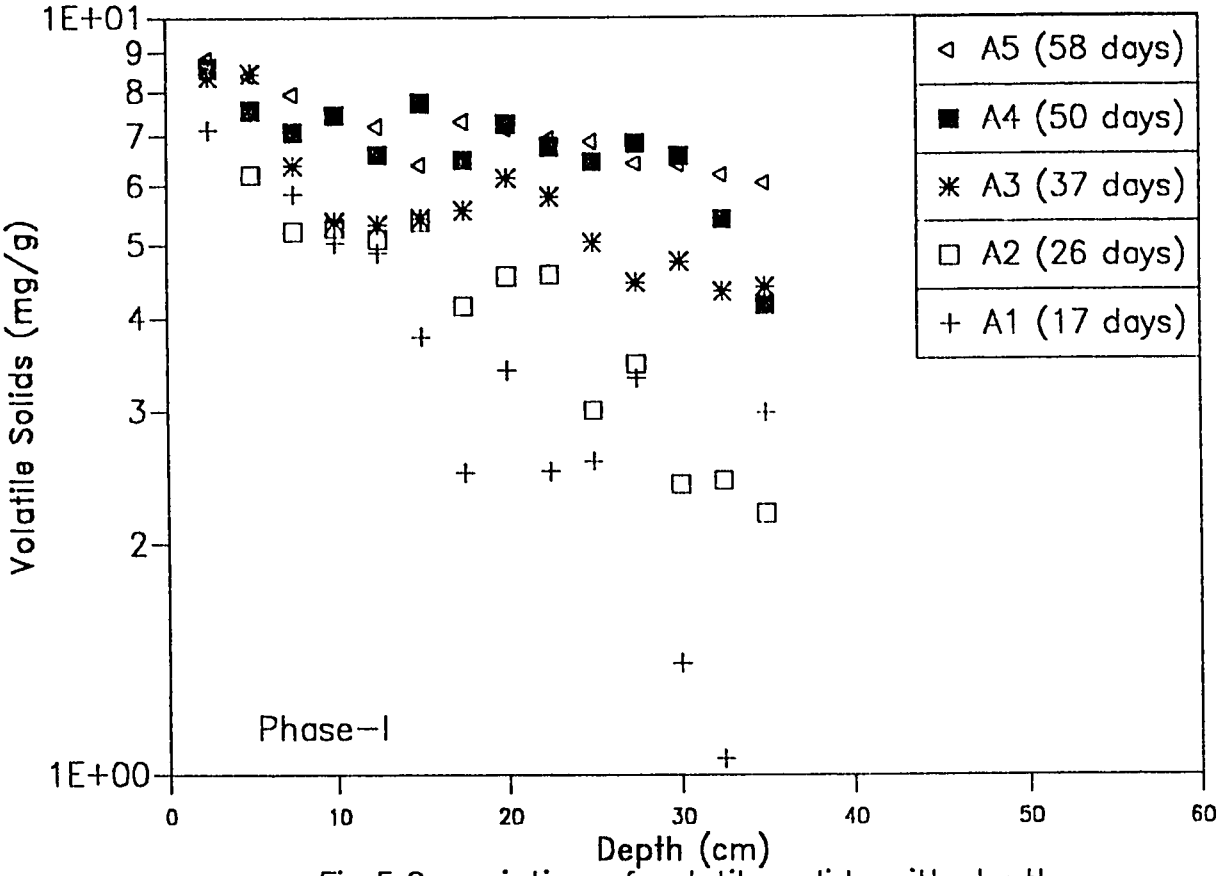

Fig.5.9: variation of volatile solids with depth through columns A1–A5 in the coarse sand

biomass in their two reactors which were dismantled at the end of the experiment (196 days). They did not simultaneously monitor the time and spatial distribution of biomass contained in the porous medium at intervals of time as has been done in this study (see Figures 5.9-5.12). The maximum bacterial density found in their study was 1.25 mg/g of soil (size of sand used was 0.7-mm), whereas in our case, for the coarse sand, it is around 9.2 mg/g of sand. The relatively very low hydraulic conductivity levels observed in this study in comparison with Taylor's work are therefore explained by the high bacterial density which was more than 7-fold that of Taylor *et al.* (1990a). A comparison of the steady-state flow rate and substrate removal rate may provide an explanation for the widely discordant volatile solids data. Methanol removal rate ranged from 30-61 mg methanol/day compared well with the 48 mg phenol/day in this study. Although the substrate yield coefficients of 0.53 mgVSS/mg phenol (Nakhla and Harazin, 1992) and 0.52 mgVSS/mg methanol (Chudoba,1988) compare very well, the much higher decay rate for methanol utilizing organisms and the much higher biological SRT result in observed yield that vary about one order of magnitude. Temperature effects and specific surface area effects tend to accentuate biomass differences.

The variation of volatile solids with depth through three different sizes of sand is shown in Figure 5.12. As it can be noticed from the figure, at the bottom of the columns, the volatile solids in the finer and medium size sand have the same value of 6.2 mgVSS/g, compared

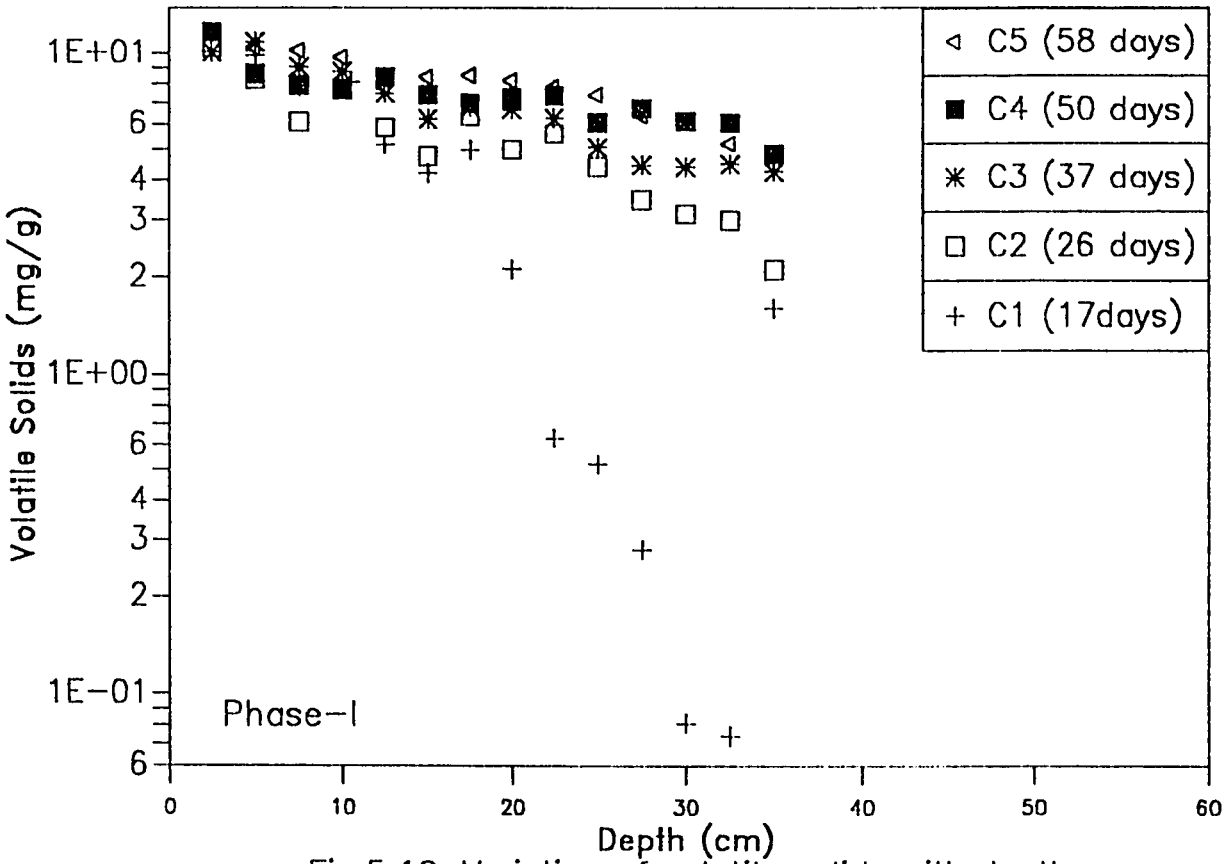

Fig.5.10: Variation of volatile solids with depth through columns C1–C5 in the fine sand

123

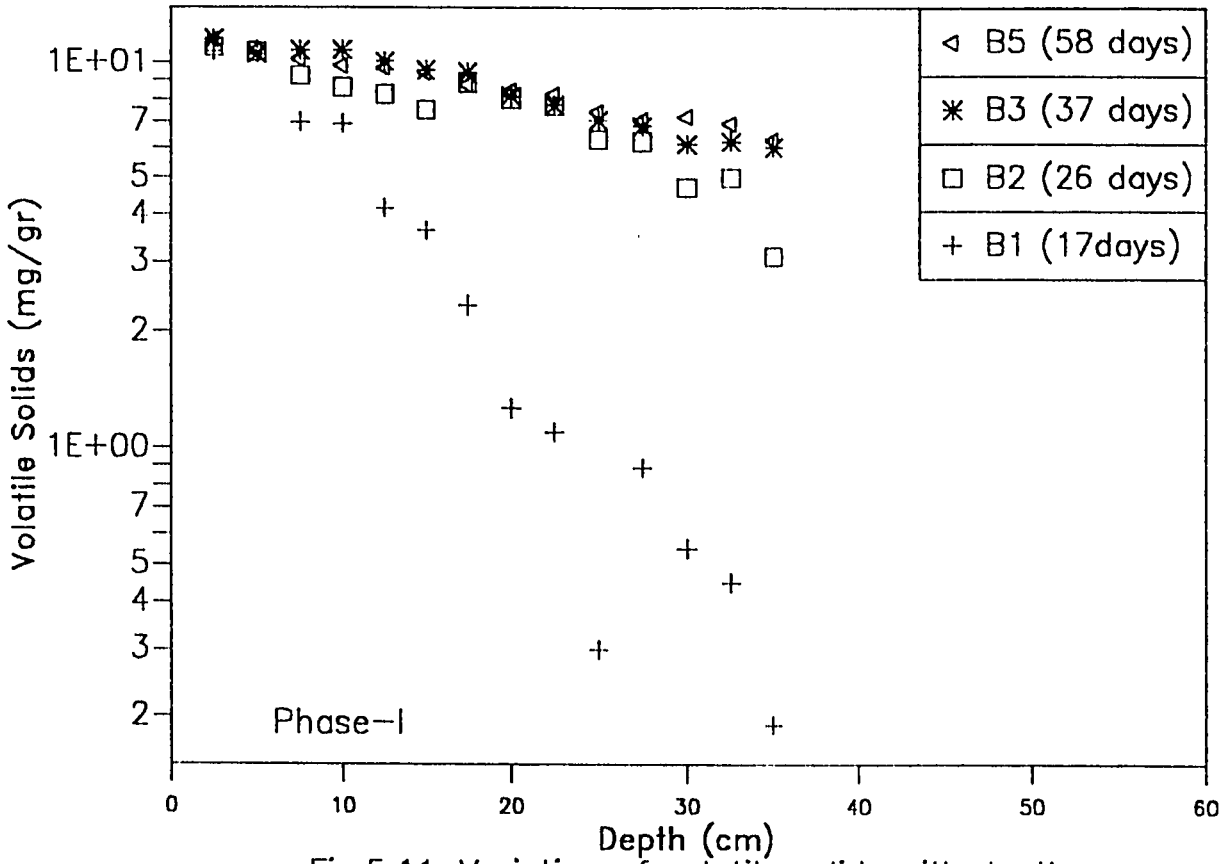

Fig.5.11: Variation of volatile solids with depth through columns B1–B5 in the medium sand

123

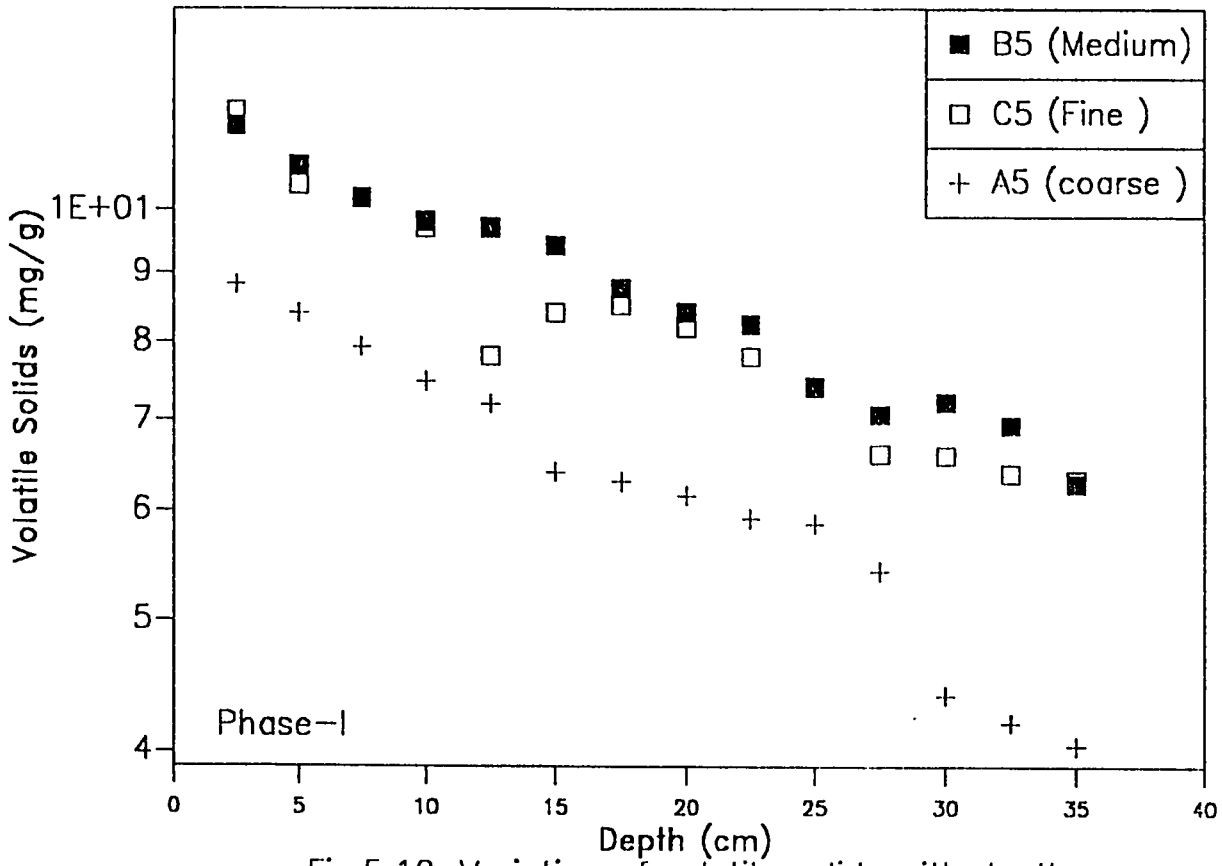

Fig.5.12: Variation of volatile solids with depth through different sizes of sand

123

to the coarse sand which has a value of 4.04 mgVSS/g of sand. The observed variations in volatile solids are entirely consistent with the final permeability reduction profiles discussed previously (Figures 5.1-5.4), and obviated by the specific surface area of the different types of sand used in this study.

5.4 Total Count of Bacteria

Figures 5.13, 5.14, 5.15 display the total counts in all 15 columns for the three sizes of sand. The data depicted in Figures 5.13-5.15 clearly demonstrate the increased active microbial density with time for the three sizes of sand. The highest active microbial density after 58 days of operation at the top 5-cm of the columns were $2.8*10^{13}$,$2.88*10^{13}$,and$2.92*10^{13}/ml$ in the coarse, medium, and fine sands respectively, while the lowest values at the bottom 5-cm were $1.48*10^{13}$,$1.56*10^{13}$,and$2.06*10^{13}/ml$ in the coarse, medium, and fine sands respectively. Therefore no significant difference in active microbial density existed between the three sand sizes in light of the precision of total count analysis. This corroborates the identical phenol removal efficiencies discussed earlier. However, the spatial distribution of active microbes is particularly interesting. In contrast to the volatile solids profiles, initially a rather uniform distribution of total counts is depicted by data of columns A1, B1, and C1. Furthermore with time, a rather uneven spatial profile of active microbial density is observed in all sizes, consistent with the high substrate removal efficiencies and substrate utilization kinetics. Microbial

activity at low substrate concentrations near the column effluent contribute to the low measured values of total counts.

A scrutiny of the volatile solids and total counts data reveals this contrast quite vividly. Therefore, while substrate utilization kinetics do not postulate an explanation for the observed volatile solids profile, the total counts, a measure of viable microbial density, conforms to the substrate patterns. It appears that initially inactive bacterial cells represented a higher proportion of total biomass at the top, though diminishing with time. The opposite is true for biomass at the outlet. With continued operation, inactive cells which are more readily detached (Robinson *et al* 1984) are transported and attached downwards. Additionally, biomass decay at low substrate concentration contributes appreciably to the build-up of inactive cells at the lower sections of the column reactors. It can be concluded that volatile solids and total counts are both very important parameters to be monitored, since permeability reduction is better indicated by volatile solids while total counts is more pertinent to understanding the fate of the pollutant in the aquifer. Although the time and spatial profile of volatile solids and total counts do not match very closely; however, at pseudo-steady state condition, a correlation between the two has been observed. The detailed calculations are given in the following table 5.1:

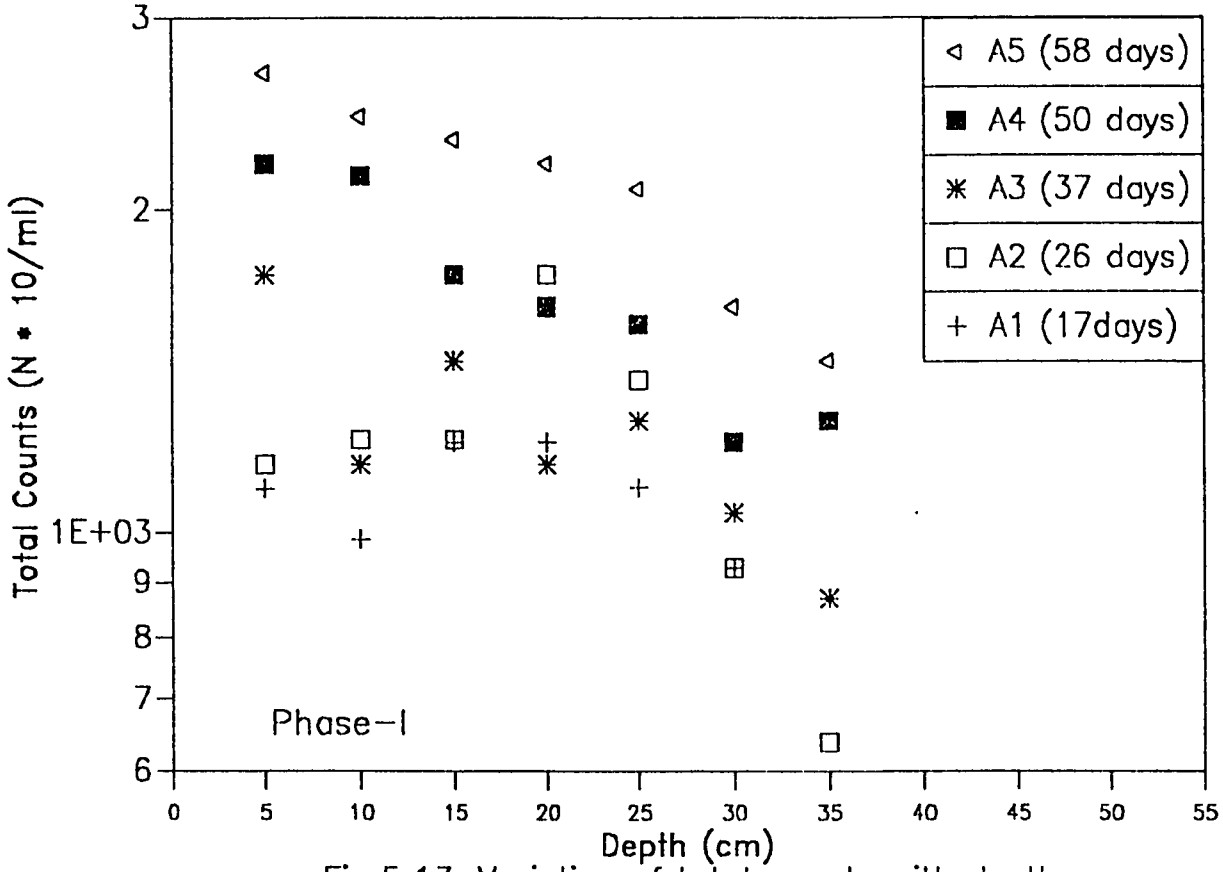

Fig.5.13: Variation of total counts with depth through columns A1–A5 in the coarse sand

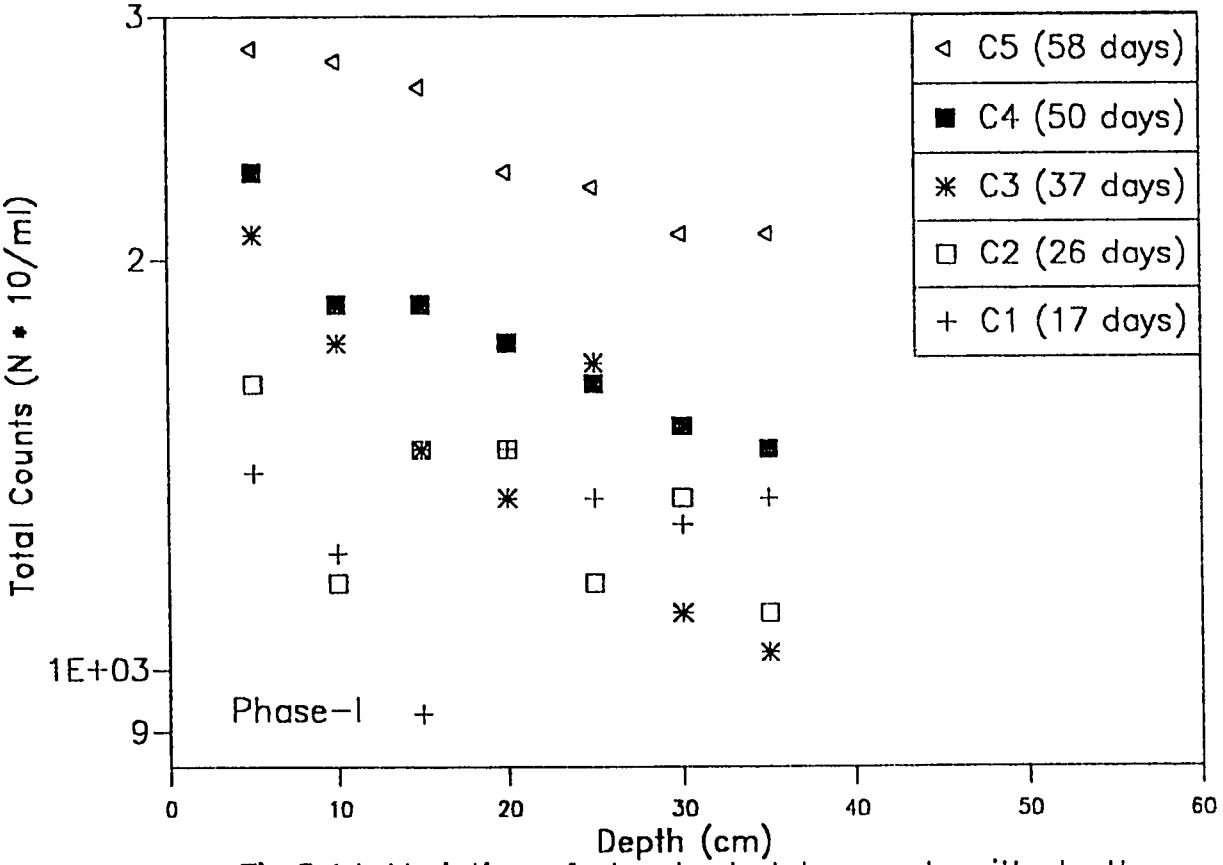

Fig.5.14: Variation of standard plate counts with depth through columns C1–C5 in the fine sand

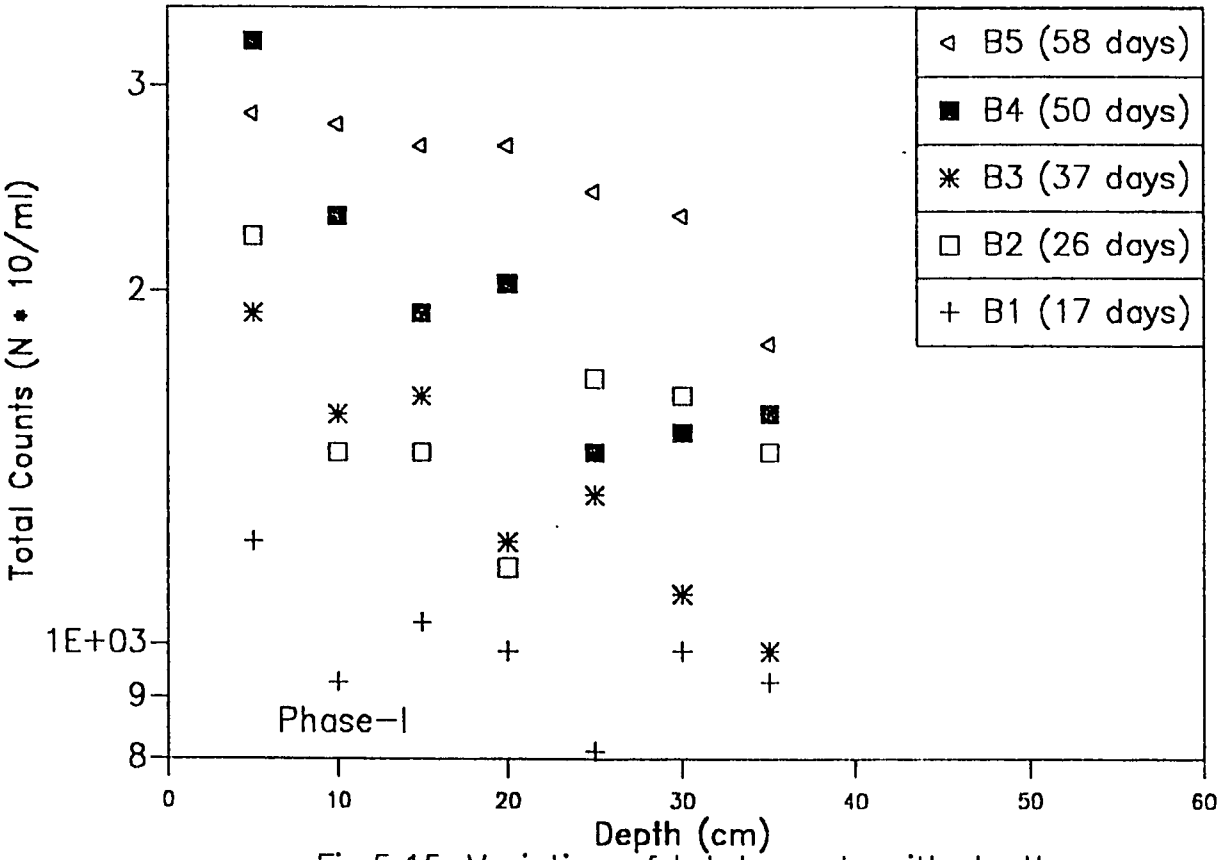

Fig.5.15: Variation of total counts with depth through columns B1–B5 in the medium sand

123

Table 5.1: Ratios of Volatile Solids & Plate Counts after 58 days for different sizes of sand

Soil Type (Diameter)	K1	K2	K= K1/K2
0.4 mm	2.04	1.89	1.08
0.3 mm	1.81	1.85	0.98
0.2 mm	1.90	1.42	1.33

K1 is the ratio between the volatile solids at the inlet and outlet of the columns, and k2 is the ratio between the standard plate counts at the inlet and outlet of the columns. Nutrient salts were added periodically to the system to ensure that phenol was the growth-limiting substrate. The composition of the nutrient salts is given in Table 5.

b) Phases I, II, III

5.5 Biomass Growth and Substrate Removal

Figure 5.16 to 5.18 depicts the spatial distribution of biomass through fine sand after 16, 26, and 35 days, respectively, for phases I-III. A comparative look at the data in Figure 5.16 reveals that the initially very high biomass density gradient between top and bottom dimished with time in all three phases of the study. This biomass redistribution phenomenon has been elaborately discussed earlier in the chapter. The interesting aspect of it however, is its dependence on substrate concentration. A relatively more uniform distribution of biomass is exhibited in the sand reactor treating 100 mg/l of phenol vis-a-vis the one treating 15 mg/l after 35 days. While high biomass densities at the bottom of the reactor is obviated by the relatively higher effluent substrate concentrations, biomass shearing of the thick biofilm at the column influent contributes significantly to transport of microbial cells down the soil reactor.

A very important observation is apparent in Figure 5.17, i.e., the biomass density at the top 10 cm of the sand column is initially independent of the substrate concentration, but displays some dependence there after (Figure 18). Although phenol biodegradation has been observed to follow both the Monod non-inhibition model (Brown et al; 1990) as well as the Haldane self-inhibition model (Rozich et al; 1985), the Haldane inhibition concentration is much greater than 100 mg/l and thus identical biomass densities at ambient phenol

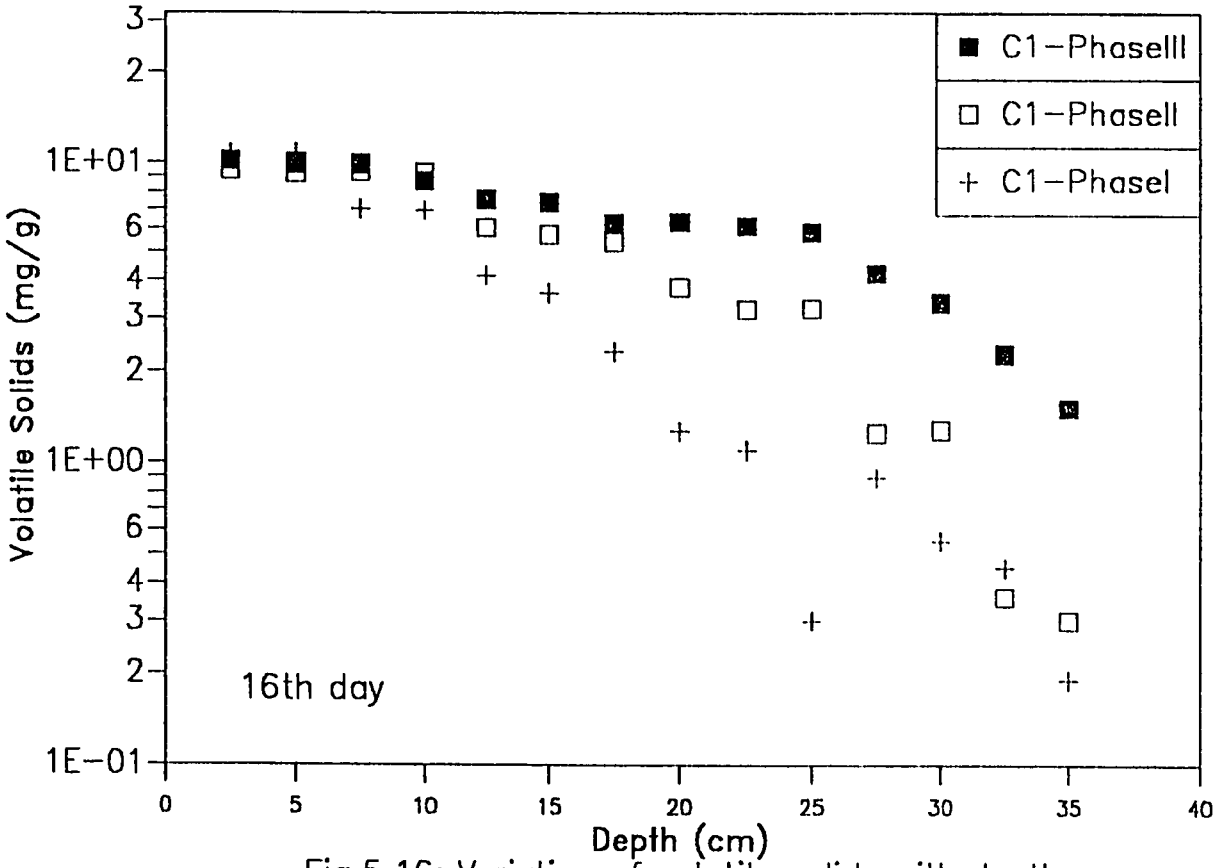

Fig.5.16: Variation of volatile solids with depth through fine sand of 1st set of three phases

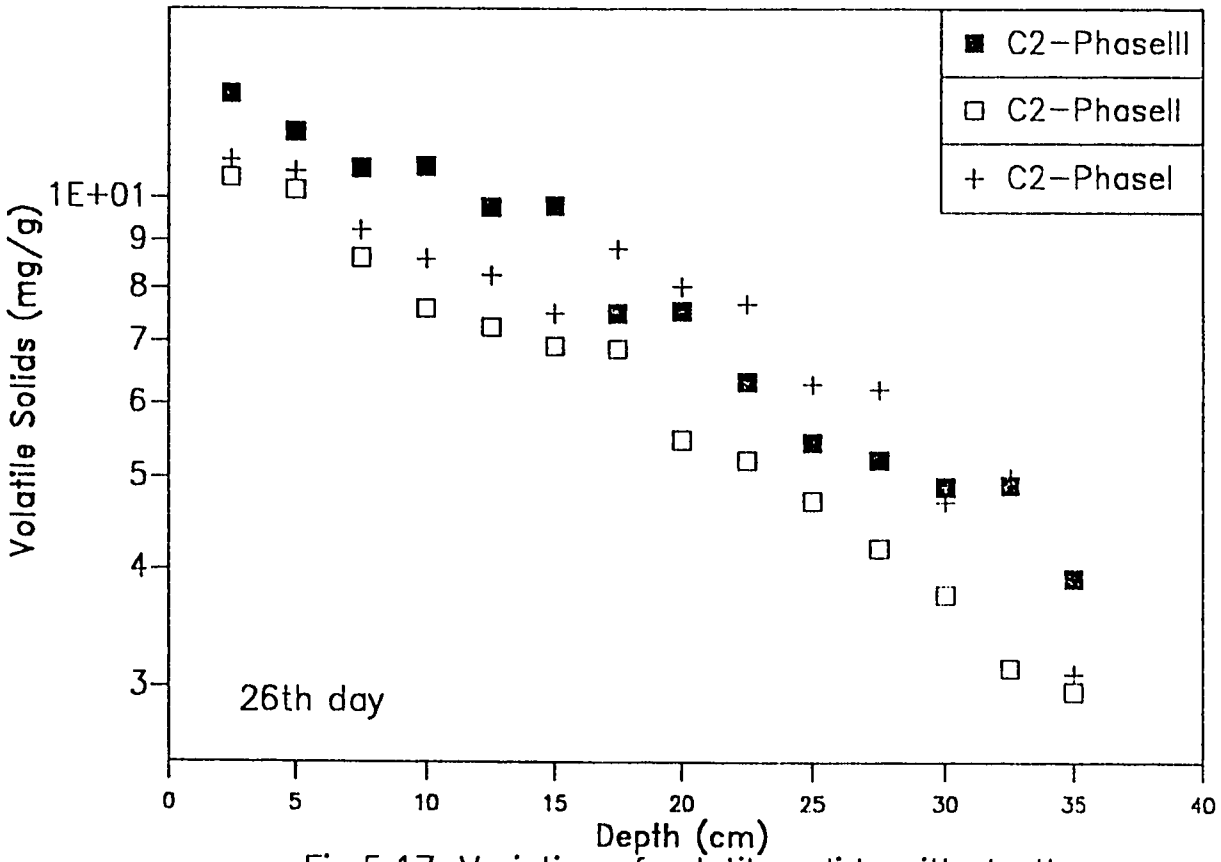

Fig.5.17: Variation of volatile solids with depth through fine sand of 2nd set of three phases

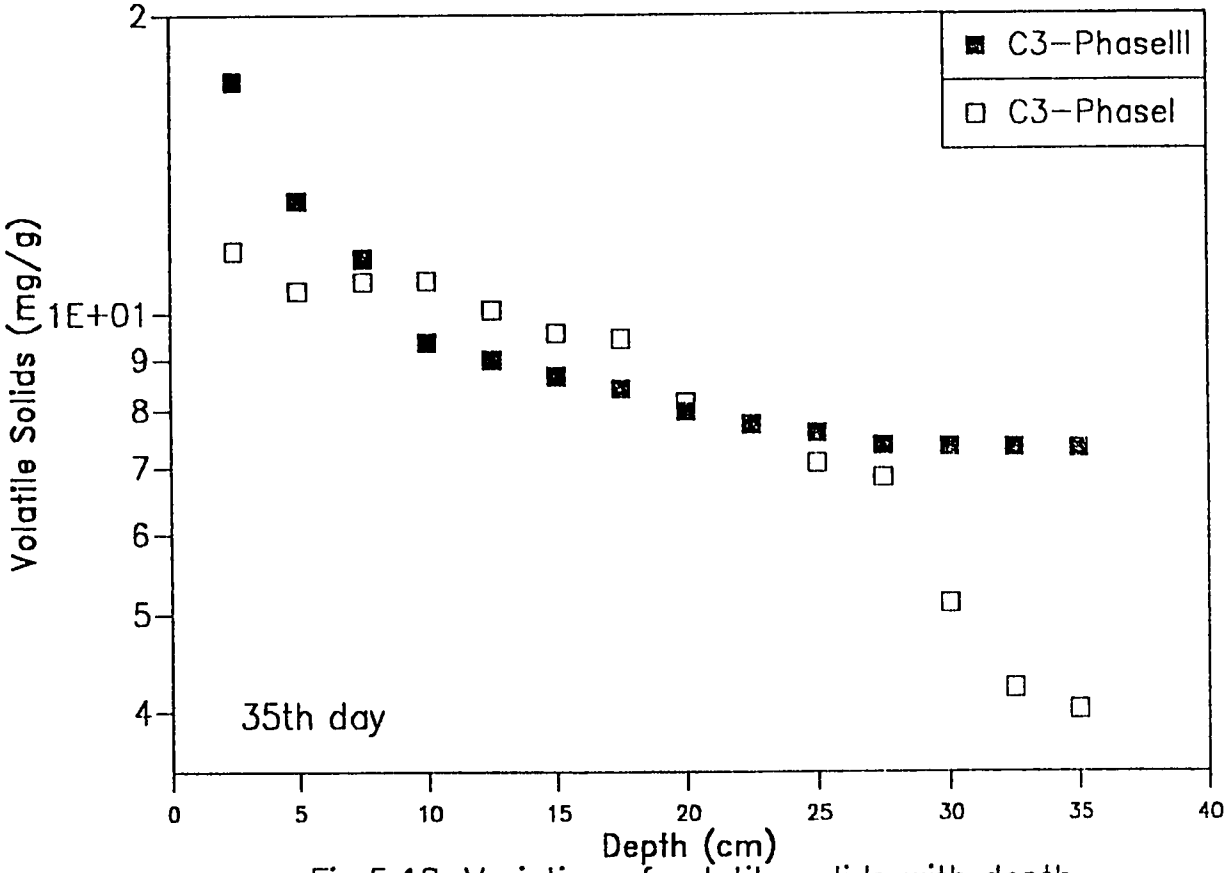

Fig.5.18: Variation of volatile solids with depth through fine sand of the 3rd set of two phases

concentrations varying from 15- 100 mg/l can not be explained by inhibition. Furthermore, had inhibition accounted for this biomass limitations, the picture would not have changed over time. Although diffusion of oxygen has been implicated in limiting microbial biofilms growth rates when substrate concentrations are normally greater than 9 times the dissolved oxygen (Williamson & McCarty, 1976), an investigation of this possibility for this case when phenol concentration is about 3.5 times the DO is highly merited. Oxygen limitation is likely to occur when $S_0/S_p < D_{fp}*V_o*MW_o/D_{fo}*V_p*MW_p$

The subscript o denotes oxygen and p denotes phenol, Df is the diffusivity inside the biofilm ($L^2T^{1)}$, Mw is the molecular weight and v is the stoichiometric coefficient. The work of Stratton et al.(1983) suggested that a DO concentration of 1 mg/l at the interface required 2 mg/l of phenol as COD to cause oxygen limitation. Therefore with influent DO concentration around 30 mg/l, phenol concentrations above 25 mg/l may cause oxygen limitations. The coincidence of biomass densities at the top 10 cm of the sand columns in the three phases after 16 days is thus explained by oxygen limitation. Interestingly enough after 35 days the biomass densities at the top and bottom 10 cm of the sand columns receiving the 100 mg/l phenol solution were significantly higher than the 15 mg/l column. It appears that an anaerobic culture developed in the system where oxygen limitations were quite severe, which slowly then started to flourish as evidenced both by the microbial densities as well as the effluent substrate

concentration profiles illustrated in Figures 19-21. In all three phases phenol removal increased significantly with time approaching 93%, 90%, and 93% in phases I-III respectively after 35 days. The relatively higher effluent phenol concentrations with increasing influent concentrations on day 16 should have sustained higher biomass densities at the top provided that the sand columns maintained aerobic heterotrophic biofilms and oxygen was not limiting. But the close agreement between the overall biomass densities in phase I and phase II reactors after 16 days strongly corroborates the oxygen limitation at the reactors influent discussed earlier.

Furthermore as evident from Figure 5.21 from day 16 to day 35, effluent phenol concentration dropped from about 3 mg/l to 1 mg/l in phase I as compared with a drop from 40 to < 10 mg/l in phase III. It is interesting that the effluent DO in phase I was over 6 mg/l decreasing to about 2.4 mg/l in phase III, thus ascertaining the prevalence of oxygen limitations in phases II & III reactors.

Therefore the more dramatic increase in phenol removal efficiency after day 16 is mostly attributed to the growth of an anaerobic or facultative bacterial film. It must be asserted that despite the relatively high biomass densities observed in this study compared to literature values of 3.5 mgVSS/g sand (Huwang et al; 1985), removal of phenol by adsorption onto biosolids computed by the following equation (Stratton et al; 1983): Phenol Sorption Capacity= $S_0 * K_{oc} *$ Mass of Solids

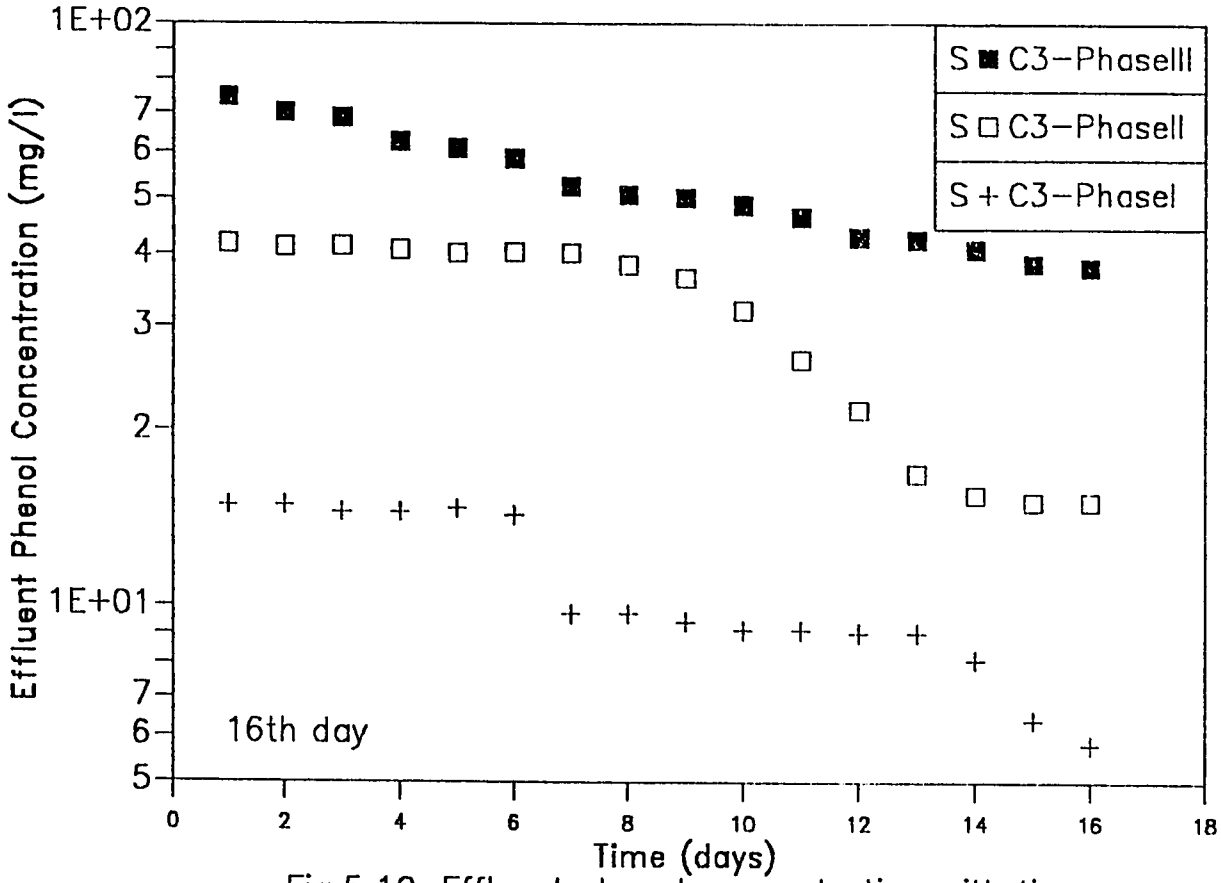

Fig.5.19: Effluent phenol concentration with time through fine sand of the 1st set of three phases

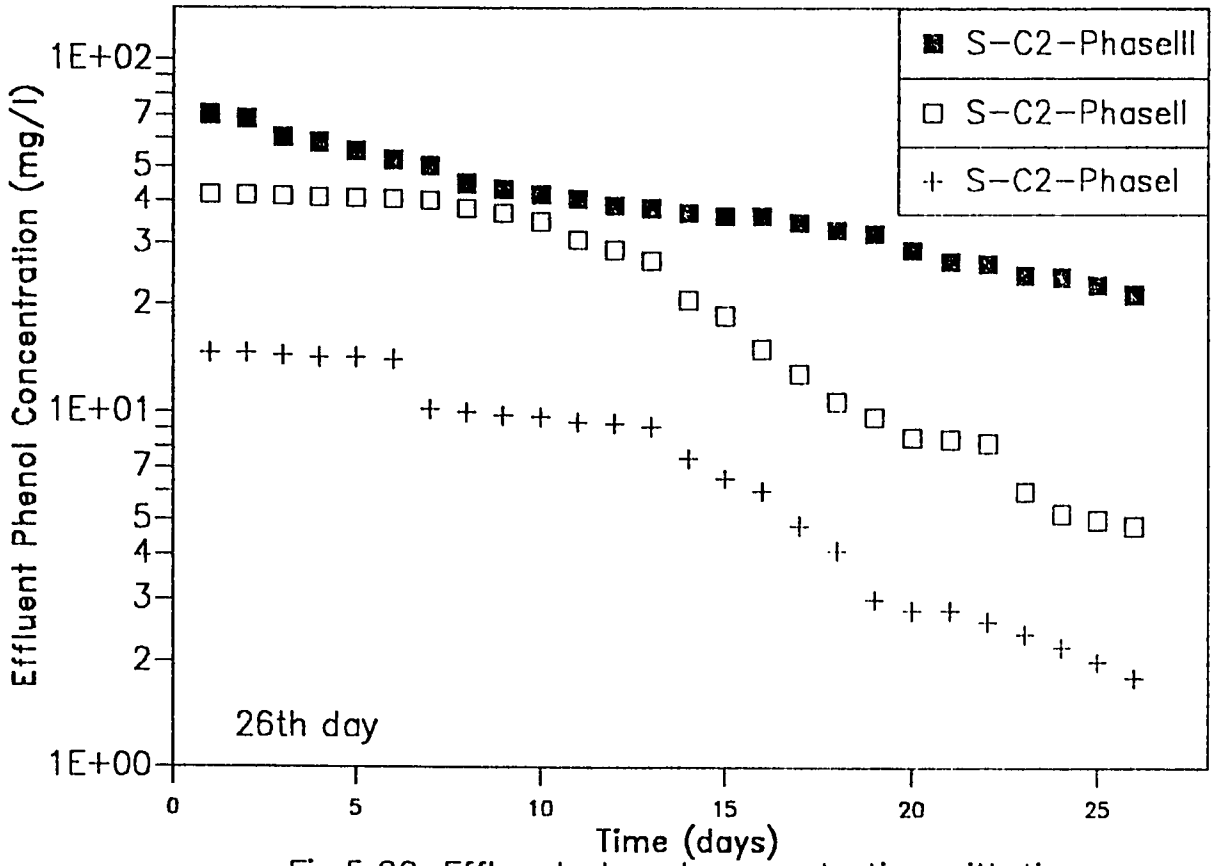

Fig.5.20: Effluent phenol concentration with time through fine sands of 2nd set of three phases

123

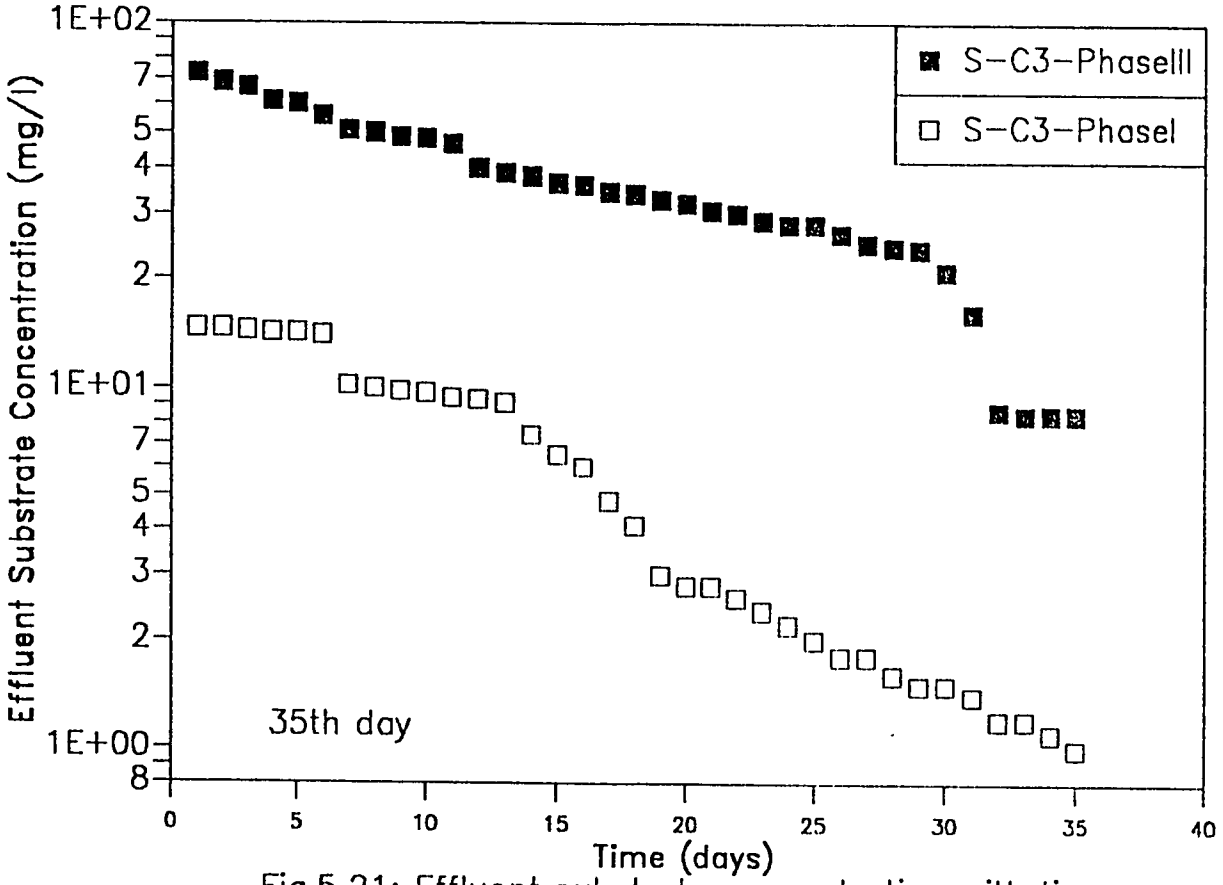

Fig.5.21: Effluent substrate concentration with time through fine sand of the 3rd set of two phases

123

where S_0 is the influent phenol concentration and K_{oc} is the organic carbon-water partition coefficient, which for phenol at room temperature is 18.5 mg H2O/mg C ranged only from 0.4-2.8 mg despite the very insignificant fraction of the phenol application rates which spanned 25-150 mg/day. Thus phenol removal was mostly by biodegradation since the sand sorptive capacity for phenol is also negligible. Figures 5.22-5.24 display the variation of volatile solids with depth in the medium size sand for the columns dismantled after 16, 26, and 35 days, respectively. The tendency of microorganisms to proliferate at the column inlet, which has been observed previously (Moltz et al; 1986) is quite conspicuous. Biomass densities varied from 8 mgVSS/g at the top of the column in the three phases to 1.8 mgVSS/g in phaseIII and 0.2 mgVSS/g in phases I & II at the column's effluent 16 days. At 35 days however, biomass densities were more uniform throughout the entire depth of the columns. For phase III biomass density ranged from 19 to 6.8 mgVSS/g. Similarly, for phases I & II densities spanned 10 to 5 mgVSS/g and 17 to 4 mgVSS/g respectively.

The identical biomass densities at the column's inlet on day 16 corroborates the oxygen limitations elaborated upon earlier. The relatively higher biomass densities at the bottom of phase III columns vis-a-vis phase II columns at all times are consistent with the higher effluent phenol concentrations depicted in Figures 5.25, 5.26, and 5.27. Phenol removal efficiencies increased with time in all columns.

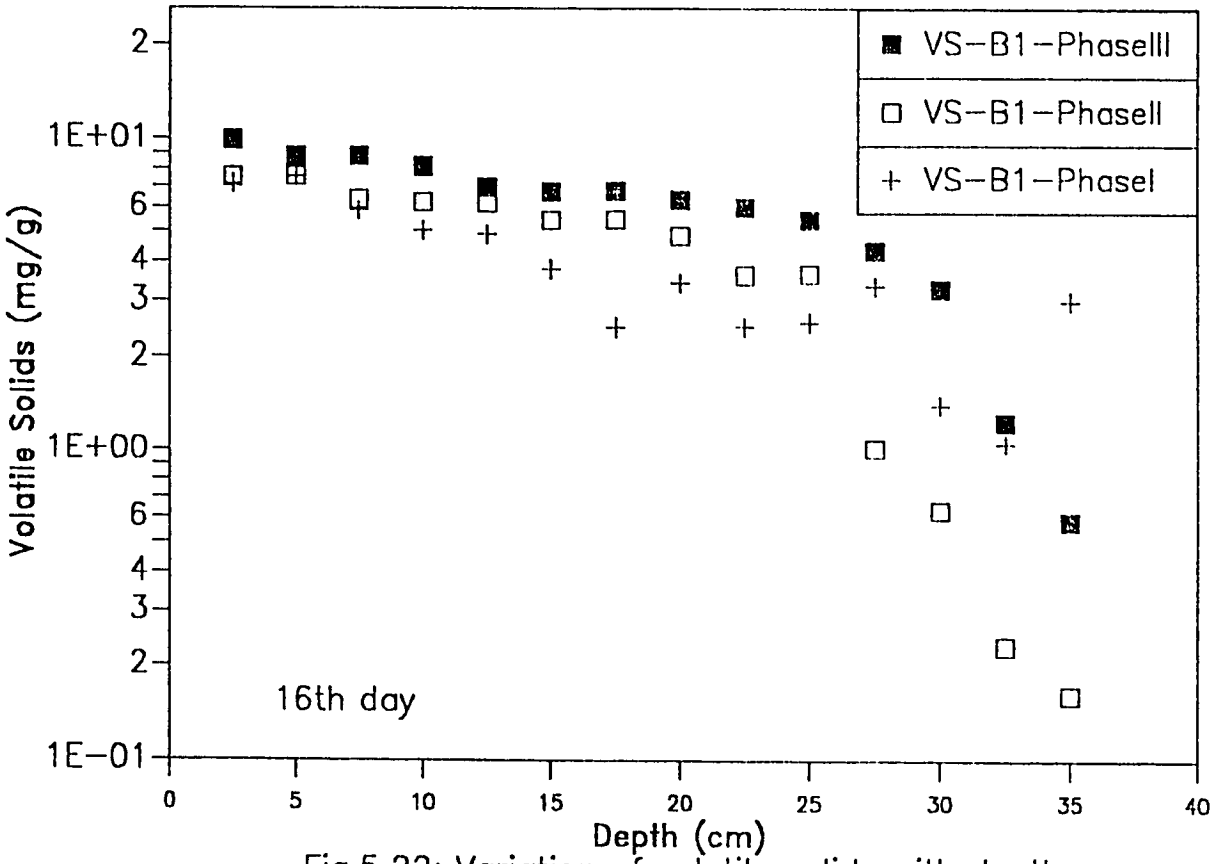

Fig.5.22: Variation of volatile solids with depth through medium sand of 1st set of three phases

123

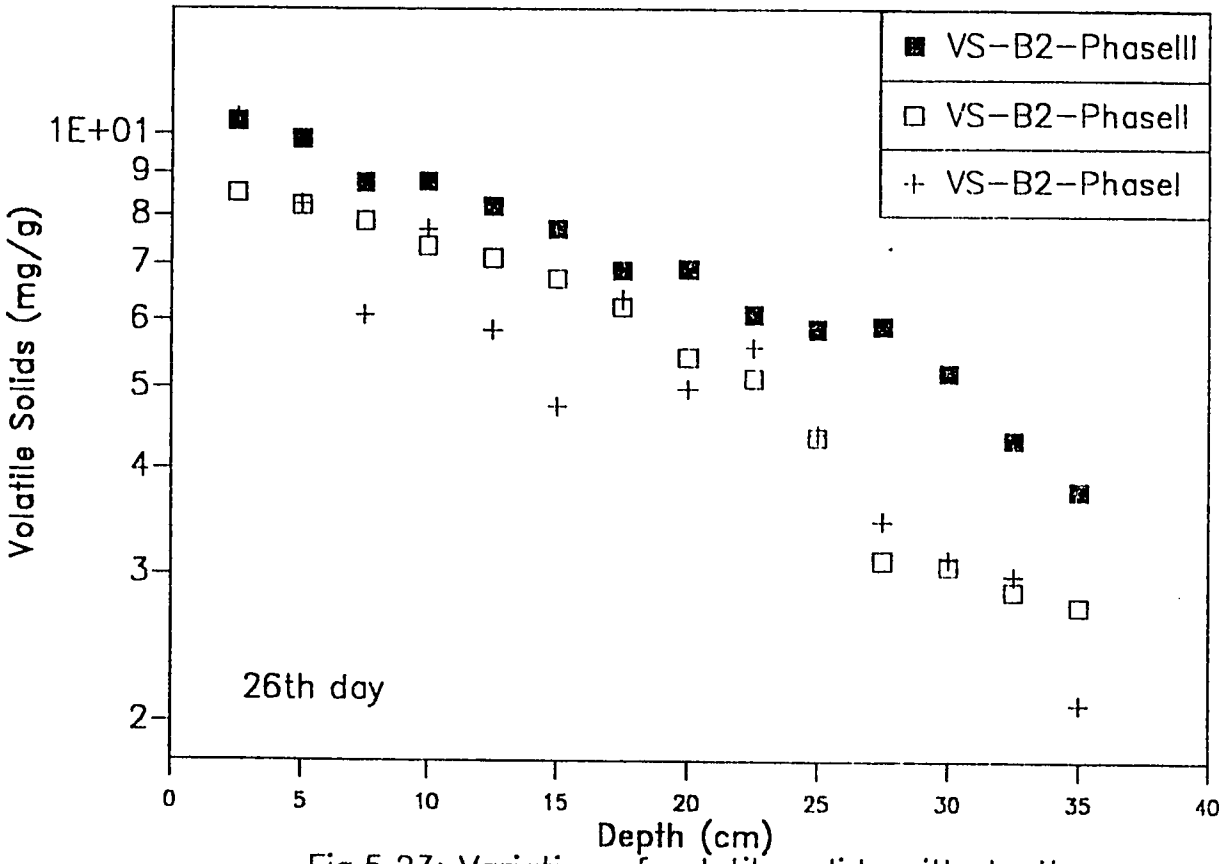

Fig.5.23: Variation of volatile solids with depth through medium sand of 2nd set of three phases

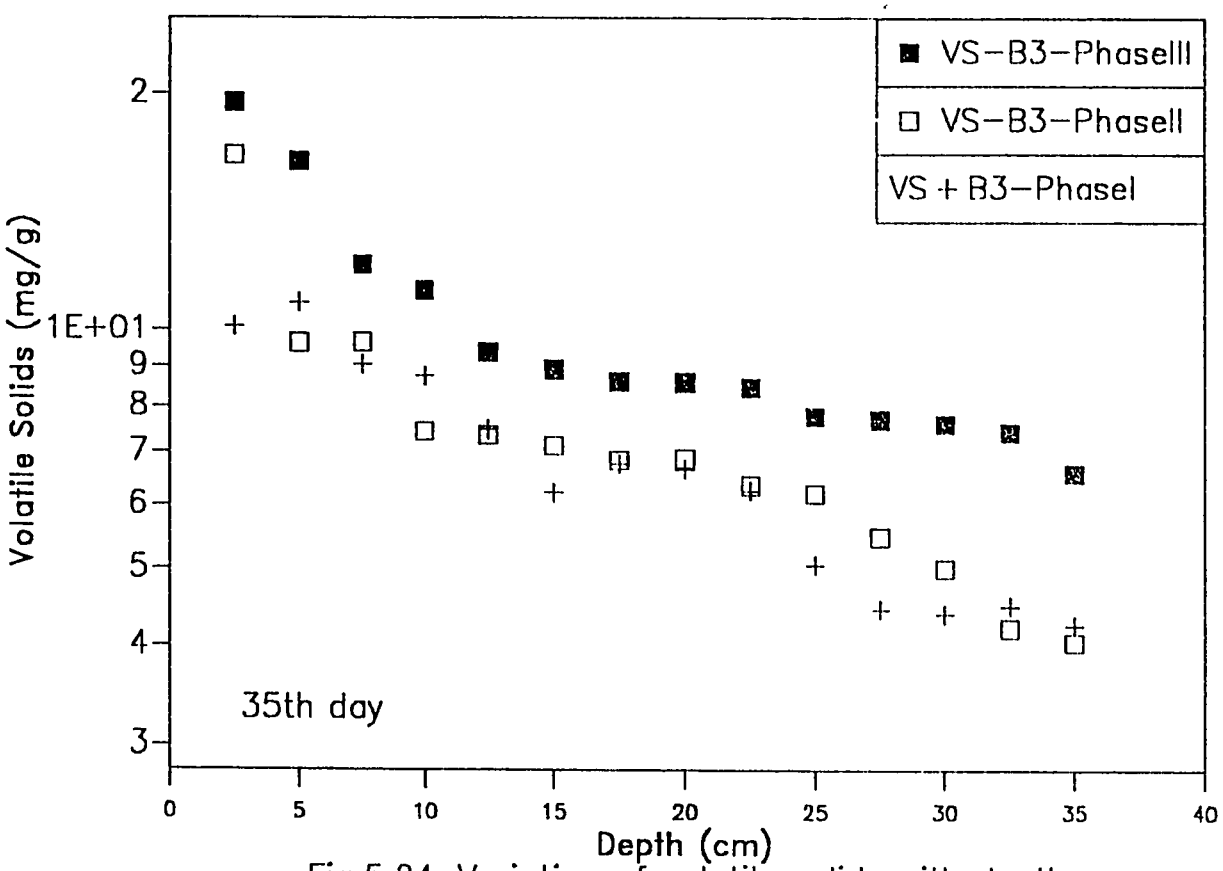

Fig.5.24: Variation of volatile solids with depth through medium sand of the 3rd set of three phases

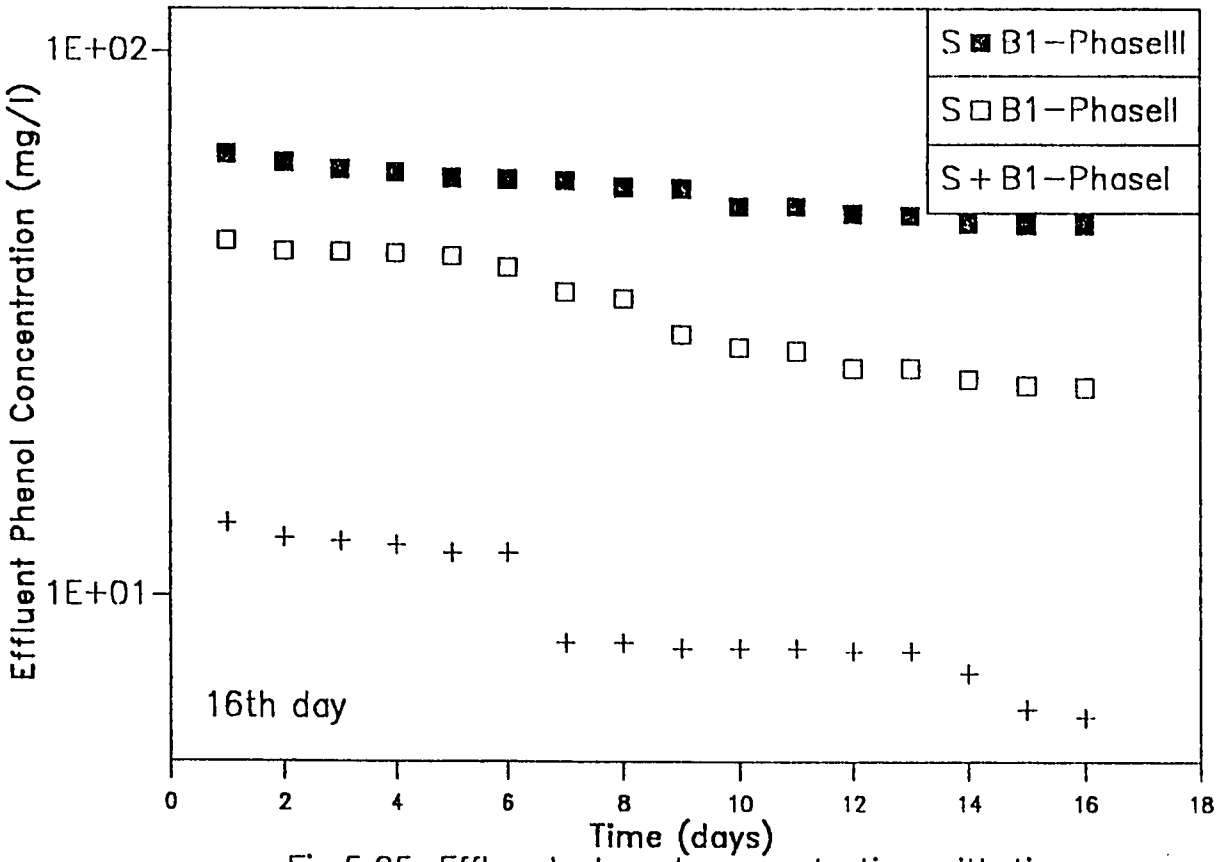

Fig.5.25: Effluent phenol concentration with time through medium sand of the 1st set of three phases

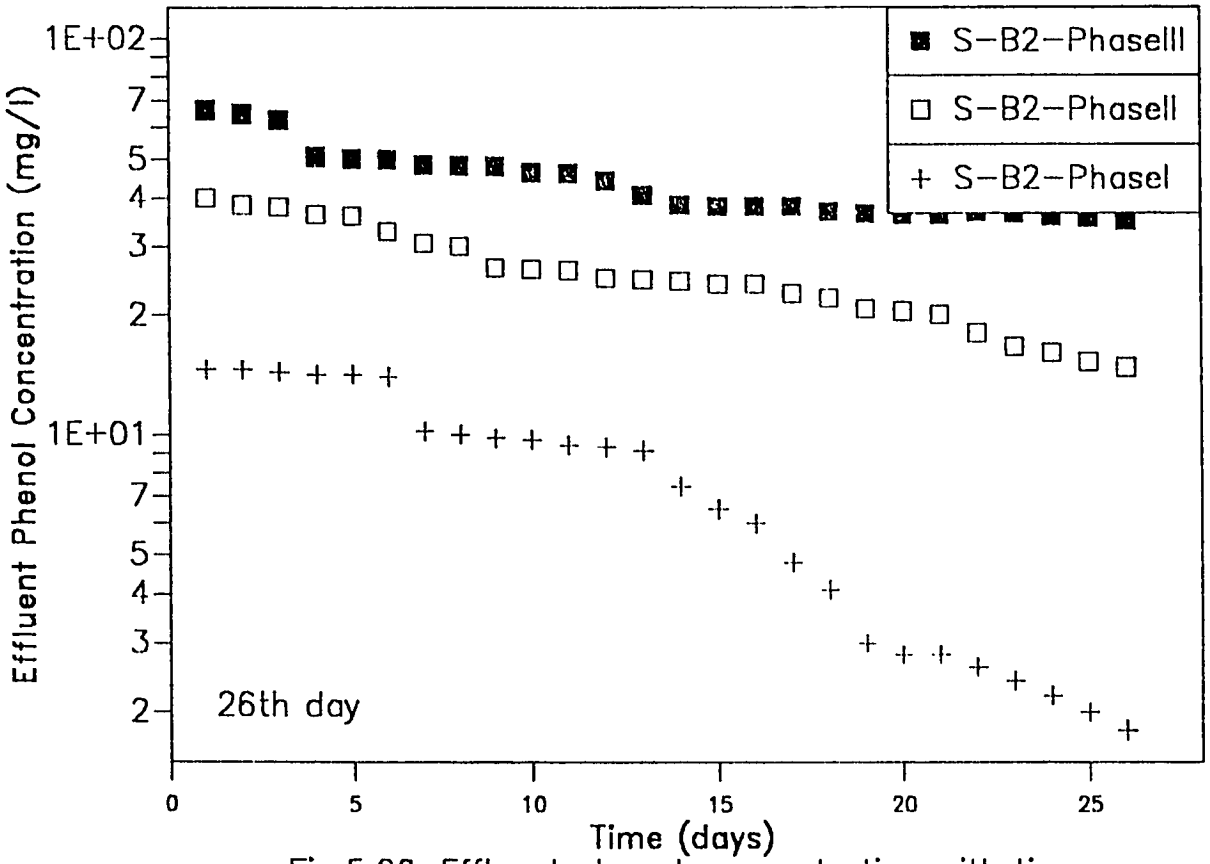

Fig.5.26: Effluent phenol concentration with time through medium sand of 2nd set of three phases

123

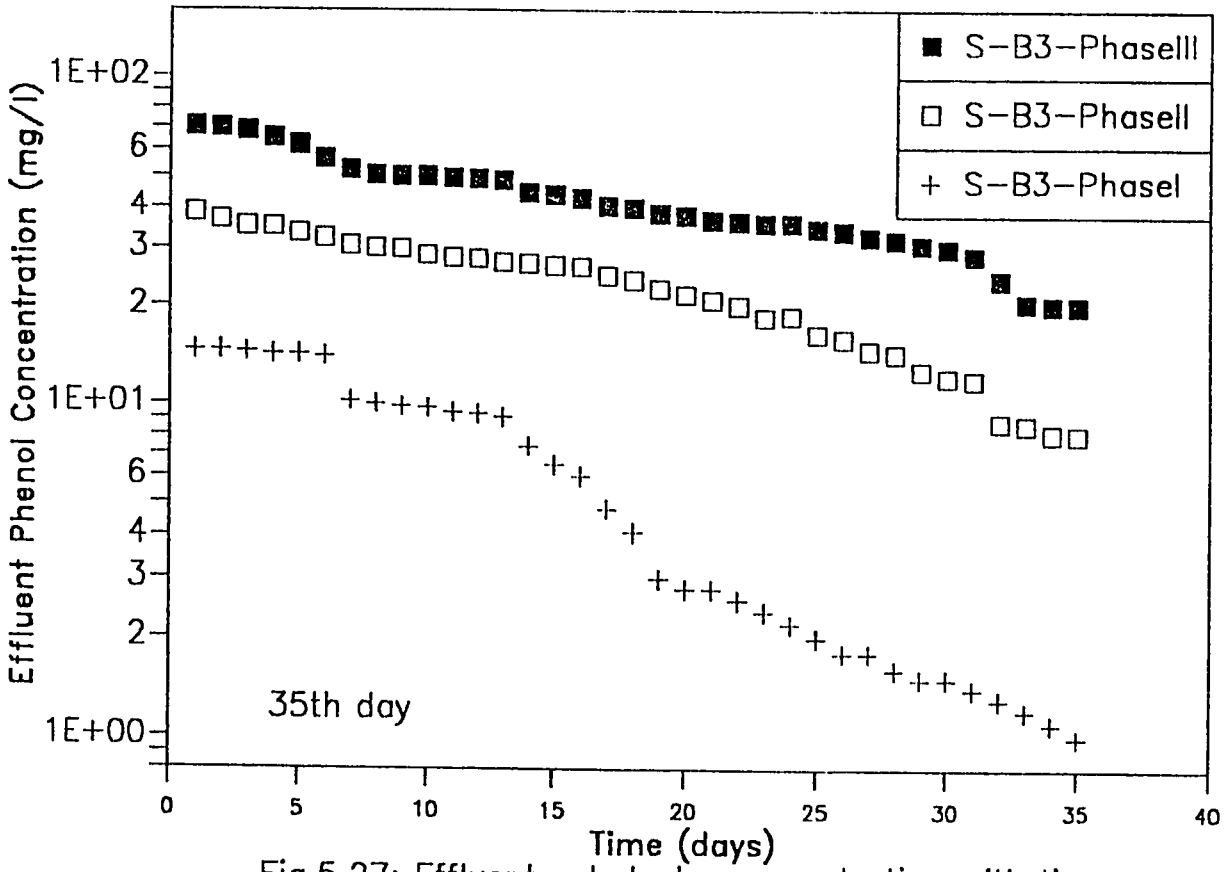

Fig.5.27: Effluent substrate concentration with time through medium sand of the 3rd set of three phases

Phenol removal efficiencies at 16 days in phase I-III were 38%, 52%, and 52% increasing to 93%, 94%, and 91% at 35 days. Effluent phenol concentrations stabilized after about 30 days in phases II & III while continuing to subside very slowly in phase I. A comparison of the effluent phenol data from the fine and medium sand columns at any time in phases II & III suggests that phenol removal efficiencies increased slightly with specific surface area. In phase I, however, differences in effluent phenol concentrations between fine and medium sand were much less pronounced , suggesting that the surface area was not limiting microbial growth and contaminant biodegradation.

Figures 5.28 to 5.30 and 5.31 to 5.33 display the variation of volatile solids with depth and effluent phenol from the coarse sand column, respectively. It is interesting to note that despite the relatively higher phenol concentrations detected in the effluent of phase II (Figure 5.33), after 16 days, biomass densities at the lower end of the columns were significantly below phase I. The significant spread between biomass densities at the bottom of the columns in phase I & II is rather unique to this sand size. As the specific surface area decreases with size, the biofilm thickness is proportional to the diameter for a given biomass concentration and biofilm density. Thus the oxygen limitations at the column inlet in phase II are only exacerbated by the high biofilm thickness in comparison with the fine and medium size sand. With time as anaerobic films proliferate in the column, the disparities between the aerobic biofilm (phase I) and the predominantly anaerobic biofilm (phase II) diminish. This microbial

population shift is further substantiated by the biomass and effluent data on day 35 (Figures 5.30 & 5.33). The relatively very low biomass densities at the column outlet in phase II are inconsistent with the higher effluent phenol concentrations in phase II as compared to phase I since higher bulk phase substrate concentration sustain high attached microcolonies.

Furthermore, the high biomass density at the top in phase II sustained by the high substrate concentration at the column inlet, can only be explained by anaerobic microbial activity unlimited by the supply of oxygen. Visual observation of the reactors indicated the presence of few anaerobic "pockets" but it is also likely that anaerobic activity may have been predominant in the basal layer of the biofilm where diffusion of oxygen is impeded by the biofilm thickness. Phenol removal efficiency increased from 33% and 43% in phases I & II respectively at 16 days to 88% in both phases after 35 days. At all times, effluent phenol concentrations from the coarse sand reactors were apparently higher than the fine and medium size sands.

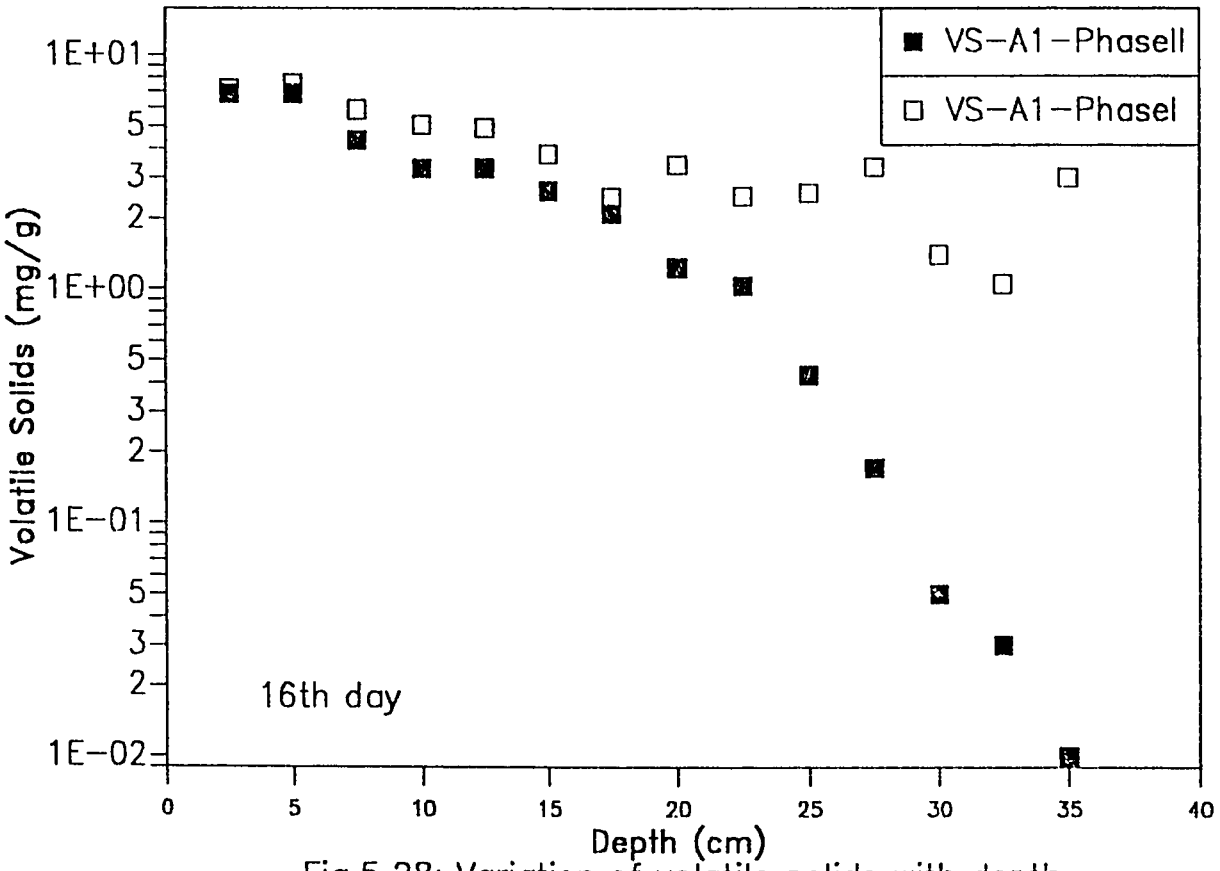

Fig.5.28: Variation of volatile solids with depth through coarse sand of 1st set of two phases

123

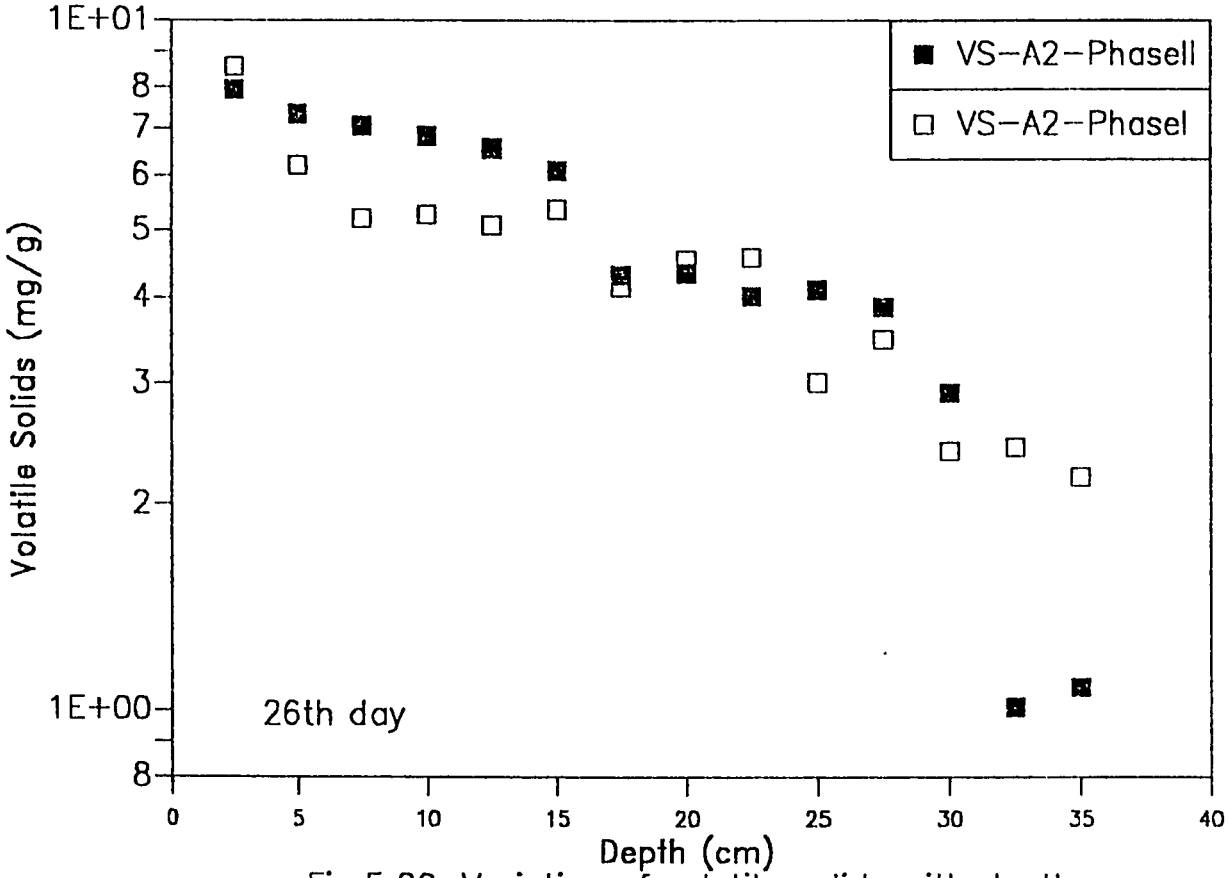

Fig.5.29: Variation of volatile solids with depth through coarse sand of the 2nd set of two phases

123

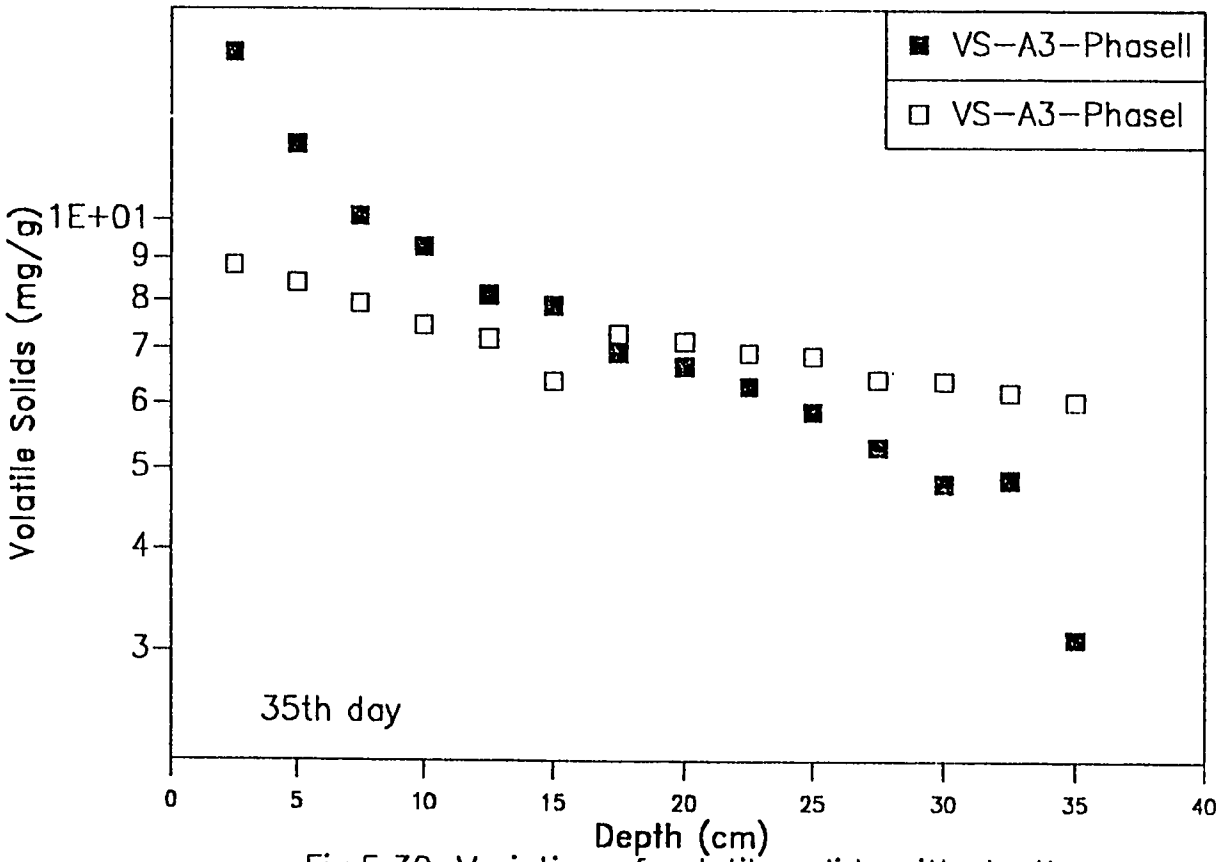

Fig.5.30: Variation of volatile solids with depth through coarse sand of 3rd set of two phases

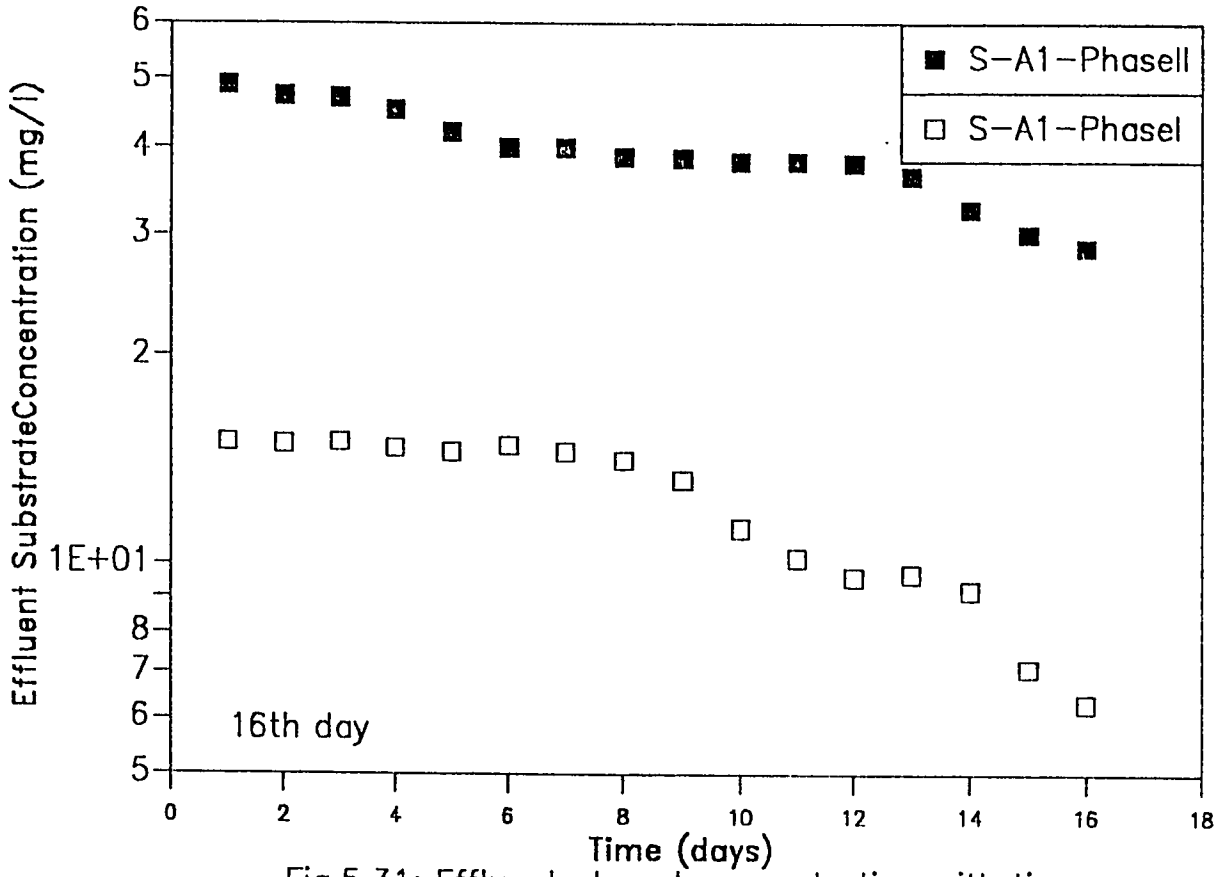

Fig.5.31: Effluent phenol concentration with time through coarse sand of the 1st set of two phases

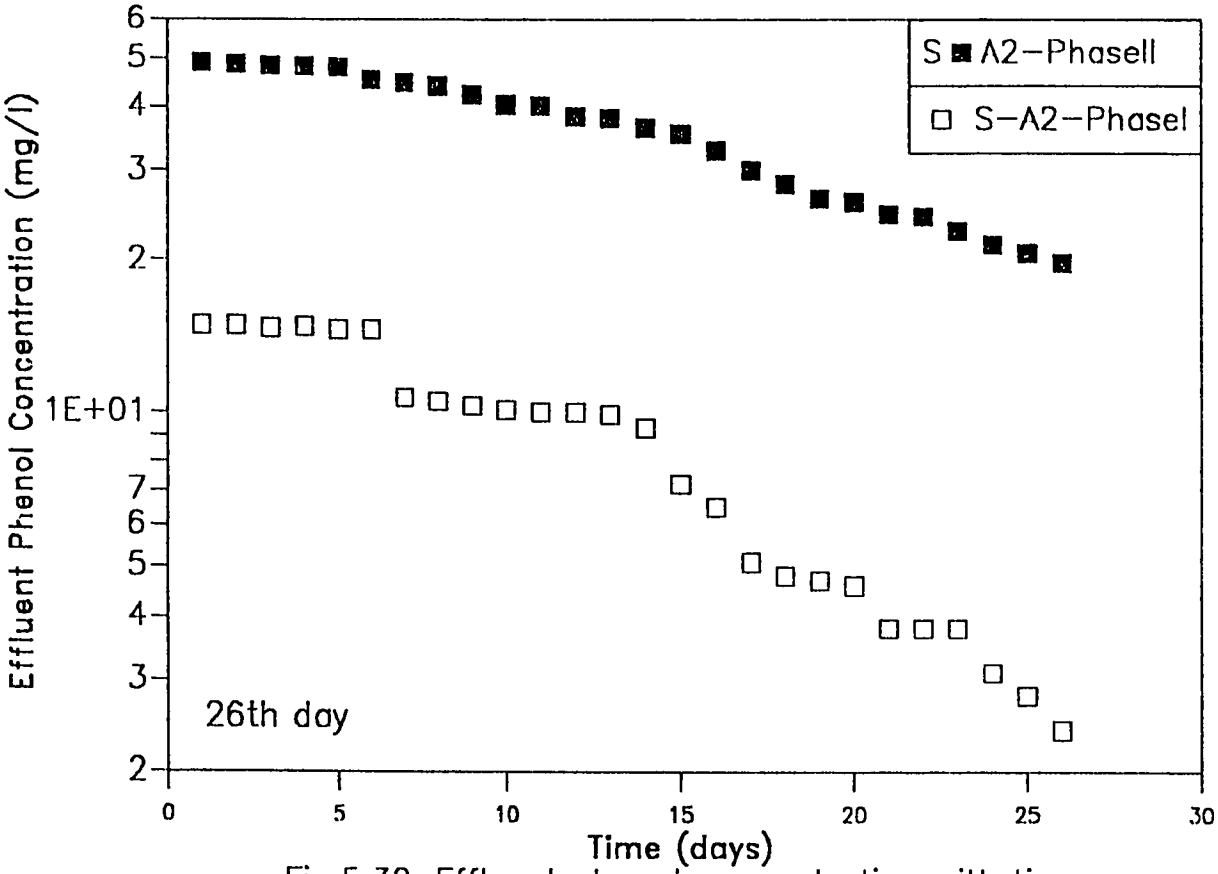

Fig.5.32: Effluent phenol concentration with time through coarse sand of 2nd set of two phases

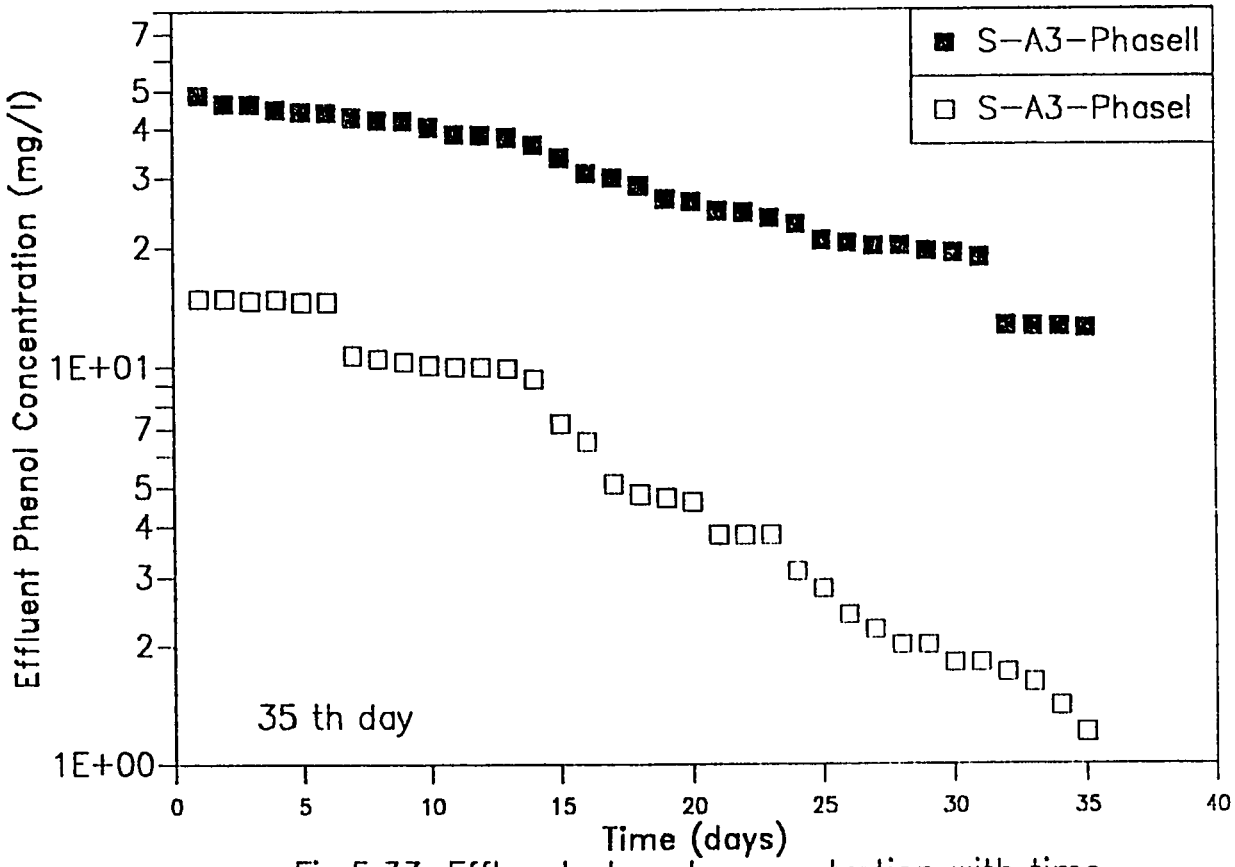

Fig.5.33: Effluent phenol concentration with time through coarse sand of 3rd set of two phases

123

Table 5.2 presents the average biomass densities in the columns and the respective yields computed as the product of the biomass density per gram and mass of sand column (2600 g) divided by the total mass of phenol removed.

Table 5.2 Average Biomas Densities in the Columns and the Respective Yields

Column	Phase I		Phase II		Phase III	
	Density mgVSS/g	Yield gVSS/g	Density mgVSS/g	Yield gVss/g	Density mgVss/g	Yield gVSS/g
C1	3.74	0.104	5.11	0.065	5.83	0.042
C2	7.37	0.094	6.06	0.036	6.96	0.023
C3	8.63	0.075			9.21	0.026
C5	8.70	0.034				
B1	4.25	0.127	4.80	0.062	6.35	0.047
B2	5.44	0.078	5.63	0.039	6.96	0.025
B3	6.77	0.062	7.35	0.039	10.8	0.033
A1	5.06	0.239	3.97	0.077		
A2	4.66	0.088	5.77	0.065		
A3	5.97	0.070	7.69	0.057		
A5	7.11	0.044				

It is interesting to compare the microbial densities on sand with those reported by Huwang et al; (1985) who observed a biomass density of 3.5 mgVSS/g during the treatment of 1000 mg/l sucrose solution at DO concentrations of 3, 5, and 16 mg/l. The notably higher biomass densities achieved in this study are attributed to the relative abundance of oxygen in phase I as well as the very short detention time of 15 minutes used in the aforementioned study. The yield for the aerobic hetrotrophic biofilm of phase I ranged from 0.062-0.239 gVSS/g phenol. For the mixed aerobic-anaerobic biofilm of phases II & III, the yield ranged from 0.023-0.077 gVSS/g phenol. Once again the relatively lower yields of phase II & III vis-a-vis phase I confirm the substantial contribution of anaerobic activity to substrate biodegradation. It can be inferred from Table 5.2 that for a given sand size and phenol concentration, the average yield decreases with time. The net yield (Y-observed) is given by the following equation $Y_{obs} = Y/(1+b*0_{c})$ where Y is the true yield (mgVSS/mg phenol), and 0_c is the solids residence time (days), and b is first order decay coefficient. For first order shear loss (Rittman, 1982), b is the sum of the first-order decay and shear loss coefficients. Thus the decrease in hydraulic conductivity with time and the concomitant rise in biofilm, first-order shear loss coefficient reduces the observed yield. generally speaking a close agreement between the yields in the respective reactors throughout all phases of the work is observed. Furthermore scrutiny of phase II and phase III yields for the various reactors strongly indicates that the net yield decreases

with grain size diameter. Although the biokinetic constants for the predominantly anaerobic biofilms in phases II & III should be independent of media characteristics, the relatively lower permeabilities and consequent higher shear stresses for finer and medium result in greater shear loss coefficients. The hydraulic conductivities of fine, medium, and coarse sand columns dismantled after 35 days is shown in Figures 5.34, 5.35, and 5.36, respectively. Although the overall biomass densities in the fine sand columns during phases I & III are very close (Table 5.2), the hydraulic conductivities particularly towards the end are divergent. The hydraulic

conductivities of fine sand in phase I & III decreased to 11.7% and 4.7% of the original value respectively. Similarly, hydraulic conductivity for the coarse sand dropped from an initial value of 9 cm/hr to 2.2 and 0.55 cm/hr in phases I & II respectively. The biomass distribution throughout the columns discussed earlier (Figures 5.18 & 5.37) do not suggest that surface plugging due to high biomass concentration at the column inlet, is the reason for this disparity in hydraulic conductivities between the various phases of this study. Thus while the overall biomass densities were essentially the same, the difference in hydraulic conductivity can only be attributed to biochemical nature of the biofilm. The data of two sand sizes in this study provides evidence of anaerobic biofilms impeding the flow of water than aerobic colonies. Previous work has documented that anaerobic bacteria reduce permeability more than aerobic films at identical biofilm thickness by reduction of pore volume due to release of the

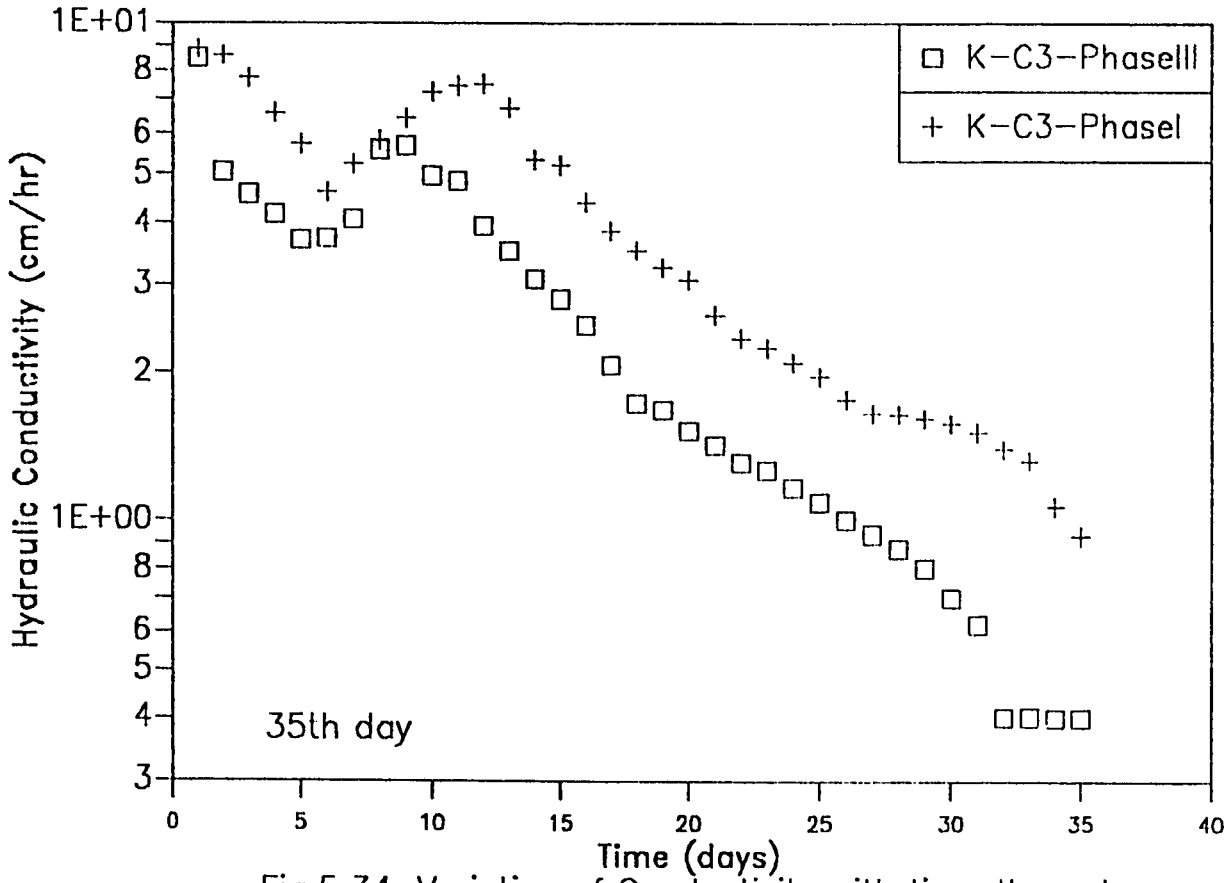

Fig.5.34: Variation of Conductivity with time through fine sand of two phases

123

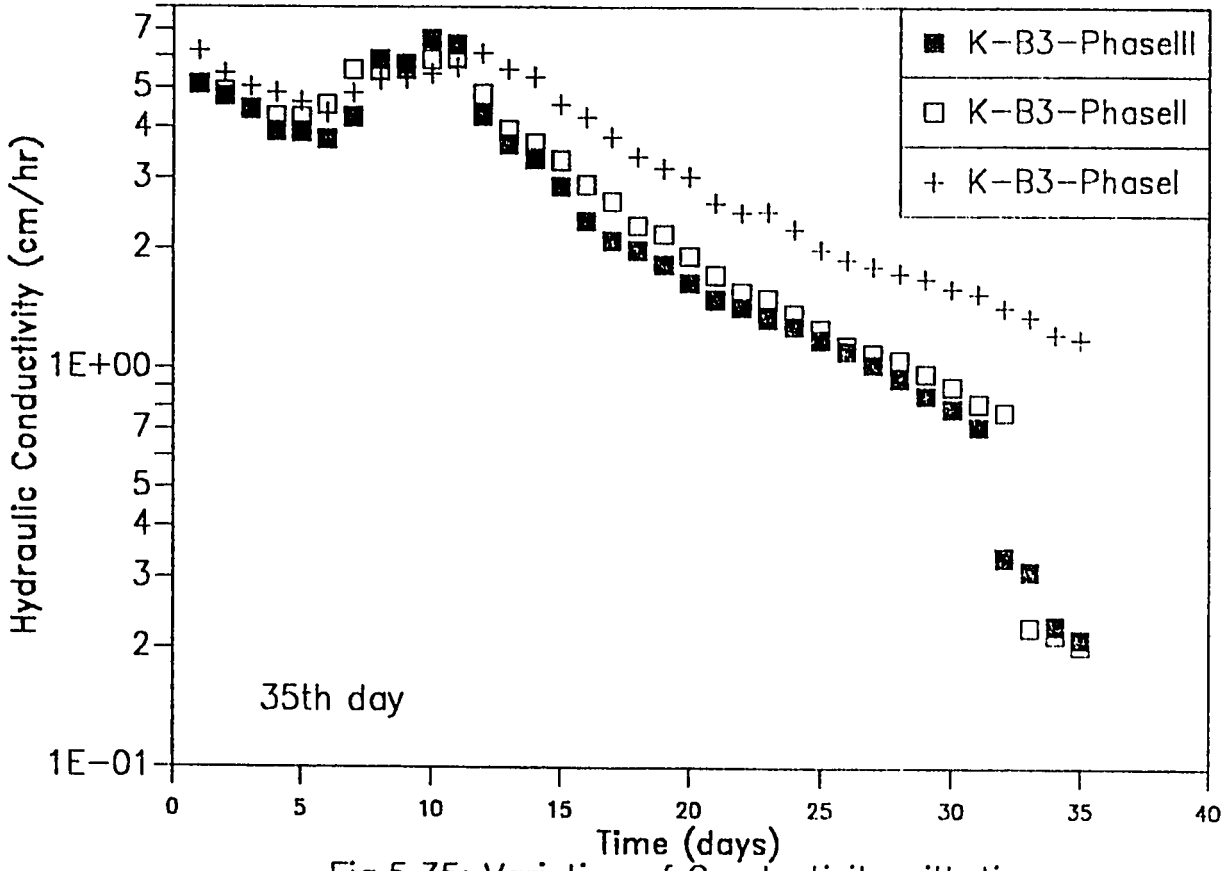

Fig.5.35: Variation of Conductivity with time through the medium sand of the three phases

123

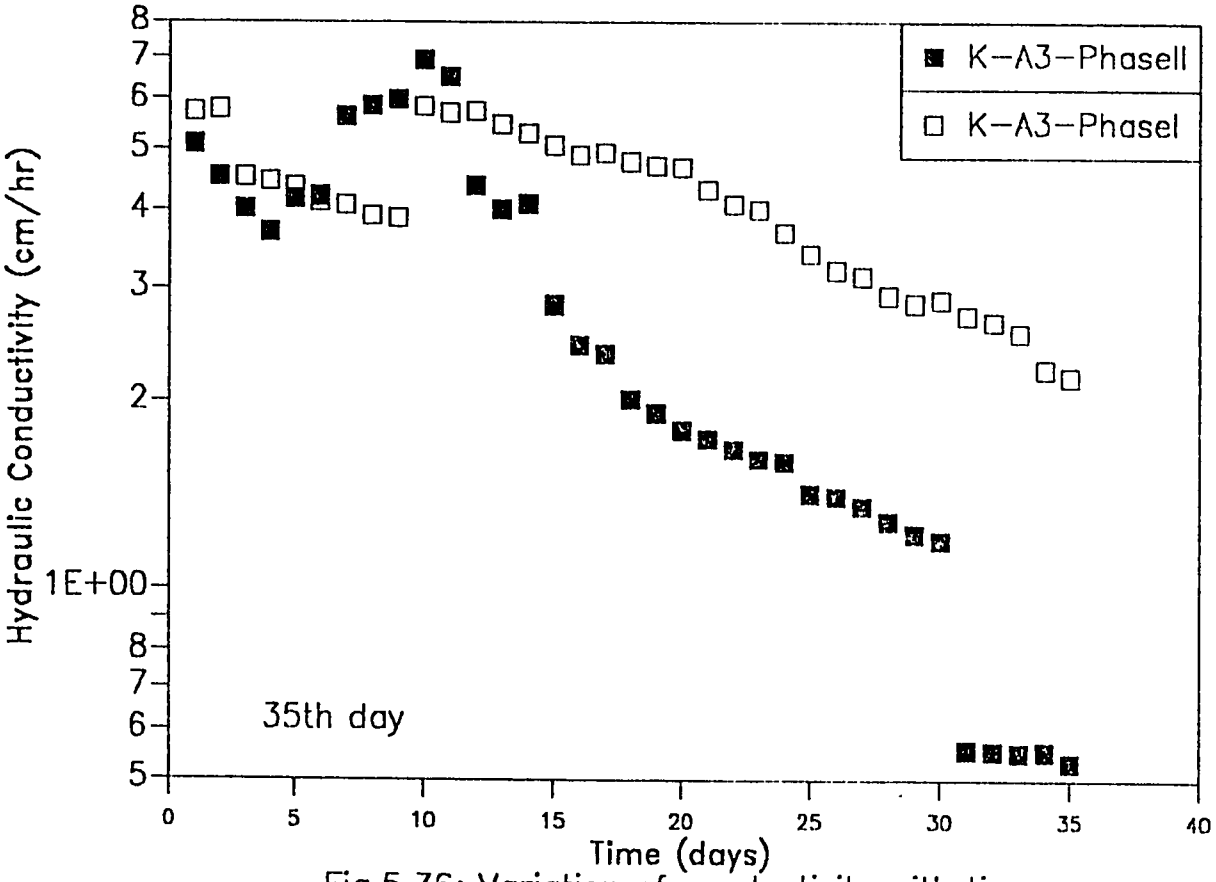

Fig.5.36: Variation of conductivity with time through coarse sand of the 3rd set of two phases

123

gaseous end products of biodegradation. The data of the medium size sand (Figure 5.35) confirms the increased resistance to water flow posed by the predominantly anaerobic microbial films. The clean surface hydraulic conductivity of medium sand was 5.6 cm/hr, decreasing to 1.1 , 0.21, and 0.23 cm/hr in phases I-III respectively. Similar hydraulic conductivity reductions of three to four orders of magnitude were observed by Vandevivere et at; (1992) at bacterial densities of 4 mgVSS/g sand.

Figure 5.37 shows a comparison between the hydraulic conductivities of the three sand sizes in phase I. While the average biomass densities in the columns C3, B3, A3 were 8.63, 6.77, 5.97 mg/g respectively, conductivities of columns B3 and C3 were very similar but much lower than the coarse sand. Assuming a constant biofilm density, the biofilm thickness is proportional to the product of biomass density per unit biomass and the diameter and therefore the biofilm thickness is greater in the coarse sand but it appears that this is offset by the significant reduction in pore volume.

The effect of grain size on hydraulic conductivity of anaerobic biofilms is presented for phases II & III in Figures 5.38 and 5.39 respectively. It is interesting to note that in phase II not only all three sizes accomodated essentially identical quantities of biomass as apparent from Table 5.2 but also the hydraulic conductivities were almost identical. Similarly, in phase III, biomass densities in the fine and medium sand reactors were in close agreement as were the

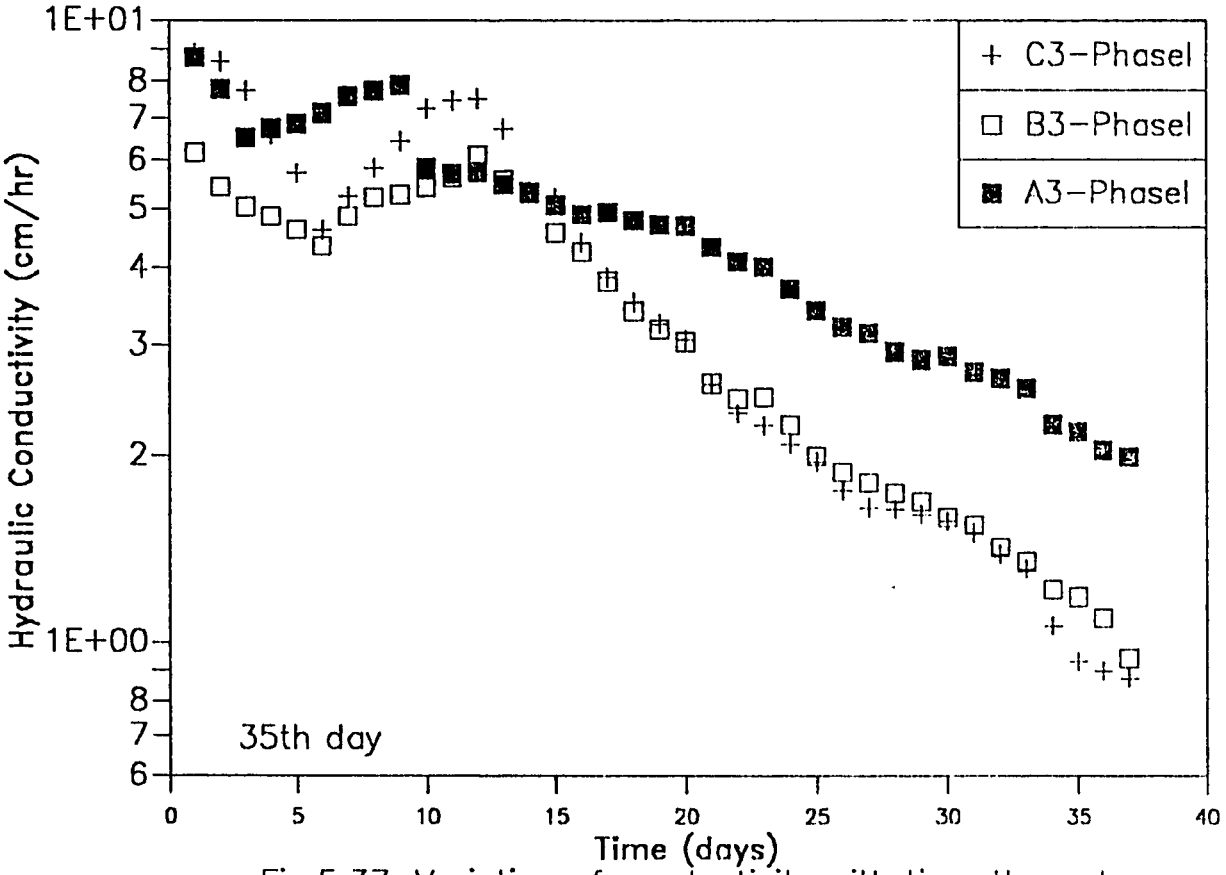

Fig.5.37: Variation of conductivity with time through three different sizes of sand of the 3rd set of 1st phase

123

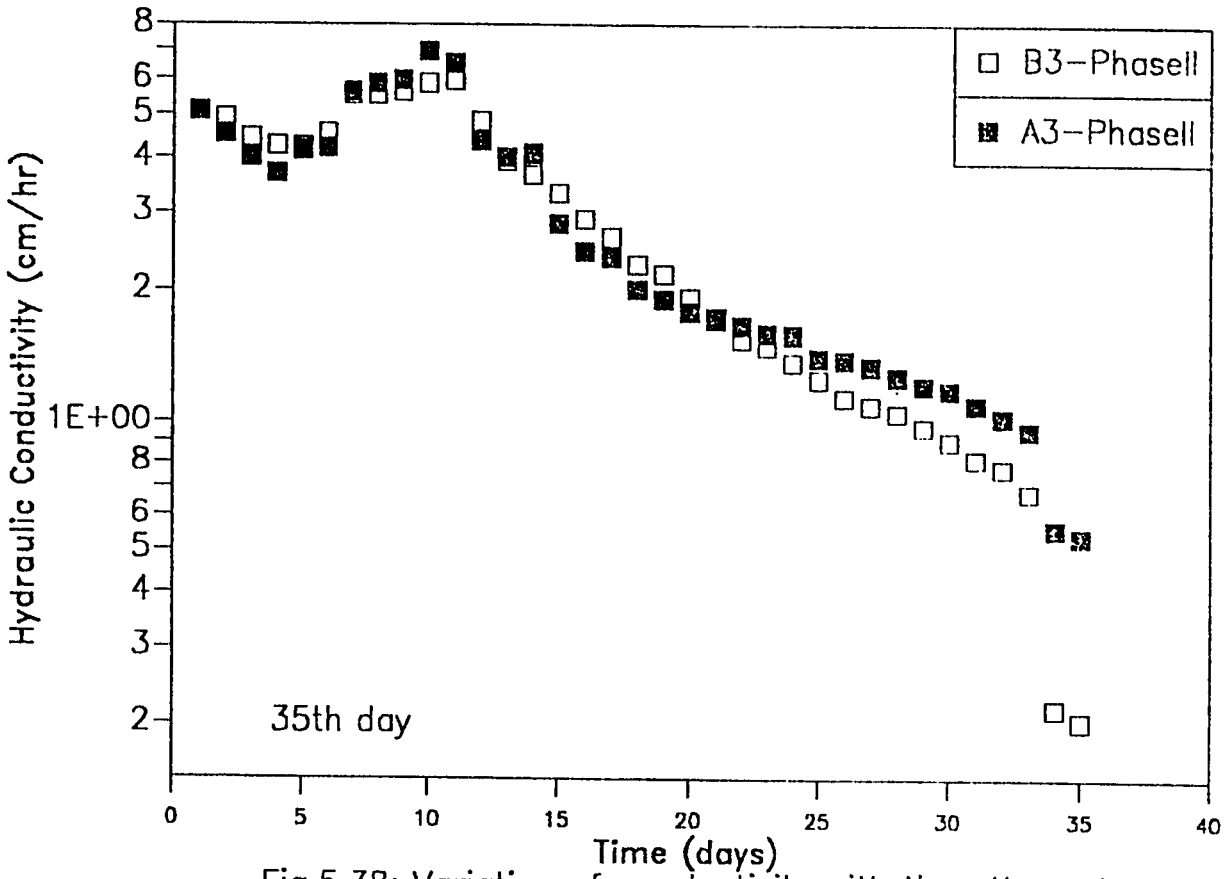

Fig.5.38: Variation of conductivity with time through two different sizes of sand of the last set of 2nd phase

123

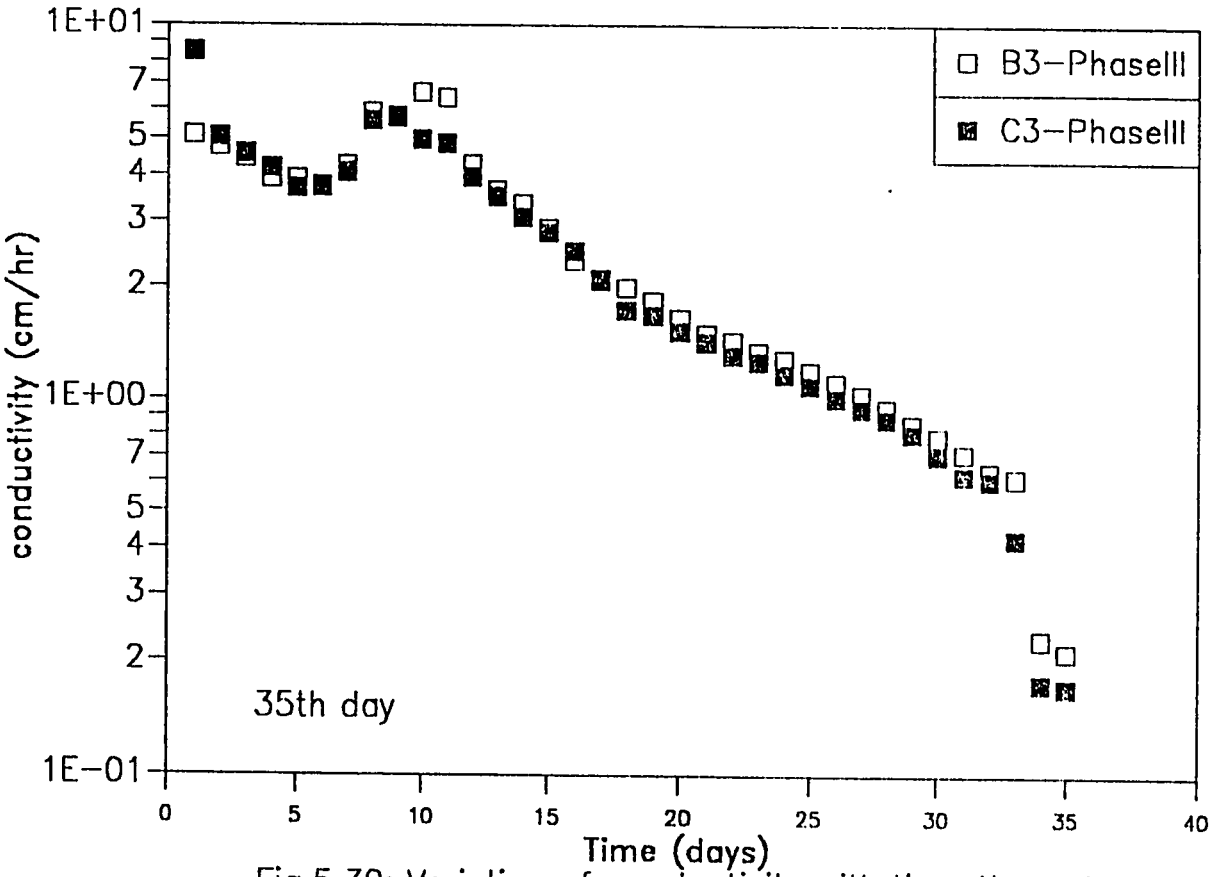

Fig.5.39: Variation of conductivity with time through two different sizes of sand of the last set of the 3rd phase

hydraulic conductivities. Thus it appears that hydraulic conductivity was a function of total biomass and not biofilm thickness. Given the relatively high biofilm density for anaerobic microorganisms vis-a-vis aerobic films which are limited by diffusion of oxygen. Therefore at comparable biomass densities per unit mass of sand, the anaerobic biofilm is much thinner than the aerobic one, and thus its resistance to the flow of water would not be mostly due to reduction of pore volume.

The findings of this study may have profound implications for the in-situ remediation of contaminated groundwaters. Although biomass mediated changes in hydrodynamic properties of the medium in the vicinity of injection wells, are of most importance the overall permeability of the aquifer is strongly influenced by the biochemical properties of bacteria films as well as their distribution in the subsurface environment. The findings of this study provide evidence of biomass redistribution in the medium over time and a strong correlation between average biomass density in the entire medium and permeability. The increased hydraulic conductivity reduction caused by anaerobic biofilms emphasize the importance of oxygen availability. Thus oxygen availability is not only important from a biodegradation perspective but also from a hydrodynamic view point. Sufficient availability of oxygen and maintenance of aerobic hetrotrophic biofilms would enhance the transport of water, nutrients, microbial cells, and substrate through the porous medium, which will improve downstream biodegradation of pollutant and achieve more comprehensive and

effective clean-up of polluted aquifers.

5.6 Change of Porosity with Biofilm Thickness

One of the goals of this investigation is to determine the biofilm thickness indirectly since the direct measurement is very difficult to accomplish. Growth of a biofilm in a porous media reduces the average size of the pores. The change in the pore space is easily quantified when certain geometric assumptions are made. We assume that the porous medium is rigid and saturated with a single fluid, the flow is Darcian, and the biofilm has negligible permeability. It is assumed also that the microbes are utilizing growth substrate under aerobic conditions. It follows that the problem is primarily one of relating changes in pore geometry, caused by biofilm growth, to changes in porosity. Many different modeling approaches for the treatment of single-phase porosity have been described in the literature.

Kozeni-Carman model has been extensively used to describe the change in porosity affected by biofilm thickness (Marshall, 1958; Taylor et al., 1990). In this study, the modified Kozeni-Carman model developed by Taylor et al. (1990) is used. This model assumes the porous medium to be equivalent to a conduit, the cross section of which has a complicated shape but a constant area. From hydraulic theory it is known that the conduit diameter is taken to be 4 times the hydraulic radius. Kozeni- Carman equation, as discussed in the literature review, was utilized to analyze this data as follows:

$$K = c_0 n^3 / M^2 \qquad (5.3)$$

where, n is the porosity, M is the specific surface, and c a constant for which Carman (1937) suggests a value of 1/5.

Assumptions regarding the packing of the solid phase were made. It was assumed that the solid phase was comprized of uniform spheres packed in a stable manner. In any arrangement, each sphere tangentially contacts a certain number of neighbouring spheres, and the number of contact points m can be used to characterize the packing arrangement. The value of m for the sphere arrangement is 6. The packing factor alpha for the sphere is 1.0 (Taylor et al; 1990)

Assuming that a biofilm develops in a porous medium comprized of spheres of equal diameter. Biofilm growth increases the volume and decreases the surface area of the solid phase. Expressions for the biofilm affected porosity n and specific surface M can be derived from the geometry of the sphere coated with a constant biofilm thickness L_f. The equations developed by Taylor et al.(1990) are discussed in chapter IV.

The biofilm-affected permeability for the sphere model was found by substituting the biofilm affected porosity and specific surface into equation 4.1, assuming that C_0 does not vary with biofilm growth. Applying this model, a set of figures relating porosity with biofilm thickness was obtained. The spatial distribution of biofilm thickness

was estimated for the column experiments discussed earlier, using the permeabilities that were observed at the end of the experiments. Mathematically, the problem consists of solving equation 4.1 for L_f given the biofilm affected permeability K_b

Figures 5.40 to 5.45 show the changes of porosity due to biofilm thickness. The figures show that as biofilm coats the pore space the porosity and cosequently the permeability decreases. The columns considered in Figure 40 and 41 were B3 which were fed a substrate concentration of 100 mg/l, and 50 mg/l, respectively. From Figures (5.40, 5.41, and 5.42) it can be noticed that in the early days of the experiment, when the biofilm thickness is small there is a direct relation between the biofilm thickness and the reduction in porosity. As the biofilm increases in thickness this linear relationship ceases to exist due to the predominantly anaerobic films which developed with time. The perturbations which are evident in these figures could be due to the combined effect of aerbic/anaerobic activities.

Figures 5.43 to 5.45 show the relation between the porosity and biofilm thickness in a coarse, medium, and fine sands.The columns considered were A3, B3, and C3 which were fed with 15 mg/l phenol. In these figures, perturbations due to oxygen limitations are not evident, and surface areas of the sands were not limiting microbial growth and contaminant biodegradation. Although the model has some major limitations the Kozeni-Carman model gives physically reasonable reults to the problem of porosity and permeability reduction by a

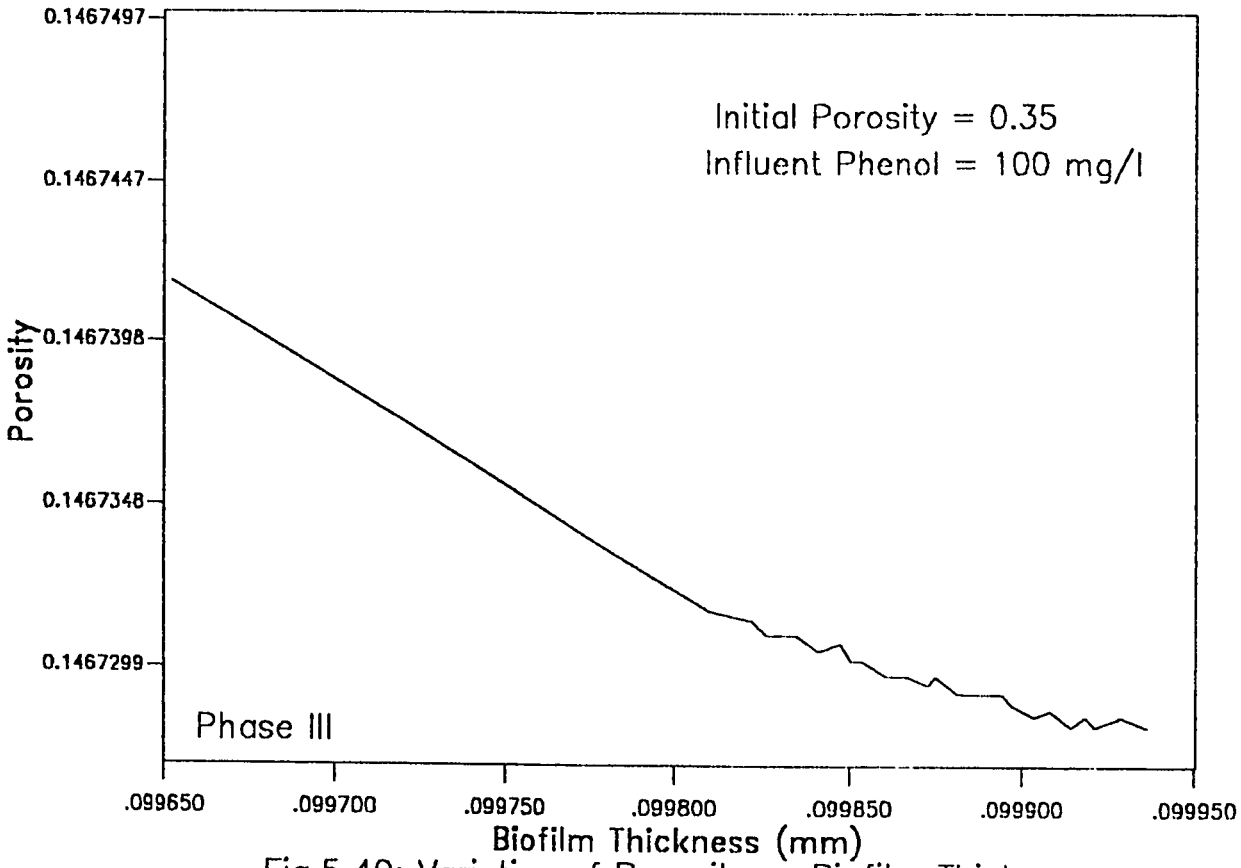

Fig.5.40: Variation of Porosity vs Biofilm Thickness in column B3 after 35 days

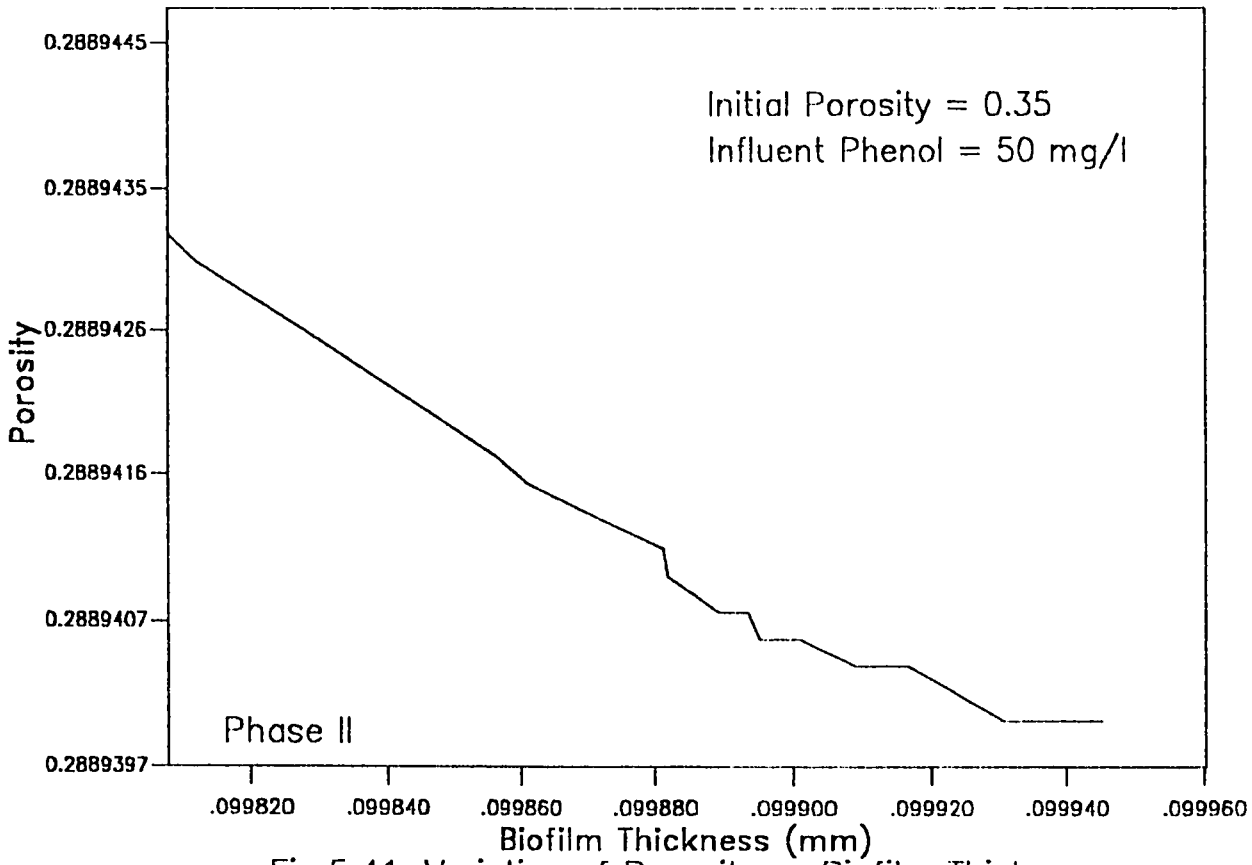

Fig.5.41: Variation of Porosity vs Biofilm Thickness in column B3 after 35 days

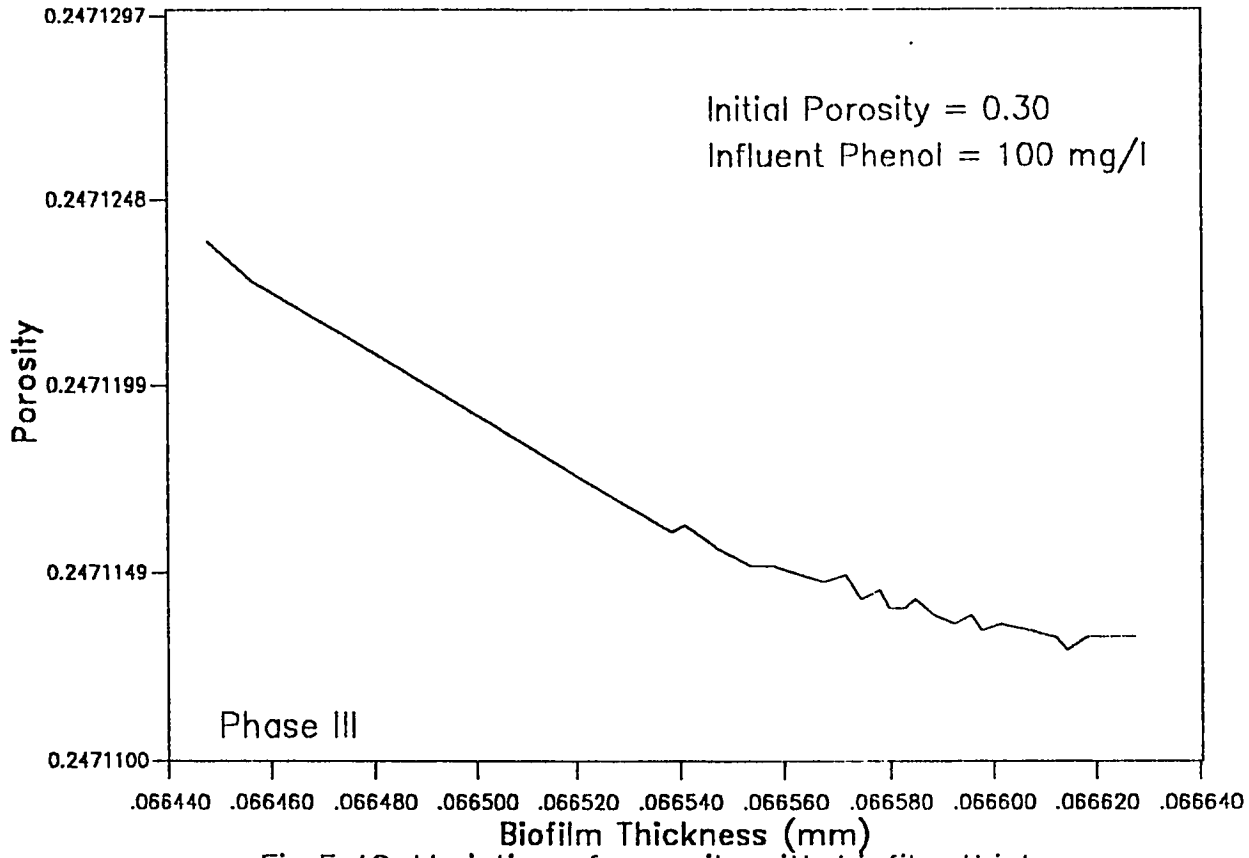

Fig.5.42: Variation of porosity with biofilm thickness through column C3 after 35 days

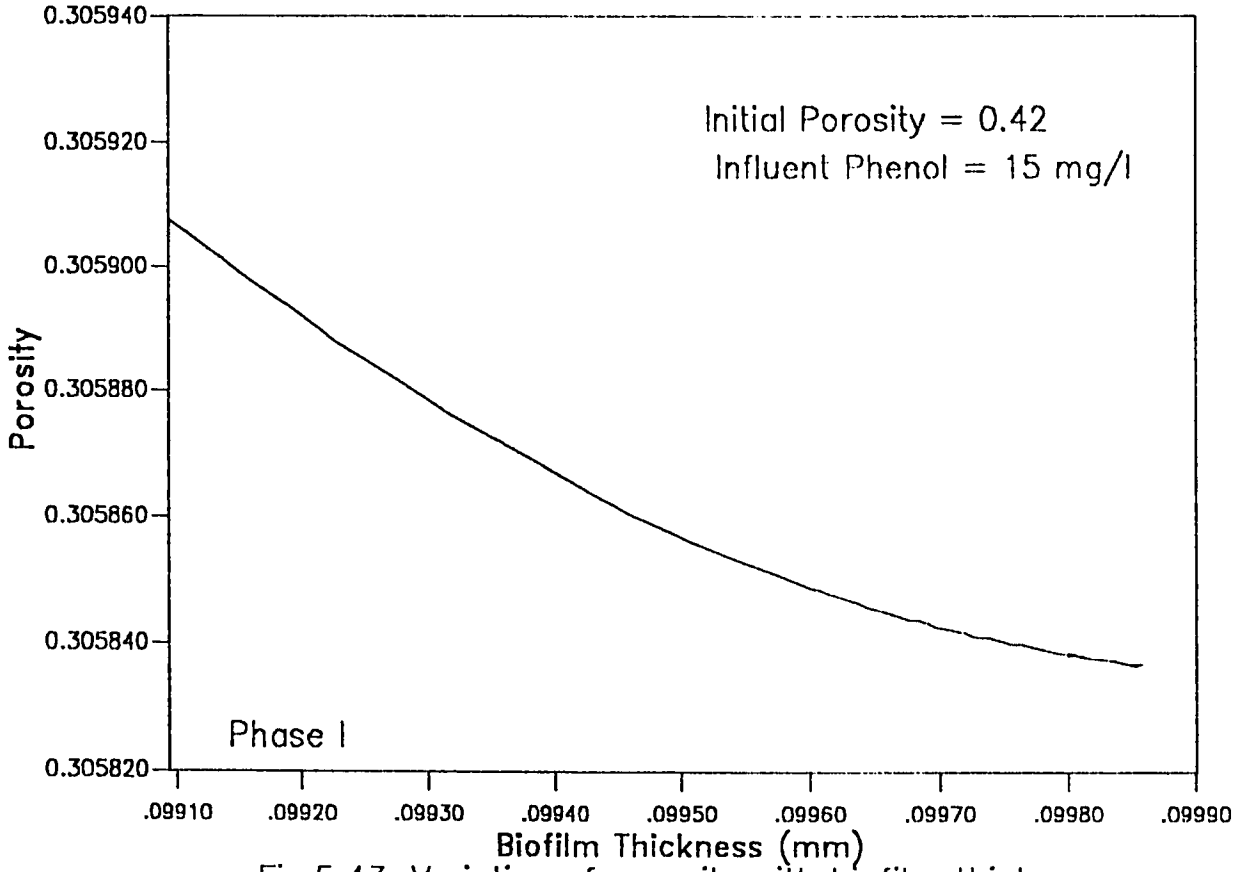

Fig.5.43: Variation of porosity with biofilm thickness through column A3 after 58 days

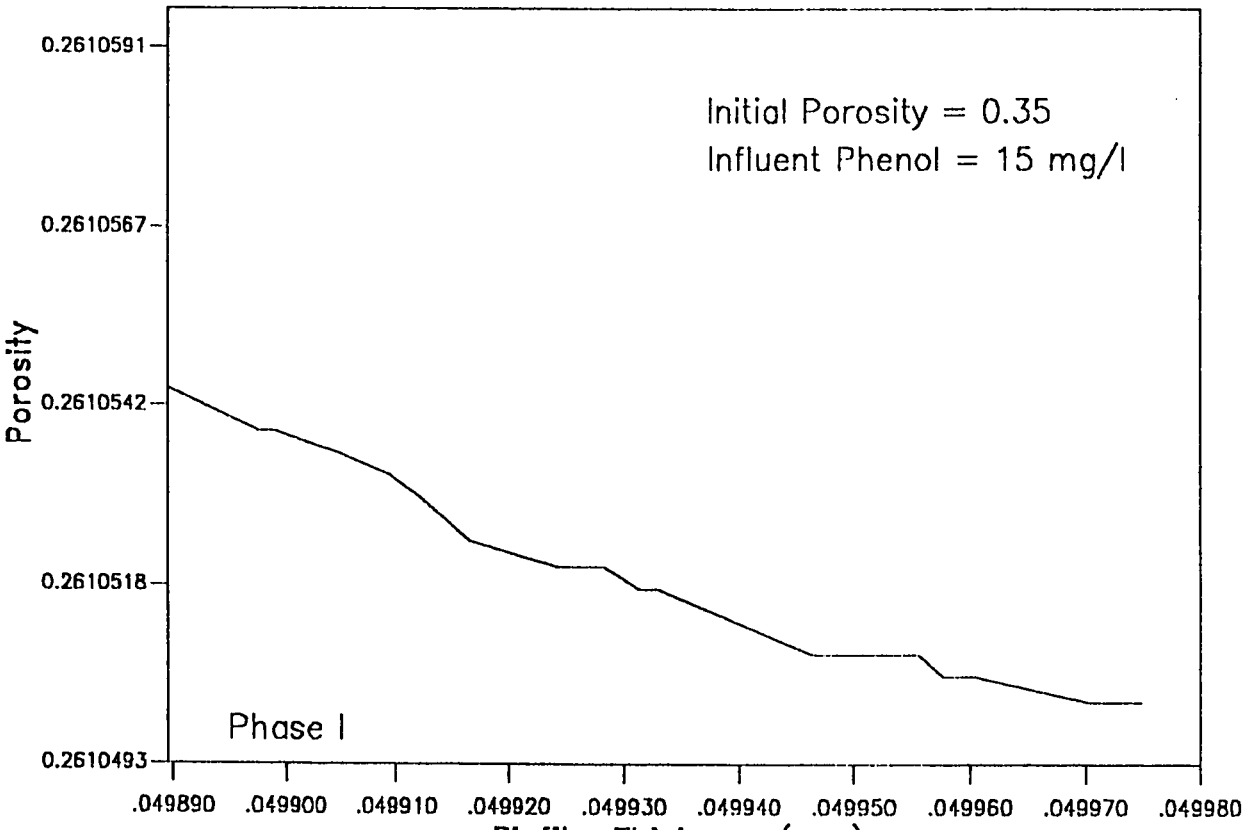

Fig.5.44: Variation of Porosity vs Biofilm Thickness in column B3 after 58 days

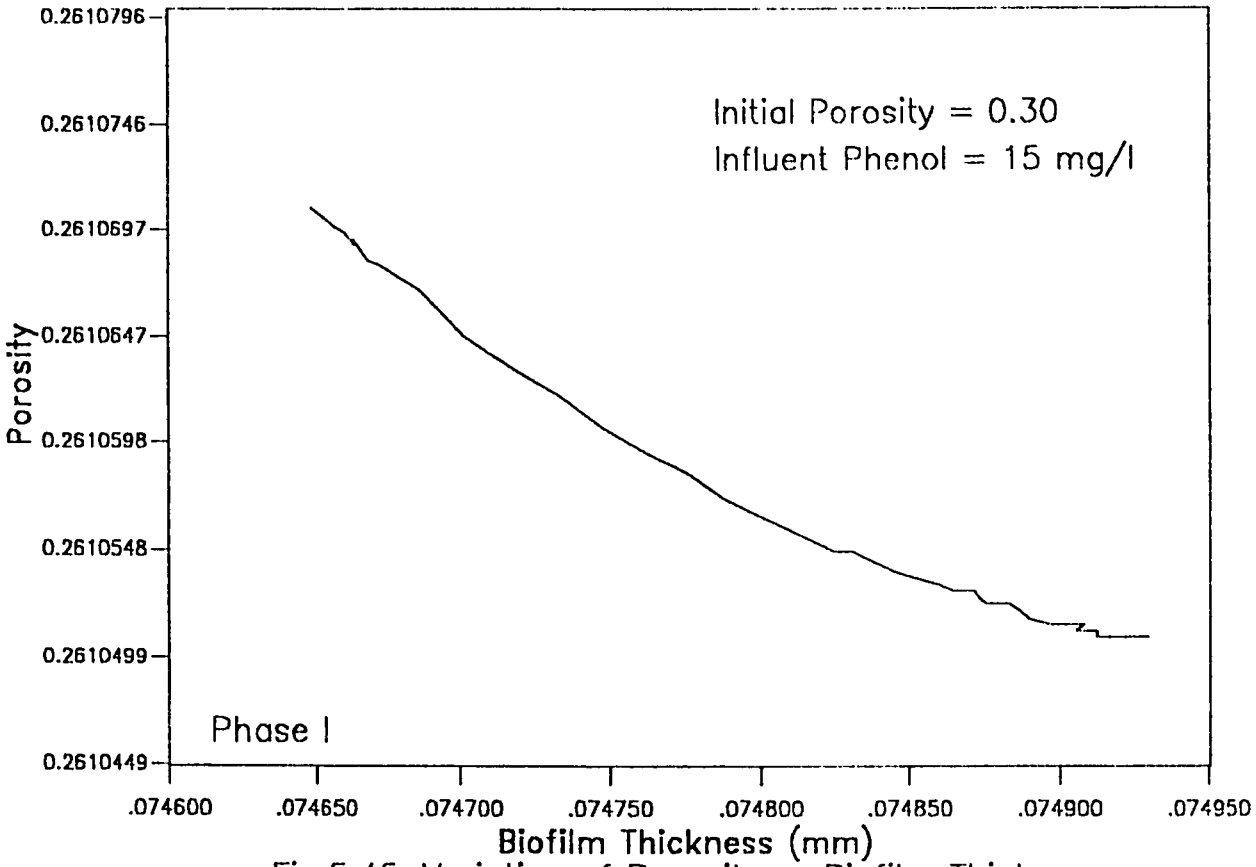

Fig.5.45: Variation of Porosity vs Biofilm Thickness in column C5 after 58 days

biofilm.

Ju-Chang Huang et al (1985) conducted a study on biofilm growth in a fixed film reactor using sucrose as substrate. In their study they succeeded to measure the biofilm thickness using a modified micrometer and a microscope. The microscope was first focused at the biofilm surface. After the sharp tip of the micrometer just touched the biofilm surface, the reading on the micrometer was taken. Then the tip was forced through the biofilm to touch the plastic surface. At this time, a second reading was taken. The difference between these two readings gave the biofilm thickness. Since the thickness of biofilm varied from one place to another at a given time, about 25 thickness measurements were taken at random. The average biofilm thickness found in this study was 0.13 mm compared to our study which gave from 0.66 to 0.98 mm in the different columns. This difference is due to the fact that higher concentration of substrate was used in their study compared to ours.

5.7 Statistical Correlation Between Various Parameters of the Experiment

One of the objectives of this study was to develop a mathematical correlation between the volatile solids, and influent substrate concentration. In this study these two variables are related and it seemed important to model and explore this relationship. To do that a simple program was developed and used.

5.7.1 Correlation Between the Influent Phenol Concentration and Volatile Solids

Since the mathematical correlation, between influent substrate concentration and volatile solids, was one of the objectives of this study, it was prescribed the conditions for the efficient operation of the experiment in such a way that the data is likely to provide the desired information within the framework of the adopted statistical model. The statistical anlysis used serves as a basis for the formulation of a relationship between the physical quantities involved in the experiment. It was developed first as a linear model which did not provide a satisfactory representation of the data. The coefficient of Determination was 0.46, which meant that only 46% of the data was accounted by the model used. The best fit was acieved using exponential model which was linearized using appropriate transformation. The coefficient of determination, used to judge the adequacy of the

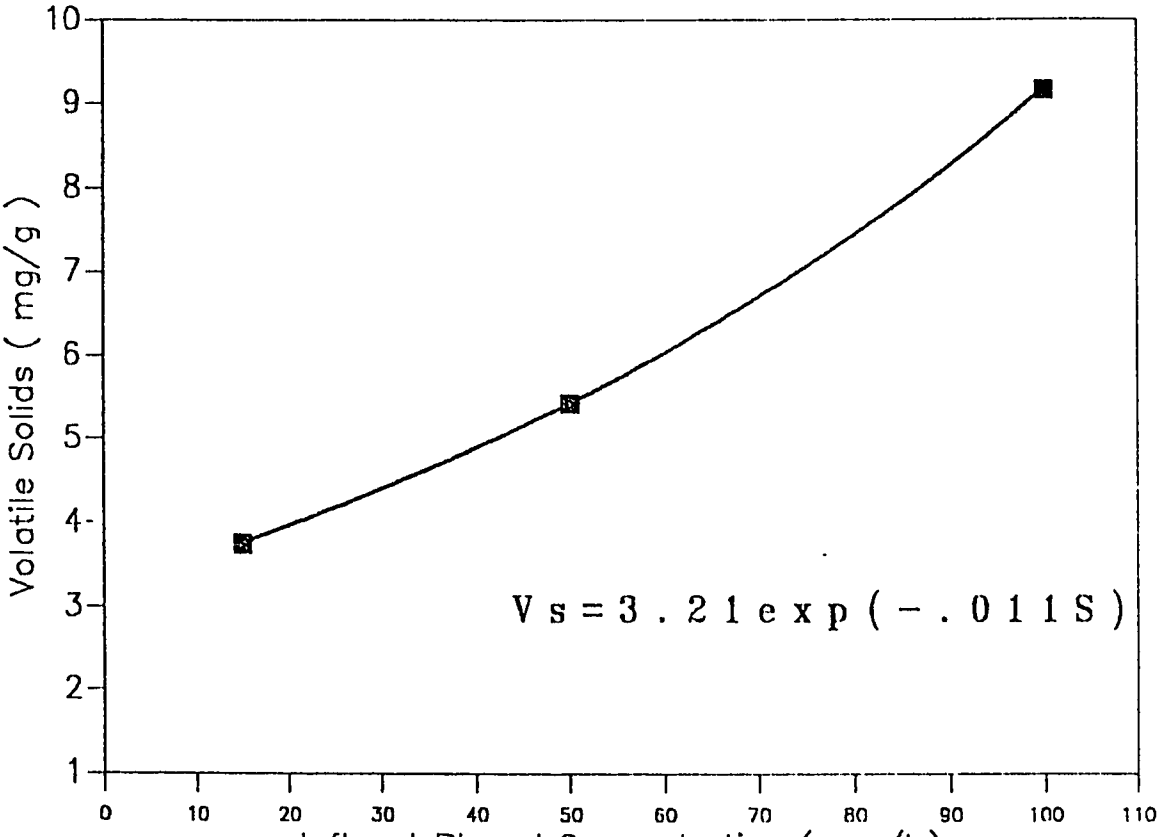

Fig.5.46: Influent Phenol Concentration Vs. Volatile Solids

regression model, was 0.93. This tells that 93% of the data is explained by the model. The coefficient of variation was 7.0 which is a good measure of precision. The results obtained show that, for three different phenol concentrations (15, 50, and 100 mg/l), volatile solids can be expressed as a function of the influent phenol concentration. The model obtained is of the following type:

ra (5.2) $$B = A^{*}EXP(CX)$$

Where

A = 3.21

B = volatile solids

C = -0.011

X = influent phenol concentration

Figure 5.46 shows the plot of the correlation between the substrate and volatile solids in the case of finer sand of the 3rd set. As it can be seen the correlation is exponential. This correlation obtained matches with the explanation given by Rittmann (1982) on the comparative performance of biofilm reactor types. This kind of correlation can not be generalized to all kinds of soil sand.

Chapter VI

SUMMARY AND CONCLUSIONS

6.1 phase I

The effect of bacterial growth in the soil column reactor environment has been investigated in this study. The growth substrate used was phenol. The different parameters studied in this work were hydraulic conductivity and porosity reductions by bacterial growth, and the determination of spatial distribution of the biomass in terms of volatile suspended solids and standard plate counts.

The salient features of the present work are summarized below:

The initial hydraulic conductivities in these columns were 9.0 cm/hr for the coarse sand, 5.2 cm/hr for the medium sand, and 8.8 cm/min for the fine sand which decreased to 0.058 cm/min for the coarse sand, and 0.033 cm/min for medium and fine sand, after 58 days of operation of the columns. The results of this study point to the existence of a limit beyond which the reduction in hydraulic conductivity becomes insignificant. This limit on conductivity reduction factor was found to be $5.8*10^{-4}$, $5.9*10^{-4}$, and $1.5*10^{-3}$, for coarse, medium, and fine sands respectively. From these value it can be deduced that the reduction in conductivity is severe for the fine sand compared to the other sizes.

The respective removal of phenol in these columns were 96% for the coarser sand, 97.9% for the medium size sand, and 98.8% for the finer sand. Steady-state effluent phenol concentrations occured simultaneously with uniform hydraulic conductivit reduction after 50 days of operation.

For a given sand size, initially biomass is mostly concentrated at the top of the reactor, but with time redistributes itself more uniformly downwards due to hydrodynamic shear.

The concentration of volatile solids near the columns inlets and outlets, after 58 days of operation, ranged between 9.8 and 4.04 mg/g for the coarse sand, 11.2 and 6.2 mg/gr for the medium size sand, and 11.8 and 6.2 mg/g of sand for fine sand, respectively. The number of colonies near the column inlets and outles were $2800*10^{10}/ml$ and $1480*10^{10}/ml$ for the coarse sand, and $2840*10^{10}/ml$ and $1520*10^{10}/ml$ for the medium sand, and $2890*10^{10}/ml$ and $2120*10^{10}/ml$ for the fine sand. Substrate time and spatial profiles were explained better by total count analysis than by volatile solids.

Although the transient data showed very poor correlation between the volatile solids and standard plate counts for the same size of sand, at pseudo-steady state the two parameters corresponded very well with the ratio of volatile solids to total counts at the inlet and outlet agreeing very closely.

6.2 Phases I, II & III

In these phases the effect of phenol concentration on biomass retention, substrate removal, and hydraulic conductivity of three sizes of sand namely 0.2 mm, 0.33 mm, and 0.4 mm were investigated. Phenol concentration of 15, 50, and 100 mg/l were studied in phases I-III. Influent dissolved oxygen concentration were maintained at about 26-30 mg/l throughout this study. Based on the findings of this study, the following conclusions can be drawn:

_ During phase I oxygen was not limiting and phenol removal efficiency of 93% and 88% were achieved in the fine and medium sand columns, and the coarse sand respectively. Hydraulic conductivity of fine sand dropped from 8.8 cm/hr to 1.2 cm/hr after 35 days. The corresponding figures for the medium and coarse sands respectively are 5.2 and 9 cm/hr diminishing to 2.2 and 2.5 cm/hr.

_ During phase II & III since oxygen was limiting bacterial growth initially an anaerobic film developed in the reactors, attested by relatively much lower yields than phase I at comparable biomass densities. Phenol removal efficiencies improved significantly with time reaching 90 and 93% in the fine sand during phases II & III respectively. Similarly, the medium sand reactors achieved 94% and 91% reduction of phenol in phase II & III respectively. The coarse sand reactor effectively removed 88% of the influent phenol in phase II. Hydraulic conductivities of the fine, medium, and coarse sands dropped substantially to reach 0.21, 0.25, and 0.55 cm/hr

respectively during phase II. Similarly in phase III, the conductivities of the fine and medium sands reached 0.20, and 0.23 cm/hr respectively after 35 days of operation.

_ Although anaerobic biofilms tend to be physically thinner than aerobic films and dense, they impede permeability by virtue of the gaseous end products of biodegradation

_ During phase I, "dirty bed", permeability was related to pore volume with the coarse sand substantially higher than the fine and medium sands. In phases II & III permeability correlated with biomass densities per unit mass of sand and was less affected by biofilm thickness and specific surface area.

_ A parabolic relationship was observed between grain size diameter and microbial growth measured as volatile solids.

_ An exponential relationship was observed between the influent substrate concentration and microbial growth measured as volatile solids.

_ The Kozeni-Carman equation was used to estimate the thickness of biological film, knowing the biofilm-affected permeability. The estimated values of the film thickness varied from 0.06 mm to 0.09 mm. A good correlation was observed between porosity and the values of biofilm thickness in low ranges.

Chapter VII

RECOMMENDATIONS

Based upon the results achieved in this study, the following recommendations have been forwarded for the future work.

1. Determination of the effects of microbial growth in subsurface environment under multiple growth substrates.

2. A mathematical model is required to generalize the relationship between biomass and the associated reduction in permeability.

3. Attempts should be made to measure the thickness of biofilm experimentally using nondestructive imaging techniques.

4. Determination of the effects of biofilm growth on the anisotropy of a porous medium.

REFERENCES

1. Aksu, L., Kutsal. "Investigation of Biosorption of Cu(II), NI(II) and Cr (VI) ions to Activated Sludge Bacteria." *Environmental Technology*. 12, 915-921.

2. Allison, L.E. "Effect of Microorganisms on Permeability of Soil under prolonged submergence." *Soil Science*, Vol. 3, 1947, pp. 439-450.

3. APHA-AWWA-WPCF (1986). *Standard Methods for the Examination of Water and Wastewaters* 16-th Edition, Washington, DC.

4. Asher Brenner and Chozick, "Treatment of a High Strength, Mixed Phenolic Waste in an SBR",.us;Water Environment Research, 64, April 1992, pp.128-133.

5. Bennett,E.O. & Kalish P.J.;"The effect of bacteria on Sandstone permeability," *Society of Petroleum Engineers*, No 17, July 1964, pp. 805-814.

6. Brian, D.Wood and Keller, "In Situ Measurement of Microbial Activity and Controls on Microbial CO2 Production in the Unsaturated Zone", .us;Water Resources Research, 29, March 1993, pp. 647-659.

7. Brown, S.C., Grady, C.P.L.Jr; and Tabek, H.H. *Water Research.24, 1990, pp.853-861*

8. Christiansen, J.E. "Effect of entrapped air upon the permeability of soils." *Soil Science*, No. 18, July 1944, pp. 355-365.

9. Chopra,S.L. & Kanwar, J.S. "Soil Analysis." *Analytical Agricultural Chemistryy*; February 1976, pp. 162-210.

10. Colvin, R.J and Rozich, Alan .R. (1986). "Phenol Growth Kinetics of Heterogeneous Populations in a Two-stage Continuous Culture System." *Journal WPCF*, 58(4), 326-332.

11. Dhawan, S. and Erickson, "Simulation of Bioremediation in Soil Beds" *Groundwater. 31, April 1993, pp.271-284.*

12. Gordon, A.Hill,"Phenol Biodegradation by Pseudomonas Putida", *Biotechnology and Bioengineering. 17, 1975, pp.1599-1615.*

13. Graham, N.J. "Slow Sand Filtration." *Water & Wastewater Technology*; October 1988, pp. 163-207.

14. Helmut, Kohnke. "soil water." *Soil Physics.* 1968, pp.6-79.

15. Hill, Gordon A. and Robinson, Campell W. (1975). "Substrate Inhibition Kinetics: Phenol Degradation by Pseudomonas Putida." *Biotech. Bioeng.* 17, 15998-1615.

16. Huang, J., Chang, S., Liu, Y. and Jiang, Z. (1985). "Biofilm Growths with Sucrose as Substrate." *ASCE, Journal of Environmental Engineering.* 111, pp.353-363.

17. Kenneth Williamson and MacCarty. (1976), "A model of substrate

utilization by bacterial films." *Journal WPCF. 48, pp.9-23.*

18. Al-Harazin, Ibrahim; Nakhla, G.F and Farooq, S. (1991). "Startup of Sequencing Batch Reactors for Toxic wastewater Treatment." *Journal of Environmental Science and Health.* A26(5), 673-687.

19. Marshall, T. J. "A Relation Between Permeability and Size Distribution of Pores." *Journal of Soil Science.* 9, 1-8.

20. Masunaga, Shigeli; Urushigawa, Y. and Yozenawa, Y. (1986). "Biodegradation of O-Cresol by Heterogeneous Culture." *Water Research 20(4), 477-484.*

21. Masunaga, Shigeli; Urushigawa, Y. (1983). "Microbial Transformation of O-Cresol to Dihydroxytoluenes by Phenol Acclimatized Activated Sludge." *Chemosphere, 12(7/8), 1075-1082.*

22. Moltz, F.G. and Widdowson, (1986). "Simulation of Microbial Growth Dynamics Coupled to Nutrient and Oxygen Transport in Porous Media," *Water Resources Research, 22, 1207-1216.*

23. Powlowsky, U. and Howell, J.A. (1973). "Mixed Culture Biooxidation of Phenol: I. Determination of Kinetic Parameters." *Biotech. Bioeng.* 15, 889-896.

24. Powlowsky, U. and Howell, J.A. (1973). "Mixed Culture Biooxidation of Phenol: II. Steady State Experiments in Continuous Culture". *Biotech. Bioeng.* 15, 889-896.

25. Pablo B.Saez "Model-Parameter estimation using least squares" *Water Research*; Vol.26, No.6, 1992, PP.789-796.

26. Radhakrishan, I. and Ray, A.K. Sinha (1974). "Activated Sludge Studies with Phenol Bacteria." *Journal WPCF*, 46(10), 2393-2417.

27. Raleich, J.T.& Flock, D.L."A study of formation plugging with Bacteria," *Petroleum Transactions*, Vol. 25, February, 1965, pp.201-206.

28. Richard J. Kolvin and Rozich,"Phenol Growth Kinetics of Heterogeneous Populations in a Two Stage Continuous Culture System", .us;WPCF,58, April 1988, pp.326-332

29. Rittmann, B.E., " Comparative Performance of Biofilm Reactor Types", *Biotechnology & Bioengineering, 24, 1982, pp.1341-1370.*

30. Rittman, B.E, "The Effect of Shear Stress on Biofilm Loss Rate", *Biotechnology and Bioengineering, 24, 1982, pp.501-506.*

31. Robert, D.H.& William D.Kovacs,"Soil classification," *Introduction to Geotechnical Engineering*; 1981, pp. 47-72.

32. Rozich, A.F., Gaudy, A.F.Jr; and D'Adamo, P.C. *Water Research, 19, 1985, pp.481-490*

33. Stewart W.Taylor & Peter R.Jaffe',"Biofilm Growth and the related changes in the physical properties of a porous medium,

Experiment," *Water Resources Research*; Vol.26, No.9, September 1990, PP.2153-2159.

34. Stewart W.Taylor & Peter R.Jaffe',"Biofilm Growth and the related changes in the physical properties of a porous medium, permeabilty," *Water Resources Research*; Vol.26, No.9, September 1990, PP.2161-2169.

35. Stewart W.Taylor & Peter R.Jaffe',"Biofilm Growth and the related changes in the physical properties of a porous medium, dispersivity," *Water Resources Research*; Vol.26, No.9, September 1990, PP.2171-2180.

36. Stewart W.Taylor & Peter R.Jaffe',"Substrate and Biomass Transport in a Porous Medium," *Water Resources Research*; Vol.26, No.9, September 1990, PP.2181-2194.

37. Stratton, R.G., Namking, E., and Rittmann, B.E. *American Water Work Association, 75, 1983, PP.463-469.*

38. Taylor, T.E. and Collins, "Microbial populations, activities and carbon metabolism in slow sand filters"
Water Research; vol.26, No 10, March 1992, pp.1319-1328.

39. Thomas J.C.& K.W.Brown "Depth variations in hydraulic conductivity within a compacted clay," *Water, Air, and Soil pollution*; Vol.65,1992, PP.371-380.

40. Williamson, K., and McCarty, P.L. *Journal of Water Pollution*

Control Federation, 48, 1976, pp.9-24.

41. Yang, D. Ren and Humphrey, Arthur E. (1975). "Dynamic and Steady State Studies of Phenol Biodegradation in Pure and Mixed Cultures." *Biotech. Bioeng.* 38, 1211-1235.

42. Youngs, E.G and Goss (1988). "Hydraulic Conductivity Profiles of Two Clay Soils." *Journal of Soil Science.* 39, 341-344.

Appendix A

Table1

Phase: 1

Daily Measurement of Hydraulic Conductivity for the 16-day period

Column A1	Column B1	Column C1
20.372	5.572	9.167
12.181	4.856	8.383
8.078	4.267	7.953
7.270	11.724	8.858
12.535	13.393	11.483
17.280	14.803	17.228
30.557	6.110	22.145
32.988	15.615	9.119
16.436	11.698	8.822
8.409	8.435	7.180
6.775	8.102	5.479
5.102	6.748	7.106
4.866	8.316	6.677
4.291	5.411	5.959
3.521	4.946	5.186
3.154	5.845	5.318

TableII

Phase:I

Daily Measurement of Hydraulic Conductivity for the 26-day period

Column A	Column B	Column C
19.132	7.823	17.203
12.535	7.035	11.910
11.360	5.309	10.313
6.991	6.544	10.669
5.416	9.703	12.886
5.111	12.231	16.277
7.115	12.787	28.116
11.340	10.398	11.875
12.096	9.231	8.822
7.040	6.562	6.194
5.261	6.430	5.447
4.901	6.093	5.845
4.714	5.659	5.061
3.935	5.536	4.628
3.928	5.922	5.258
3.877	5.922	4.561
3.997	7.239	3.838
3.951	5.404	2.785
4.029	5.171	2.785

3.879	4.991	2.657
3.688	4.444	2.740
3.494	3.798	2.553
3.458	3.406	2.394
3.276	3.844	2.257
3.061	3.863	2.148
2.999	3.375	2.175

TableIII

Phase: I

Daily Measurement of Hydraulic Conductivity for the 35-day period

Column A	Column B	Column C
8.731	6.178	8.847
7.775	5.431	8.594
6.514	5.038	7.735
6.743	4.865	6.584
6.859	4.623	5.722
7.128	4.339	4.612
7.573	4.860	5.235
7.721	5.218	5.826
7.889	5.271	6.433
5.832	5.411	7.245
5.699	5.619	7.448
5.740	6.093	7.505
5.475	5.563	6.730
5.292	5.318	5.332
5.065	4.559	5.199
4.887	4.244	4.395
4.929	3.801	3.856
4.775	3.395	3.518
4.701	3.183	3.245

4.677	3.037	3.063
4.310	2.612	2.603
4.088	2.470	2.341
4.006	2.483	2.238
3.687	2.242	2.088
3.409	1.994	1.954
3.207	1.879	1.754
3.137	1.807	1.644
2.925	1.737	1.635
2.843	1.682	1.603
2.880	1.586	1.564
2.722	1.540	1.500
2.662	1.419	1.386
2.561	1.346	1.313
2.246	1.218	1.064
2.184	1.184	0.930

TableIV

Phase: I

Daily Measurement of Hydraulic Conductivity for the 50-day period

Column A	Column B
12.601	5.648
9.616	5.883
8.291	4.787
8.483	4.213
6.632	3.714
5.138	7.055
4.912	7.422
5.241	8.542
7.979	7.976
11.141	8.543
11.500	8.658
11.884	8.869
7.572	6.882
7.120	5.432
6.437	4.653
6.320	4.642
6.042	4.316
5.816	4.244
5.594	4.042

5.171	3.908
4.529	3.340
4.297	3.219
4.083	3.070
3.745	2.810
3.594	2.654
3.364	2.442
3.026	2.298
2.778	2.232
2.657	2.125
2.519	1.938
2.439	1.849
2.339	1.724
2.273	1.633
2.020	1.500
1.922	1.434
1.776	1.322
1.717	1.220
1.675	1.163
1.600	1.137
1.551	1.095
1.485	1.045
1.448	1.008
1.374	0.952
1.308	0.813

1.100	0.706
1.033	0.622
0.930	0.555
0.811	0.476
0.561	0.446
0.523	0.421

TableV

Phase: I

Daily Measurement of Hydraulic Conductivity for the 58-day period

Column A	Column B	Column C
6.755	4.413	4.622
6.503	4.277	4.484
6.172	4.089	4.069
6.609	3.974	3.963
6.978	3.760	3.817
7.257	4.029	4.292
7.560	4.273	4.544
8.247	4.549	4.903
9.072	4.914	5.233
8.976	4.866	5.659
10.222	4.588	5.309
11.500	4.321	5.017
12.271	3.801	4.486
10.533	3.691	3.952
9.326	3.488	3.769
8.815	3.307	3.513
8.003	3.136	3.251
7.030	3.066	3.267
6.329	2.918	2.798

5.949	2.829	2.954
5.320	2.672	2.665
4.477	2.540	2.372
4.194	2.345	2.045
3.949	2.215	1.955
3.649	2.067	1.842
3.285	1.809	1.783
3.158	1.733	1.704
3.024	1.648	1.611
2.922	1.559	1.559
2.726	1.455	1.516
2.604	1.421	1.435
2.496	1.314	1.369
2.393	1.234	1.278
2.286	1.119	1.042
2.109	1.085	0.927
1.974	0.992	0.882
1.879	0.944	0.867
1.795	0.901	0.832
1.709	0.902	0.823
1.614	0.873	0.781
1.550	0.834	0.730
1.489	0.806	0.739
1.336	0.773	0.705
1.186	0.492	0.558

1.118	0.469	0.498
1.027	0.431	0.445
0.855	0.387	0.396
0.566	0.342	0.354
0.540	0.317	0.318
0.466	0.286	0.282
0.419	0.269	0.256
0.387	0.244	0.234
0.354	0.227	0.229
0.347	0.224	0.222
0.334	0.222	0.223
0.336	0.217	0.218
0.314	0.211	0.214
0.305	0.181	0.204

TableVI

Phase: II

Daily Measurement of Hydraulic Conductivity for the 16-day period

Column A	Column B	Column C
6.063	6.366	6.366
5.804	5.560	5.080
5.404	4.966	4.076
5.259	4.818	3.878
4.813	4.468	6.255
4.669	4.311	6.534
5.968	5.978	6.897
6.072	7.171	7.076
7.138	7.115	7.699
10.186	7.292	10.656
7.843	5.966	8.668
6.905	4.881	6.515
4.729	3.864	5.650
4.584	3.571	5.228
3.501	3.400	4.739
3.169	3.071	4.289

TableVII

Phase: II

Daily Measurement of Hydraulic Conductivity for the 26-day period

Column A	Column B	Column C
6.366	5.093	6.366
5.080	4.336	5.787
4.838	4.127	5.744
4.540	4.106	4.931
4.540	4.445	5.199
4.094	4.365	5.927
4.554	4.793	6.207
5.121	5.273	6.191
5.699	5.376	6.808
5.974	5.319	6.948
5.341	4.797	6.031
4.845	4.381	5.784
4.993	5.205	5.486
5.800	4.868	7.533
8.382	6.366	8.276
8.538	11.459	6.684
5.449	5.857	4.511
4.178	4.269	4.173
2.851	3.470	3.376

2.768	3.038	3.112
2.391	2.858	2.838
2.292	2.655	2.728
2.037	2.469	2.648
1.834	2.092	2.358
1.722	1.877	2.064
1.520	1.774	2.042

TableVIII

Phase: II

Daily Measurement of Effluent Phenol Concentration for the 16-day period

Column A	Column B	Column C
41.800	45.000	49.000
41.300	43.000	47.300
41.400	42.800	47.000
40.800	42.600	45.200
40.200	42.000	42.000
40.400	40.000	40.000
40.200	36.000	40.000
38.400	35.000	38.800
36.400	30.000	38.600
32.000	28.400	38.200
26.400	28.000	38.200
21.700	26.000	38.000
16.800	26.000	36.400
15.400	24.800	32.600
15.000	24.200	30.000
15.000	24.000	28.700

TableIX

Phase:II

Daily Measurement of Effluent Phenol Concentration for the 26-day period

Column A	Column B	Column C
41.600	40.100	49.100
41.500	38.400	48.700
41.300	38.000	48.400
40.800	36.400	48.200
40.600	36.000	48.000
40.400	32.800	45.300
40.000	30.600	44.700
37.900	30.000	44.000
36.800	26.400	42.300
34.700	26.200	40.400
30.700	26.000	40.200
28.700	24.800	38.300
26.700	24.600	38.000
20.600	24.400	36.400
18.600	24.000	35.400
15.000	24.000	32.800
12.800	22.600	30.000
10.700	22.000	28.200
9.700	20.700	26.400

8.500	20.400	26.000
8.400	20.000	24.600
8.200	18.000	24.300
6.000	16.600	22.800
5.200	16.000	21.400
5.000	15.200	20.600
4.800	14.700	19.700

TableXI

Phase: I

Daily Measurement of Effluent Phenol Concentration for the 16-day period

Column A	Column B	Column C
14.800	12.900	14.200
14.600	12.600	14.000
14.600	12.600	13.800
14.400	12.200	13.800
14.800	12.200	13.600
14.200	12.600	13.200
10.800	8.700	9.600
10.100	8.400	9.400
10.000	8.400	9.300
10.000	8.200	9.300
9.800	8.200	8.400
9.800	8.200	8.000
9.800	8.100	7.600
9.600	8.000	6.500
9.600	7.200	6.300
9.600	6.800	6.300

TableXII

Phase: I

Daily Measurement of Effluent Phenol Concentration for the 26-day period

Column A	Column B	Column C
14.900	13.600	14.800
14.800	12.800	14.800
14.900	12.600	14.400
14.600	12.400	14.400
14.400	12.000	14.600
14.700	12.000	14.200
14.400	8.200	9.700
14.000	8.200	9.700
13.100	8.000	9.400
11.200	8.000	9.100
10.200	8.000	9.100
9.600	7.900	9.000
9.700	7.900	9.000
9.200	7.200	8.100
7.100	6.200	6.400
6.300	6.000	5.800
5.400	4.800	4.100
5.000	4.200	4.000
4.800	4.000	3.200

4.400	3.200	3.000
4.400	3.200	3.000
4.300	3.000	2.800
4.300	3.000	2.800
4.310	2.800	2.800
4.250	2.800	2.700
4.240	2.800	2.500

TableXIII

Phase: I

Daily Measurement of Effluent Phenol Concentration for the 35-day period

Column A	Column B	Column C
14.900	12.800	14.600
14.900	12.600	14.600
14.700	12.400	14.400
14.800	12.400	14.200
14.600	12.200	14.200
14.600	11.900	14.000
10.700	8.000	10.200
10.500	8.000	10.000
10.300	8.000	9.800
10.100	8.000	9.700
10.000	7.800	9.400
10.000	7.800	9.300
9.900	7.600	9.100
9.300	6.900	7.400
7.200	6.000	6.500
6.500	5.400	6.000
5.100	4.200	4.800
4.800	3.800	4.100
4.700	3.600	3.000

4.600	3.100	2.800
3.800	3.000	2.800
3.800	2.900	2.600
3.800	2.400	2.400
3.100	2.200	2.200
2.800	1.900	2.000
2.400	1.800	1.800
2.200	1.600	1.800
2.000	1.200	1.600
2.000	1.200	1.200
1.800	1.000	1.200
1.800	1.000	1.000
1.600	0.900	0.800
1.600	0.900	0.800
1.400	0.800	0.800
1.400	0.800	0.600

TableXIV

Phase: I

Daily Measurement of Effluent Phenol Concentration for the 50-day period

Column A	Column B
14.700	13.800
14.600	13.400
14.400	13.400
14.700	12.800
14.200	12.600
14.000	12.400
9.900	8.800
9.400	8.400
9.800	8.200
9.200	8.000
9.200	8.000
9.000	7.900
9.000	7.800
8.900	6.300
7.000	6.000
7.000	5.300
6.800	4.000
4.300	3.600
4.100	3.000

4.000	2.800
4.000	2.900
3.900	2.700
3.900	2.400
3.000	2.300
2.700	2.000
2.300	1.800
2.400	1.500
2.000	1.200
2.000	0.900
1.800	0.800
1.800	0.800
1.600	0.740
1.600	0.700
1.600	0.650
1.400	0.650
1.400	0.600
1.200	0.600
1.200	0.500
0.900	0.500
0.800	0.500
0.700	0.450
0.700	0.400
0.600	0.360
0.600	0.360

0.600	0.360
0.600	0.340
0.600	0.340
0.500	0.320
0.500	0.310
0.480	0.300

TableXV

Phase: I

Daily Measurement of Effluent Phenol Concentration for the 58-day period

Column A	Column B	Column C
14.800	13.800	14.800
14.800	13.600	14.200
14.800	13.200	14.000
14.700	12.600	14.000
14.700	12.600	13.800
14.300	12.400	13.400
10.100	9.200	9.500
10.000	8.800	9.500
9.800	8.400	9.300
9.400	8.100	9.200
9.400	7.900	9.000
9.300	7.900	9.000
9.100	7.900	8.900
8.800	6.600	7.600
6.900	5.800	6.300
6.800	5.000	6.100
6.200	4.100	4.300
5.000	3.200	4.100
4.800	2.800	3.300

4.400	2.400	2.800
4.000	2.400	2.700
4.000	2.500	2.400
3.800	2.200	2.200
3.200	2.000	2.000
3.000	1.700	1.800
2.800	1.300	1.600
2.500	1.700	1.300
2.200	1.000	1.000
2.200	0.900	0.800
2.000	0.650	0.600
2.000	0.600	0.600
1.800	0.600	0.600
1.800	0.550	0.500
1.600	0.500	0.500
1.600	0.450	0.500
1.400	0.450	0.450
1.200	0.400	0.400
1.200	0.400	0.400
1.000	0.400	0.400
0.800	0.400	0.400
0.800	0.320	0.400
0.700	0.300	0.380
0.700	0.300	0.380
0.650	0.300	0.360

0.650	0.300	0.360
0.650	0.280	0.360
0.600	0.280	0.300
0.600	0.280	0.300
0.600	0.280	0.300
0.600	0.280	0.300
0.600	0.280	0.300
0.500	0.280	0.250
0.480	0.240	0.230
0.440	0.230	0.200
0.430	0.210	0.170
0.410	0.190	0.110
0.400	0.180	0.100
0.320	0.120	0.080

TableXVI

Phase: I

Measurement of Standard Plate Counts for the 16-day period

Column A	Column B	Column C
1100.000	1392.000	1218.000
986.000	1218.000	928.000
1218.000	928.000	1044.000
1218.000	1450.000	986.000
1102.000	1334.000	812.000
928.000	1276.000	986.000
870.000	1334.000	928.000

TableXVII

Phase: I

Measurement of Standard Plate Counts for the 26-day period

Column A	Column B	Column C
1160.000	1624.000	2230.000
1225.000	1160.000	1450.000
1225.000	1450.000	1450.000
1740.000	1450.000	1160.000
1392.000	1160.000	1682.000
928.000	1334.000	1624.000
638.000	1102.000	1450.000

TableXVIII

Phase: I

Measurement of Standard Plate Counts for the 35-day period

Column A	Column B	Column C
1740.000	2088.000	2320.000
1160.000	1740.000	1856.000
1450.000	1450.000	1856.000
1160.000	1334.000	1740.000
1276.000	1682.000	1624.000
1044.000	1102.000	1508.000
870.000	1030.000	1450.000

TableXIX

Phase: I

Measurement of Standard Plate Counts for the 50-day period

Column A	Column B
2204.000	2320.000
2146.000	1856.000
1740.000	1856.000
1624.000	1740.000
1566.000	1624.000
1218.000	1508.000
1276.000	1450.000

Table XXI

Phase: I

Measurement of Standard Plate Counts for the 58-day period

Column A	Column B	Column C
2668.000	2842.000	2842.000
2436.000	2784.000	2784.000
2320.000	2668.000	2668.000
2204.000	2320.000	2668.000
2088.000	2262.000	2436.000
1624.000	2088.000	2320.000
1450.000	2088.000	1800.000

TableXXII

Phase: I

Measurement of Volatile Solids for the 16-day period

Column A	Column B	Column C
7.130	11.120	11.720
7.530	9.810	11.770
5.850	7.810	6.980
5.030	8.100	6.910
4.880	5.170	4.160
3.780	4.210	3.630
2.480	4.960	2.330
3.410	2.110	1.270
2.490	0.630	1.100
2.570	0.520	0.300
3.330	0.280	0.890
1.400	0.081	0.550
1.050	0.074	0.450
2.990	1.600	0.190

TableXXIII

Phase: I

Measurement of Volatile Solids for the 26-day period

Column A	Column B	Column C
8.560	10.450	10.980
6.210	8.270	10.680
5.210	6.090	9.240
5.270	7.710	8.600
5.090	5.850	8.260
5.360	4.750	7.510
4.150	6.360	8.820
4.540	4.980	8.030
4.570	5.580	7.690
3.010	4.400	6.290
3.480	3.470	6.210
2.390	3.130	4.710
2.420	2.990	4.990
2.190	2.100	3.100

TableXXIV

Phase: I

Measurement of Volatile Solids for the 35-day period

Column A	Column B	Column C
8.370	10.110	11.560
8.440	10.850	10.540
6.390	9.050	10.770
5.370	8.750	10.780
5.320	7.480	10.080
5.420	6.220	9.560
5.560	6.770	9.440
6.140	6.660	8.150
5.800	6.260	7.740
5.040	5.060	7.070
4.460	4.450	6.830
4.750	4.390	6.120
4.340	4.490	6.220
4.400	4.250	6.020

TableXXV

Phase: I

Measurement of Volatile Solids for the 50-day period

Column A	Column B	Column C
8.600	11.680	11.520
7.560	8.610	10.780
7.080	7.930	10.210
7.450	7.650	9.810
6.600	8.390	9.710
7.720	7.390	9.420
6.490	6.970	8.760
7.240	7.240	8.410
6.760	7.370	8.240
6.460	6.050	7.420
6.830	6.700	7.060
6.570	6.110	7.210
5.400	6.030	6.930
4.160	4.820	6.270

TableXXVI

Phase: I

Measurement of Volatile Solids for the 58-day period

Column A	Column B
8.820	11.810
8.400	10.440
7.930	10.200
7.480	9.710
7.200	7.810
6.400	8.410
7.300	8.520
7.150	8.200
6.920	7.800
6.870	7.400
6.430	6.400
6.400	6.100
6.200	5.200
6.040	4.840

TableXXVII

Phase: II

Measurement of Volatile Solids for the 16-day period

Column A	Column B	Column C
9.430	7.500	6.810
9.230	7.560	6.850
9.300	6.360	4.340
9.280	6.210	3.270
6.050	6.180	3.290
5.720	5.430	2.620
5.400	5.460	2.100
3.800	4.830	1.230
3.200	3.610	1.030
3.230	3.650	0.430
1.250	1.010	0.170
1.280	0.630	0.050
0.360	0.230	0.030
0.300	0.160	0.010

TableXXVIII

Phase: II

Measurement of Volatile Solids for the 26-day period

Column A	Column B	Column C
10.510	8.520	7.930
10.200	8.230	7.330
8.630	7.880	7.060
7.600	7.360	6.830
7.250	7.120	6.560
6.920	6.720	6.100
6.870	6.230	4.310
5.480	5.430	4.330
5.210	5.130	4.010
4.720	4.360	4.100
4.210	3.120	3.870
3.760	3.070	2.900
3.140	2.870	1.010
2.970	2.750	1.080

TableXXIX

Phase: II

Measurement of Volatile Solids for the 35-day period

Column A	Column B
16.720	15.930
9.630	12.360
9.650	10.130
7.440	9.310
7.360	8.130
7.130	7.890
6.840	6.930
6.870	6.670
6.350	6.310
6.210	5.870
5.480	5.310
5.010	4.800
4.210	4.850
4.040	3.110

TableXXX

Phase: III

Measurement of Volatile Solids for the 16-day period

Column A	Column B
9.880	10.170
8.730	9.870
8.760	9.900
8.120	8.680
6.940	7.530
6.730	7.360
6.770	6.270
6.330	6.300
5.970	6.130
5.430	5.830
4.320	4.210
3.260	3.370
1.230	2.280
0.580	1.510

TableXXXI

Phase:III

Measurement of Volatile Solids for the 26-day period

Column A	Column B
10.350	12.930
9.870	11.760
8.760	10.750
8.790	10.800
8.210	9.770
7.710	9.810
6.880	7.510
6.900	7.550
6.100	6.330
5.870	5.440
5.910	5.210
5.210	4.880
4.330	4.900
3.770	3.910

TableXXXII

Phase: III

Measurement of Volatile Solids for the 35-day period

Column A	Column B
19.480	17.110
16.440	12.990
12.130	1.360
11.240	9.370
9.360	8.990
8.110	8.660
7.310	8.410
6.910	7.980
6.760	7.430
6.780	7.130
6.100	6.200
5.610	6.230
5.130	5.400
4.590	5.360

TableXXXIII

Phase: III

Daily Measurement of Effluent Phenol Concentration for the 16-day period

Column A	Column B
64.800	74.400
62.600	70.100
60.800	68.600
60.000	62.400
58.600	60.700
58.200	58.400
58.000	52.400
56.400	50.600
56.000	50.000
52.000	48.600
52.000	46.400
50.400	42.800
50.000	42.400
48.200	40.800
48.000	38.600
48.000	38.000

TableXXXIV

Phase:III

Daily Measurement of Effluent Phenol Concentration for the 26-day period

Column A	Column B
66.200	70.200
64.800	68.400
62.600	60.700
50.800	58.700
50.200	55.400
50.000	52.300
48.400	50.400
48.200	44.800
48.000	43.200
46.400	41.600
46.200	40.400
44.200	38.700
40.600	38.000
38.300	36.800
38.000	36.000
38.000	36.000
38.000	34.500
36.800	32.800
36.400	32.000

36.000	28.600
36.000	26.600
36.700	26.200
36.400	24.300
35.800	24.000
35.400	22.800
35.100	20.400

TableXXXV

Phase:III

Daily Measurement of Effluent Phenol Concentration for the 35-day period

Column A	Column B
70.400	72.600
70.000	68.600
68.400	66.400
65.300	60.800
62.300	60.000
56.400	55.500
52.400	50.800
50.400	50.000
50.000	48.600
50.000	48.200
49.300	46.600
49.000	40.000
48.600	38.800
44.600	38.000
44.000	36.400
42.800	36.000
40.600	34.500
40.000	34.000
38.600	32.800

38.000	32.000
36.800	30.600
36.400	30.000
36.000	28.700
36.000	28.000
34.600	28.000
34.000	26.400
32.700	24.800
32.000	24.200
30.800	24.000
30.000	22.800
28.600	22.000
28.000	20.600
16.400	16.400
9.110	7.110
9.020	6.240

TableXXXVI

Phase: II

Daily Measurement of Effluent Phenol Concentration for the 35-day period

Column A	Column B
38.700	48.800
36.800	46.400
35.100	46.200
35.000	44.800
33.600	44.200
32.400	44.000
30.700	42.800
30.200	42.200
30.000	42.000
28.700	40.400
28.200	38.800
28.000	38.600
27.200	38.000
27.000	36.400
26.600	33.700
26.400	30.800
24.800	30.000
24.000	28.600
22.600	26.400

21.600	26.000
20.800	24.600
20.000	24.400
18.400	23.600
18.600	22.800
16.400	20.700
15.800	20.400
14.600	20.000
14.200	20.000
12.600	19.400
12.000	19.200
11.800	18.700
11.400	18.600
10.600	18.200
3.100	16.210
3.000	16.100

TableXXXVII

Phase: III

Daily Measurement of Hydraulic Conductivity for the 26-day period

Column A	Column B
6.366	5.093
4.848	4.356
4.365	4.289
4.053	4.100
4.422	4.375
4.851	4.787
5.498	4.934
5.900	5.889
5.984	6.366
7.176	6.872
5.930	6.247
6.243	6.278
6.234	6.897
7.390	7.958
6.920	7.830
7.061	10.823
4.419	5.116
3.855	3.747
3.020	3.035

2.908	2.709
2.674	2.574
2.533	2.272
2.247	2.010
2.138	1.867
1.888	1.718
1.804	1.626

TableXXXVIII

Phase:II

Daily Measurement of Hydraulic Conductivity for the 35-day period

Column A	Column B
5.093	5.093
4.906	4.525
4.434	4.022
4.259	3.689
4.237	4.170
4.539	4.208
5.541	5.628
5.541	5.851
5.626	5.978
5.869	6.930
5.952	6.512
4.826	4.371
3.939	4.009
3.654	4.086
3.326	2.827
2.900	2.449
2.637	2.375
2.288	2.010
2.180	1.910

1.919	1.790
1.719	1.735
1.553	1.666
1.501	1.607
1.376	1.588
1.259	1.411
1.139	1.396
1.093	1.348
1.049	1.273
0.970	1.216
0.898	1.188
0.813	1.095
0.772	1.021
0.676	0.952
0.217	0.555
0.203	0.533

TableXXXIX

Phase: III

Daily Measurement of Hydraulic Conductivity for the 35-day period

Column A	Column B
5.093	8.488
4.769	5.054
4.434	4.564
3.911	4.171
3.901	3.702
3.741	3.720
4.244	4.072
5.869	5.578
5.730	5.683
6.614	4.962
6.406	4.838
4.279	3.944
3.640	3.508
3.356	3.077
2.871	2.801
2.351	2.489
2.098	2.069
1.981	1.726
1.824	1.670

1.639	1.515
1.491	1.415
1.425	1.304
1.331	1.258
1.273	1.160
1.179	1.084
1.104	1.000
1.021	0.936
0.940	0.877
0.853	0.803
0.788	0.702
0.711	0.621
0.637	0.602
0.612	0.423
0.228	0.174
0.211	0.170